Fire, Charcoal, and the Biogeochemistry of Carbon and Nitrogen in Pacific Northwest Forest Soils

Melissa Rose Ann Pingree

A dissertation

submitted in partial fulfillment of the

requirements for the degree of

Doctor of Philosophy

University of Washington

2017

Reading Committee:

Thomas H. DeLuca, Chair

David Butman

Darlene Zabowski

Program Authorized to Offer Degree:

Environmental and Forest Sciences

University of Washington

Abstract

Fire, Charcoal, and the Biogeochemistry of Carbon and Nitrogen in Pacific Northwest Forest Soils

Melissa Rose Ann Pingree

Chair of the Supervisory Committee:
Professor Thomas H. DeLuca
School of Environmental and Forest Sciences

The rain shadow forests of the Olympic peninsula represent a unique, mixed-severity fire regime class in the midst of a highly productive landscape where spatial heterogeneity of fire severity may have significant implications for below and aboveground post-fire recovery. The purpose of this study was to quantify the impacts of wildfire on forest carbon (C) and nitrogen (N) pools and assess the influence of charcoal in a mixed-severity ecosystem on the Olympic Peninsula, Washington, USA. We established a fire chronosequence in forest stands ranging in time since fire (TSF) from 3 to 115 years prior to site establishment. At each site, we measured vegetation abundance, overstory composition, and attributes of surface mineral soil to a depth of 10 cm and forest floor organic matter that included pH, texture, bulk density, and C and N pools (dissolved organic C [DOC], phenol, ammonium, nitrate). Non-ionic resin lysimeters were buried at the

interface of organic and mineral soil to measure the O-horizon leached DOC that would contact charcoal particles on the forest floor. Charcoal particles collected from the chronosequence sites were used in adsorption batch experimentation with phenol as a sorbate and measured an average 29.70 (± 6.23) μg phenol mg charcoal^{-1} adsorption capacity, which did not differ significantly between chronosequence sites. Wildfire-produced charcoal along the chronosequence showed high variability in adsorption capacity, which was partially explained by the thermogravimetric region of volatilized adsorbed compounds onto charcoal surfaces. The O-horizon leachate averaged 1.05 (SD ± 2.87) g DOC m^{-2} year^{-1} and increased significantly along the TSF gradient (Pearson's r = 0.52; p < 0.0001). Multivariate, non-parametric analysis of soil and vegetation factors showed a significant relationship with the time since fire gradient between sites (p-value < 0.01) but not within sites. The TSF gradient was significantly correlated to charcoal mass in the O-horizon (r = -0.4), O-horizon C (r = 0.4), phenolic content in both O-horizon (r = 0.4) and mineral soils (r = 0.2), and potentially mineralizable N (r = 0.4). Recent sites contained higher mineral soil total N and inorganic available N, though not significantly correlated with the TSF gradient. Over time, soils appear to shift toward phenolic-rich organic and mineral soils, higher moss cover, and a higher potentially mineralizable nitrogen index. This study provides evidence of a multivariate, belowground soil response that is less sensitive to wildfire disturbances than the aboveground vegetation.

TABLE OF CONTENTS

LIST OF FIGURES

LIST OF TABLES

ACKNOWLEDGEMENTS

There are many, many people who helped this research project become a reality. My committee chair and members provided the time, patience, and mentorship in preparation for and throughout each of the rigorous exams. Amanda Bidwell worked countless hours in the field and laboratory on this project and provided council on questions concerning sample processing and analysis. I was also lucky to have the help of undergraduate students Teddy McFall, Andrew Wells, Felipe Grigoleto, Ryan Contreras, Daylen Issac, Norah Hummel, Teresa Wang, and laboratory assistants Katie Kryston, Florence Miller, Ian Evans, and Alvin Lieu. Council from my fellow graduate students Si Gao, Anna Simpson, Oliver Jan, Jason James, and Sean Jeronimo was paramount. Andrew Kim facilitated the use of the Chemical Engineering Brindra Innovation Lab and Fernando Resende graciously provided his lab equipment for my work. The School of Environmental and Forest Sciences administrative personnel, especially Amanda Davis, Michelle Trudeau, and David Campbell, played a more important role than I could have imagined. Thank you everyone.

DEDICATION

To my grandmother

Barbara Ann Stevens

who reminds me to hold my head up with pride

Chapter 1. INTRODUCTION

1.1 WILDFIRE AND ANTHROPOGENIC FIRE ON THE OLYMPIC PENINSULA

The Olympic peninsula, located in northwest Washington, USA, is a rugged 7,000 km^2 body of land surrounded by the Pacific Ocean on the west, the Strait of Juan de Fuca on the north, and the Puget Sound on the east. Within this area is a pronounced precipitation gradient of 50 – 500 cm annually, dictated by the orographic effect of Mount Olympus and local weather patterns of the Pacific Ocean. The Olympic mountain range produces an orographic and adiabatic precipitation effect as moist, warmer air is pushed from the Pacific Ocean, over the mountains where southwest-facing slopes receive 50% more precipitation than valley bottoms (Gavin and Brubaker, 2015). Temperatures of the peninsula diverge in the summer, where the moderate Pacific Ocean sea breeze impedes maximum summer temperatures on the west side of Mt. Olympus at 18°C and allows for higher temperatures of 24°C on the east side (Daly et al., 2002; Gavin and Brubaker, 2015).

The entirety of the Olympic peninsula exhibits a unique contrast in ecosystem disturbances that are related to the precipitation gradient (Franklin and Dyrness, 1973; Gavin and Brubaker, 2015). The dense, highly productive forests of the Olympic peninsula consist of *Pseudotsuga menziesii* dominated stands with *Tsuga heterophylla* and *Picea sitchensis* climax communities in the rain shadow and coastal temperate rain forests, respectively (Franklin and Dyrness, 1973). Disturbance regimes, similar to climax communities, shift from wind-driven in the west to fire-driven in the east (Agee, 1993). Fire is the primary disturbance agent in forest ecosystems of the rain shadow forests of the Olympic peninsula. High wind events and fire disturbances create

divergent forest structure, composition, and biogeochemical cycles along a precipitation gradient from the Pacific coast to the Puget Sound of western Washington.

On the west coast of the peninsula, wind is the primary disturbance influencing tree growth and forest regeneration. High wind events with gusts of 179 knots occurred approximately 1.23 times annually from 1701-2002 as measured by tree-ring analysis of *P. sitchensis* and *P. menziesii* along the western Oregon coast (Knapp and Hadley, 2012). Forests in the *P. sitchensis* zone are highly prized for both economic and ecologic values due to the size and longevity of *P. sitchensis*, high biomass production, and high species richness, which have led to considerable social and political conflicts (Franklin and Johnson, 2012; Thomas et al., 2006). Fire frequency is limited by high rates of annual precipitation (200 – 300 cm yr^{-1}) and mild temperatures (4.3 – 15.6°C range) on the west coast of the peninsula (Agee, 1993). Although fires are rare (500-1100 years) and of moderate fire intensity, they often result in high mortality due to the abundance of fire avoiding vegetation with minimal defenses even low severity fire disturbances (Agee, 1993; Fahnestock and Agee, 1983; Huff, 1995).

In contrast, the *T. heterophylla* forest zone in the rain shadow of the Olympic Mountains receives less summer rainfall, about 30% of total coastal precipitation, and higher maximum summer temperatures (24°C compared to 18°C). Since the end of the Little Ice Age (1850), extensive, climate-driven fires have ceased and the diversity of fire size and occurrence now reflects human activity and seasonal or decadal weather cycles (Agee, 1993). The forests of the *T. heterophylla* zone experience fire between 90 – 150 years and are characterized by a mixed-severity fire regime (Franklin and Dyrness, 1973; Gavin and Brubaker, 2015; Halofsky et al., 2011b;

Weisberg, 2004). Mixed-severity fire regimes poorly characterized, difficult to predict, and the most difficult to measure in terms of fire effects because of the high spatial and temporal variability typical in these fire regimes (Marcoux et al., 2013; Perry et al., 2011).

Similar to many western US forests, timber harvest and fire exclusion on the Olympic peninsula has led to increased forest density and homogeneity of forest structure where non-stand-replacing natural fires would otherwise maintain a mixed-severity fire regime (Weisberg, 2004). An investigation of prescribed fire on the peninsula established the viability of using low-intensity surface fire as a restoration tool in an old growth *P. menziesii* stand (Fonda and Binney, 2011). The Elwha River watershed shows a particularly extensive fire history as evidenced by a detailed dendrochronological investigation of the lower watershed from 1568 – 2007 through cross-referenced and adjacent tree-ring methods (Wendel and Zabowski, 2010). These methods increased the accuracy of fire-scar dating and resulted in conservative estimates of fire history by requiring at least three fire scars to indicate a fire event. The authors reported a mean fire return interval (MFRI) of 127 years in the lower Elwha River watershed. Frequent and infrequent fire periods were segregated into topographic and anthropogenic influences. Fires were more frequent on south-facing aspects and frequency increased with elevation for both north and south aspects. Natural fire rotation also coincided with periods of native inhabitants, low population, homesteading, and fire suppression. Decadal climate fluctuations correlate with fire frequencies of the Elwha River watershed. It is likely that the presence and behavior of humans responded to climatic conditions to create the rich fire history of the Olympic peninsula's *T. heterophylla* forest zone.

In a nearby river drainage located about 15 miles to the west of the lower Elwha River valley, a dendrochronology study of the Morse Creek area describes similar patterns of high fire frequency and low fire intensity since the mid-17th century (Wetzel and Fonda, 2000). The authors measured establishment dates and fire-release markers in 318 *P. menziesii* tree cores to make inferences about fire history, fire severity, and species composition. Findings from this study, similar to Wendel and Zabowski (2010), indicate the time periods of 1687 – 1720 and 1897 – 1904 were extensive burning periods while smaller fires burned in the drainage throughout the previous 650 years. The mean FRI is dependent on spatial scale and ranges from 106 years (>0.001 ha), 44 years (0.1 – 1 ha), 21 years (200 ha), and 3 years (2500 ha) in the Morse Creek area. At four different spatial scales, the authors reported the most appropriate mean FRI as 21 years over an area of 200 ha.

Fire in the rain shadow *T. heterophylla* forests of the Olympic peninsula has been significantly influenced by the behavior of human inhabitants and climactic conditions. The history of fire on the Olympic peninsula reflects an importance to both Native American and European habitation (Wray and Anderson, 2003), which has helped create the current distribution of vegetation and, likely, underlying biogeochemical cycles associated with wildfire disturbances. The unique complexity of the Olympic peninsula landscape provides diverse and specialized habitats for organisms to recover from disturbances via a variety of mechanisms, although this complexity is reduced in lower elevation forests where landscapes are highly altered by humans and landforms are more homogeneous (Peterson et al., 1997). The added complexity of mixed-severity fire regimes in this region, coupled with expected increases in fire frequency, distribution, and extent

(Halofsky et al., 2011b), provides a clear impetus to understand wildfire effects in forests of the rain shadow Olympic peninsula that remain largely unstudied and sparsely documented.

1.2 Wildfire Effects on Forest Soils

Studies of long-term wildfire effects that span a fire return interval provide insight to the function of fire in a particular ecosystem, rather than ephemeral effects of a fire event, and often use a space-for-time substitution approach (i.e. chronosequence). These studies rely on indirect measures of successional changes or soil development over an appropriate time series that represent an ongoing 'natural experiment' (Fukami and Wardle, 2005). A fundamental assumption of this design is a successional trajectory wherein the younger sites develop in a temporal pattern that resembles the older site development (Walker et al., 2010). In order for the chronosequence to provide a meaningful interpretation, the temporal scale of the study design must be appropriate for the specific process or organismal lifespan around which the study is designed to measure. Misuses of this design approach fail to consider multiple successional development trajectories and imply mechanisms from patterns along the chronosequence sites (Fastie, 1995; Johnson and Miyanishi, 2008). Chronosequence study designs provide meaningful insight into the effects of wildfires and the absence of fire, e.g. trends in vegetation abundance and surface soil nutrients, when they encompass at least one typical fire cycle, focus on processes likely to change over the fire cycle period, and avoid mechanistic implications without a direct measure of wildfire effects.

Short-term fire effects provide relevant immediate management implications for physical effects (i.e. erosion, runoff, water-repellency), mechanistic understandings of biotic responses, guidance for re-vegetation efforts, or other post-fire management activities (salvage logging), but fail to

encompass the broader functionality of fire as an ecosystem disturbance agent of secondary succession. For example, studies conducted in *Pinus ponderosa/P. menziesii* forests the eastern Cascade Mountains of Washington State, USA, measured lower C and N content in O-horizon and A-horizon soils subjected to a variable intensity wildfire in comparison to an unburned control (Baird et al., 1999). Similar sites in the on the Mission Creek National Fire and Fire Surrogate study area that had been repeatedly burned in low-intensity lightning-strike wildfires revealed no differences in C and N concentrations (nutrient capital was not measured) or other measures of soil properties (pH, cation exchange capacity, base saturation, hydrophobicity, and extractable phosphorus) compared to unburned control soils (Hatten et al., 2005). A comparison of these studies reiterates the importance of long-term space-for-time substitutions; immediate fire effects implied that the ecosystem would be greatly affected by a wildfire event, however, the longer-term study sites revealed no differences due to wildfire. Fire severity and alterations of historical fire regimes provide an added layer of uncertainty in wildfire studies where the majority of sites show little evidence of fire severity and a change in fire regime (e.g. from low-intensity and frequent to high-intensity and infrequent) may negate previously measured trends.

A suite of studies in temperate conifer and boreal forests provide a below-ground perspective of fire effects and collectively support the hypothesis that the occurrence of fire in historically fire-maintained ecosystems contributes to the long-term sustainability and resilience of forest ecosystem processes such as N cycling, C storage, and organic matter turnover (Cutler et al., 2016; DeLuca et al., 2006; DeLuca and Sala, 2006; Hart et al., 2005; MacKenzie et al., 2004; Zackrisson et al., 2004). The immediate effects of fire are dominated by the combustion of vegetation, organic matter, and heating of underlying mineral soil. Long-term effects of fire

resonate through the successive interactions between vegetation, soil, and organisms via fluctuations in temperature, moisture, nutrient pools, pH, and leachates (Certini, 2005; Certini, 2014; Knicker, 2007; Neary et al., 1999). Meanwhile, the post-fire soil biotic communities remain, recolonize, replace, or disappear compared to pre-fire soils (Hart et al., 2005). Fire temperature and duration provide a context to compare fire intensity in the soil environment, which typically only directly impacts the surface 5 – 10 cm of mineral during a low to moderate severity wildfire or prescribed fire (Mataix-Solera et al., 2013; Monsanto and Agee, 2008; Santín et al., 2013; Stoof et al., 2013). Generalizations of fire effects are inherently difficult due to the complexity of fuels, ignitions, and oxygen availability during a fire event and published studies provide a limited view of the full range of fire effects on soils.

Carbon accounting is an important aspect of quantifying the effects of wildfire and prescribed fire as constant additions of CO_2 and other C-rich greenhouse gasses into the atmosphere continue to alter the global C cycle. In individual studies of temperate and boreal ecosystems, researchers have reported forest O-horizon and mineral soils accounted for variable stocks of total C: 35% (116 Mg C ha^{-1}) of the total ecosystem C in a *P. ponderosa* (Law et al., 2001), 25% (193 Mg C ha^{-1}) in old-growth Pacific Northwest forests (Homann et al., 2005), and 60% (109 Mg C ha^{-1}) in boreal forest soils (DeLuca and Boisvenue, 2012). In a mixed-severity fire regime, a high-severity fire event resulted in a loss of 23 Mg C ha^{-1} of organic and mineral soils, most of which resulted from mineral soil C loss to total 60% mineral soil C loss and 100% of organic soil loss (Bormann et al., 2008). Moderate to low-severity fire effects resulted in an average loss of 10 Mg C ha^{-1} in soils after accounting for mineral soil loss by convective heat during the fire event (Homann et al., 2011). Additional losses of C via erosion and mineralization are common

after the wildfire events (Neary et al., 2005). The combustion and pyrolysis of organic matter in surface and subsurface soils also contributes to the recalcitrant, black C pool of C in fire-affected soils (Buma et al., 2014; Liang et al., 2008b; Pingree et al., 2012; Santín et al., 2015).

Nitrogen availability in forest soils is likely the most limiting factor in forest productivity and regeneration in secondary succession forests (Vitousek and Howarth, 1991). It is required for the synthesis of a variety of compounds including amino acids, proteins, nucleic acids, and chlorophyll in plant foliage. In soils, N is found to exist as amines, proteins, nucleic acids, and more stable humic compounds (e.g. humic and fulvic acids). Nitrogen compounds in organic and mineral soils typically experience a similar fate as C with combustion of organic matter. Post-fire measurements of soil N report a loss of 57% (690 kg N ha^{-1}) from mineral soils under high-intensity fire and less than 300 kg N ha^{-1} in moderate to low-severity conditions (Bormann et al., 2008; Homann et al., 2011). However, fire disturbances also provide a catalyst for N turnover in forest ecosystems. Post-fire soils exhibit an increase mineralizable N and inorganic N that can last up to three years (as extractable NH_4^+-N and NO_3^--N) (Choromanska and DeLuca, 2001; DeLuca et al., 2006; Gundale and DeLuca, 2007; MacKenzie and DeLuca, 2006). As measured by *in situ* soil methods, the effect of fire can last for 10 – 20 years as increased mineralizable N and resin-extractable N (DeLuca and Sala, 2006; MacKenzie and DeLuca, 2006).

Chronosequence studies in boreal forests provide evidence that wildfires stimulate N cycling (DeLuca et al., 2002), reconfigure soil-microbial and soil-plant nutrient cycles (Cutler et al., 2016; Hyodo et al., 2013; Zackrisson et al., 2004), increase total biomass C (Wardle et al., 2003), redistribute spatial patterns of biotic activity (Das Gupta and Mackenzie, 2016; Lavoie and

Mack, 2012), and produce a secondary functional component: charcoal (Zackrisson et al., 1996). Nitrification and N mineralization rates were highest immediately after wildfires, as measured by ionic resin capsules: N mineralization rates decreased from 20 μg NO_3^--N + NH_4^+-N $capsule^{-1}$ to 4 μg NO_3^--N + NH_4^+-N $capsule^{-1}$ $month^{-1}$ while nitrification decreased from 6 μg NO_3^--N $capsule^{-1}$ $month^{-1}$ to 0.5 μg NO_3^--N $capsule^{-1}$ $month^{-1}$ after 300 years since the last fire (time since fire [TSF]) (DeLuca et al., 2002). In a laboratory and field N mineralization experiment Lavoie and Mack (2012) found similar trends for an interior Alaska boreal fire chronosequence that spanned 79 years where rates were highest in the early-succession stand (8 years TSF), though not always significantly. Resin capsules accumulated an average of 3,900 μg N g $resin^{-1}$ in the 8 years TSF sites, which decreased to 3,050 μg N g $resin^{-1}$ after 87 years TSF. In situ nitrification also decreased significantly along the fire chronosequence from 50 μg N g $resin^{-1}$ to a non-detectable level. Interestingly, laboratory measures of N mineralization and extractable inorganic N (NO_3^--N + NH_4^+-N) were significantly higher (ten fold and 2 fold, respectively) in the mid-succession 20 year TSF site compared to the 8 and 87 TSF sites. This inconsistency suggests a high N demand for plants and microbes that is altered when uptake and leaching pathways are removed in the enclosed laboratory environment (Hart et al., 1994). Mineralization rates should also be considered an index, rather than absolute value, due to the unknown soil mass or soil solution volume in contact with resin capsules.

In terms of C stocks along measured fire chronosequences, boreal forests have been shown to accumulate C in O-horizon soils with TSF. As reported by Lavoie and Mack (2012), the percent C in surface (0-15 cm) mineral soils increased significantly from 6.99% to 11.3% in conjunction with a significant increase in O-horizon depth (1.6 to 7.8 cm). Over a much longer fire

chronosequence, boreal islands that experienced fire more frequently due to the larger size of the island accumulated 6.4 to 27.3 kg C m^{-2} in O-horizon soils, corresponding to 585 to 3,250 years TSF, respectively (Wardle et al., 2003). While soils accumulated C in the O-horizon over the TSF gradient, aboveground total biomass C decreased as did vegetation C productivity. These findings show that O-horizon soil C is lost via combustion or decomposition stimulated by the fire event while these ecosystems also decline in aboveground productivity with TSF – an ecosystem C balance influenced by fire frequency (Wardle et al., 2003).

In frequent-fire temperate conifer forests of Montana, USA, the reoccurrence of wildfires in fire-adapted forests rejuvenates the forest floor decomposition quality (MacKenzie et al., 2004) and maintains N availability over time (DeLuca and Sala, 2006), which is in part mediated by the presence of charcoal in the O-horizon (DeLuca et al., 2006; MacKenzie and DeLuca, 2006). In this ecosystem, O-horizon depth and total C and N increased significantly (1.8 to 6.1 cm, 500 to 2,200 kg C ha^{-1}, 20 to 80 kg N ha^{-1}) along a 132-year fire chronosequence (MacKenzie et al., 2004). Phenolic compounds present in O-horizon soils also increased significantly with TSF, which the authors propose may have added to the recalcitrance of the late-succession forest floor as well as interfered with N mineralization pathways. After a short incubation period, ammonification and potentially mineralizable N increased over the TSF gradient while nitrification decreased; these trends reached an asymptote around the same time period in which fire was historically repeated (MacKenzie et al., 2004). A detailed investigation of labile C and N pools in soil solution available for plant and microbial uptake showed a decrease of labile organic N (ninhydrin-reactive N) and inorganic N (NO_3^--N + NH_4^+-N), but not labile C adsorbed onto resin capsules (MacKenzie and DeLuca, 2006). Frequently burned forests in this ecosystem

exhibited higher inorganic N in mineral soils, higher NO_3^--N adsorption on resin capsules, and elevated nitrification potential in laboratory assays, which was positively related to the addition of charcoal (DeLuca and Sala, 2006). Collectively, these studies support the close relationship between fire events and N cycling in dry, temperate conifer ecosystems.

1.3 Deposition and Function of Charcoal in Forest Soils

The quantification and characterization of fire-altered organic C (pyrogenic C [PyC]) has traditionally encompassed studies of paleobotany, geology, and archeology (Franklin, 1951; Guo and Bustin, 1998; Scott, 2000; Scott and Damblon, 2010; Taylor et al., 2009). Common traditional practices of slash and burn agriculture and incorporation of PyC into agricultural soils in many different cultures around the world (Wiedner and Glaser, 2015) has sparked research into the PyC presence and function in soils (Glaser et al., 1998; Glaser et al., 2001; Glaser et al., 2002; Sanford et al., 1985). Naturally occurring, wildfire-produced PyC in forest soils was seldom recognized or emphasized as a unique component of the forest floor and only a few studies existed prior to the 'terra preta' soil phenomena (Tryon, 1948; Wardle et al., 1998; Zackrisson et al., 1996). A dissertation published by Tryon (1948) provides a review of literature up to that time period, which describe improved fertility, an increase in carbon content, amelioration of toxins via adsorption, increase in microorganisms, and stimulation of N cycling.

Empirical measurements of PyC in surface and sub-surface forests, agriculture, grasslands, peat, shrublands, and urban soils reported by over 500 studies ranges from 0 – 60% of soil organic matter (Reisser et al., 2016). In the western US forests and as determined by a weak acid/peroxide digestion method, PyC accounts for 3 – 30% of mineral soil organic C (Bélanger

and Pinno, 2008; Buma et al., 2014; Kurth et al., 2006; MacKenzie et al., 2008; Pingree et al., 2012). No standard method exists to quantify PyC in soils (Hammes et al., 2007), therefore, the following section details a selection of studies that quantify PyC in western US forests that are comparable in assumptions and limitation.

Recently, Buma et al. (2014) reported PyC produced by a high-severity wildfire in an alpine forest zone of north central Colorado, USA. Total PyC produced by the wildfire accounted for 7,240 kg C ha^{-1} or 8.05% of total ecosystem C compared to 5,960 kg C ha^{-1} or 2.77% in unburned reference stands. This estimate includes PyC on standing live and dead boles, coarse woody debris (CWD) on the forest floor, and mineral soil and O-horizon soils. Total ecosystem C estimates encompass standing live and dead boles, living and dead coarse roots, CWD, forbs and graminoids, and mineral soil and O-horizon soils. The fine PyC fraction (< 2mm) separated from O-horizon soils in unburned reference stands, as no O-horizon existed in wildfire burned stands, was almost 5 times greater than the coarse fraction (> 2mm) or 1,290 kg C ha^{-1} and 270 kg C ha^{-1}, respectively. Lastly, PyC material in mineral soils of wildfire stands averaged 38.6% C, slightly lower than previously reported values (Baldock and Smernik, 2002; Forbes et al., 2006; Gundale and DeLuca, 2006b; Pingree, 2011), and may suggest limited pyrolysis conditions during the high-intensity wildfire.

Mineral and O-horizon soil analysis of unburned and wildfire-burned forests of the Siskiyou Long-Term Ecosystem Productivity experiment reported by Pingree et al. (2012) remains one of the few direct quantifications of PyC produced by a single wildfire event (Clark et al., 1998; Santín et al., 2015). O-horizon soils measured one year after the wildfire increased in PyC from

35 kg C ha^{-1} (pre-fire) to 311 kg C ha^{-1}. This represents 3.2% of coarse (> 10 cm diameter) and fine (1-10 cm diameter) fuels consumed during the fire event. Total surface fuels in post-wildfire stands, which include thinned, prescribed burn, and control treatments with no harvest or prescribed fire, averaged 7,180 kg C ha^{-1} (Raymond and Peterson 2005). The PyC produced from the wildfire event, including all treatments, represented 4% of total soil and surface fuel C if PyC is assumed to be 50% C, an average value reported by Pingree (2011) as determined by the peroxide-nitric acid digestion method. This value does not incorporate living and dead biomass C or PyC of standing boles, which represents a potential long-term input of PyC into soil as bark sloughs onto the forest floor and standing snags fall to the ground (Makoto et al., 2012).

A study in northern Idaho and western Montana quantified charcoal along a fire chronosequence where multiple fires from 1870 to 1992 shaped aboveground and belowground forest dynamics (DeLuca and Sala, 2006). Charcoal, or PyC, separated from the O-horizon yielded an average of 1000 kg charcoal ha^{-1} with the lowest values reported for sites burned once and highest values at sites burned multiple times (Brimmer, 2006). Interestingly, the fire frequency and charcoal mass relationship seems to suggest variable charcoal production, charcoal consumption by subsequent fires, or alterations in charcoal recalcitrance. Charcoal deposited by wildfires, though recalcitrant in nature, does not escape decomposition and oxidation (Ascough et al., 2011; Cheng et al., 2008; Singh et al., 2012). Mineral soils in these stands averaged 9,390 charcoal C kg^{-1} (Kurth et al., 2006). Collectively, these PyC values represent about 14% of total C in a *Pinus ponderosa/ Pseudotsuga menziesii* ecosystem (DeLuca and Aplet, 2008).

This high-C and low-N fire residue exhibits a number of physical and chemical properties that may alter soil nutrient cycling in acidic forest soils, such as providing micro- and macro-pores (Chia et al., 2015), stimulating net and gross nitrification (Berglund et al., 2004; DeLuca et al., 2006; DeLuca et al., 2002) and altering soil solution chemistry by adsorption of organic compounds (Cornelissen and Gustafsson, 2004; Hale et al., 2015; Keech et al., 2005; Pingree et al., 2016). Dissolved organic matter incorporated in forest soils from O-horizon DOC leachate and O-horizon leachate represents a significant source of C, N, and P, as well as organic compounds with the potential to alter soil solution chemistry and nutrient cycling (Kalbitz and Kaiser, 2008; Michalzik et al., 2001; Qualls and Haines, 1991). This solution is most likely to be in contact with PyC deposited on the forest floor during a fire event. Given the numerous properties that PyC displayed in forest soils, this material provides an essential catalyst for nutrient cycling recovery in wildfire affected soils where organic matter inputs are low and surface soil bacterial and fungal activity is reduced (Hart et al., 2005).

The adsorption capacity of charcoal particles may have a significant effect on N cycling in post-fire forest soils. Previous studies of temperate and boreal forest soils have shown an increase in net nitrification with the addition of charcoal through the production of nitrate (NO_3^--N), which otherwise show minimal net nitrification (Ball et al., 2010; DeLuca et al., 2006; DeLuca et al., 2002; Kurth et al., 2014; MacKenzie and DeLuca, 2006). There are multiple pathways to result in an increase in NO_3^--N after the addition of charcoal. Charcoal may release nitrifier activity by adsorption of allelopathic C compounds or immobilization of NH_4^+, which results in a total reduction of nitrification potential (Paavolainen et al., 1998; Uusitalo et al., 2008). Also, the presence of heterocyclic C compounds, in the form of terpenes, may provide a source of organic

C and immobilize NH_4^+ (Bremner and McCarty, 1988). Mineralization of organic N by heterotrophic bacteria or fungi results in the production of NH_4^+ and soluble organic N while autotrophic bacteria oxidize NH_4^+ into NO_3^- (Paul, 2007). The nitrification process occurs first through the oxidation of ammonia (NH_3) to nitrite (NO_2^-) by obligate aerobes and is mediated by the ammonia mono-oxygenase enzyme, which can also oxidize non-polar compounds such as phenol and methane. Nitrite is then oxidized via the reversible oxidoreductase enzyme to NO_3^-. The presence of charcoal may also reduce the complexation of high molecular weight compounds, such as tannins, and indirectly alter the N and C cycles of soils via the adsorption of allelopathic organic carbon compounds (Gundale et al., 2010; Kraus et al., 2003).

Charcoal physical structure contains local graphite-like layers, aromatic-aliphatic C compound from residual volatiles and ash, and various sized pores and cracks – attributes that create microsites for pore space, water, nutrients, and metals (Kleber et al., 2015). Recent literature has explored mycorrhizal network interactions that expand the zone in which plant roots interact with allelopathic chemicals in soil solution (Barto et al., 2011). The presence of charcoal may also serve an important role in bioactive zones via adsorption of allelopathic compounds and interactions with fungal hyphae (DeLuca et al., 2002; DeLuca and Sala, 2006; Jones et al., 2011; Pietikäinen et al., 2000). The ‘charosphere’ describes the soil immediately surrounding a PyC particle that is directly influenced by the physical and chemical attributes of the particle and most likely to affect plant-microbe-soil interactions (Quilliam et al., 2013). Charcoal particles have been proposed as creating a novel substrate for microbial growth and as physical habitat for microbes (Pietikäinen et al., 2000; Quilliam et al., 2013; Thies et al., 2015), which may aid in the recovery of surface soils exposed to wildfires or intense prescribed fires.

Chapter 2. ADSORPTION CAPACITY OF WILDFIRE-PRODUCED CHARCOAL FROM PACIFIC NORTHWEST FORESTS

2.1 INTRODUCTION

Naturally ignited wildfires are a major driver of forest ecosystem disturbance that are reported in the paleoecological record as fossilized charcoal and pollen since the Devonian era (Glasspool et al., 2006; Scott, 2000). Forest fires are responsible for tree mortality, combustion of organic matter horizon (OM) on the forest floor, loss of mineral soil where high intensity convection and erosion transport particles, and stimulation of nutrient transformations (Agee, 1993; Bormann et al., 2008; DeLuca and Sala, 2006). Charcoal, a byproduct of incomplete combustion of OM and woody debris, is one of the few lasting legacies of wildfires (DeLuca and Aplet, 2008; Preston and Schmidt, 2006). This high-carbon (C) and low-nitrogen (N) residue exhibits a number of physical and chemical properties that may alter soil nutrient cycling in acidic forest soils, such as providing micro- and macro-pores (Braida et al., 2003; Jaafar et al., 2015; Wildman and Derbyshire, 1991), stimulating net and gross nitrification (DeLuca et al., 2006; DeLuca et al., 2002; Gundale and DeLuca, 2006a) and altering soil solution chemistry via adsorption of organic compounds (Cornelissen et al., 2004; Gundale and DeLuca, 2007; Keech et al., 2005). Dissolved OM incorporated in forest soils from O-horizon DOC leachate represents a significant source of C, N, and phosphorus, as well as organic compounds with the potential to alter soil solution chemistry and nutrient cycling (Kalbitz and Kaiser, 2008; Qualls and Haines, 1991). Charcoal can provide a functional and active component of nutrient cycling in wildfire-affected systems (DeLuca and Sala, 2006; MacKenzie and DeLuca, 2006) where OM inputs are low and surface-horizon bacterial and fungal activity is reduced (Dooley and Treseder, 2012; Hart et al., 2005).

The ability for charcoal particles, as well as other pyrogenic C molecules such as biochar and activated carbon, to adsorb non-polar, organic molecules is a fundamental mechanism that may alter soil solution chemistry (Bormann et al., 2008; Brimmer, 2006; Cornelissen et al., 2004; Keech et al., 2005; Zackrisson et al., 1996) and nutrient cycling of forest soils (Berglund et al., 2004; DeLuca et al., 2006). Wildfire-produced charcoal contains aromatic C rings, aliphatic C structures from residual volatiles and ash, and various sized pores and cracks – the fractions of these attributes dictate physical structure and chemical composition (Gundale and DeLuca, 2006b; Preston and Schmidt, 2006; Zackrisson et al., 1996). Charcoal is a less graphitic, amorphous constituent of the BC continuum model, which describes physical and chemical attributes of pyrogenic C materials along a temperature gradient (Hedges et al., 2000).

Although many environmental conditions alter the physical and chemical characteristics of charcoal during the thermal degradation process, such as heating ramp and the presence of water, the oxidation temperature provides the greatest source of variation in residual charcoal particles (Gundale and DeLuca, 2006b; Lua et al., 2004; Manyà, 2012). Wildfire temperatures are spatially and temporally variable, which would theoretically result in a similarly large range in the surface area and adsorption capacity of charcoal deposited during fire events; however, there are few studies of wildfire-induced physical and chemical variability on adsorption behavior or capacity (Brimmer, 2006; Gundale and DeLuca, 2006b; Zackrisson et al., 1996). Surface soil wildfire temperatures in temperate forests typically range between 400 °C and 600 °C although conditions directly under smoldering coarse woody debris can exceed 700 °C (Bormann et al., 2008; Monsanto and Agee, 2008; Neary et al., 2005). The adsorption capacity of charcoal

increases asymptotically with formation temperature as graphite-like layers of aromatic double- and single-bonded covalent C molecules condense, which increases surface area and hydrophobic interactions (Cornelissen et al., 2004; Keiluweit and Kleber, 2009). An investigation of charcoal physical characteristics generated from *Eucalyptus camadulensis* reported an increased in surface area from 6 $m^2 \cdot g^{-1}$ to 490 $m^2 \cdot g^{-1}$ and an increase in adsorption using benzene as a sorbate from 10 $mg \cdot g^{-1}$ to 150 $mg \cdot g^{-1}$ in charcoal generated at 250 °C and 850 °C, respectively (Bornemann et al., 2007). Pore size distribution also increased from 17% microporosity (pores < 2nm) in the 450 °C charcoal to >90% in the 850 °C charcoal (Bornemann et al., 2007).

Charcoal formed during wildfire events is known to adsorb organic compounds present in soil solution and O-horizon DOC leachate, but there is only limited understanding of the longevity and capacity of wildfire-produced charcoal to alter the surrounding soil environment. Over time, charcoal surfaces undergo oxidation – this reduces binding sites and the adsorption capacity of charcoal particles produced by the initial formation conditions (Cheng and Lehmann, 2009; Cheng et al., 2006; Zackrisson et al., 1996). Zackrisson and others (1996) found that the ability of wildfire-produced charcoal to adsorb phenolic compounds decreased with time since fire (TSF) over a 350-year chronosequence in Swedish boreal forests. Adsorption capacity was measured by seed germination bioassay in aqueous *Empetrum hermaphroditum* leaf extracts and attributed to an allelopathic effect in seedling germination (Zackrisson et al., 1996). Charcoal that had reduced ability to adsorb organic compounds could be reactivated by heating the charcoal at 400°C –750 °C, suggesting that charcoal might regain the adsorptive capacity during subsequent fire events (Zackrisson et al., 1996). A subsequent study by Keech et al. (2005)

established low adsorption capacity by bioassay of charcoal produced by boreal gymnosperm species (< 40%) and found no correlation between the transversal porosity and adsorption capacity.

In a separate study of charcoal adsorption capacity using catechin as a sorbate, a common allelopathic compound found in *Centaurea maculosa*, maximum adsorption increased from 1,000 μg $\cdot g^{-1}$ to 4,500 μg$\cdot g^{-1}$ when combustion temperature of *Pinus ponderosa* charcoal increased from 300 °C and 750 °C, respectively (Brimmer, 2006). Weathering of charcoal surfaces is evidenced by an increase in oxygen (O) content present in hydroxyl and carboxyl functional groups, a decrease in C content (Cheng et al., 2008), and a decrease in adsorption capacity (Zackrisson et al., 1996). Current models of wildfire-produced charcoal adsorption as a functioning component of forest ecosystems exist for boreal (Zackrisson et al., 1996) and dry *P. ponderosa/Pseudotsuga menziesii* ecosystems (Brimmer, 2006; DeLuca et al., 2006) and affirm the trend of decreased adsorption capacity over time.

The purpose of the work reported was to determine differences in adsorption capacity of wildfire-produced charcoal as influenced by TSF using a fire chronosequence approach in the eastern rain shadow forests of the Olympic Peninsula, in western Washington, USA. These forests represent a unique, mixed-severity fire regime class in the midst of a highly productive landscape where spatial heterogeneity of fire severity may have significant implications for below and aboveground post-fire recovery (Franklin and Dyrness, 1973). Non stand-replacing fires alter succession trajectories, forest composition, tree diameter, and are considered within the natural historical variability of these ecosystems (Perry et al., 2011; Tepley et al., 2013;

Weisberg, 2004; Wendel and Zabowski, 2010; Wetzel and Fonda, 2000). The Olympic Peninsula is predicted to increase in annual temperature (+0.6–1.9 ºC by the 2020's) and summer potential evapotranspiration (5–18 mm by the 2040's) with climate change – conditions that will likely result in higher fire frequency and size (Halofsky et al., 2011b). The *Tsuga heterophylla* forest zone of the rain shadow region on the Olympic Peninsula experiences fire every 90–150 years and is characterized by a mixed-severity fire regime that experiences 20–70% mortality during a fire event (Agee, 1993; Franklin and Dyrness, 1973; Halofsky et al., 2011a; Weisberg, 2004).

The purpose of the following studies was to assess the *adsorption capacity* of charcoal generated during historical fire events to determine whether adsorption capacity would decrease with time since fire. The effects of formation temperature and oxidation by weathering and adsorption are discernible by advanced analytical techniques yet have an indiscernible interactive effect on adsorption capacity of wildfire-produced charcoal. Therefore, we utilized thermogravimetric analysis (TGA) to determine the mass of volatile organic C, which includes strongly adsorbed organic C theoretically acquired over time, and the mass of thermally stable C, or BC structure produced during the pyrolysis and combustion of charcoal samples. This method quantifies the mass of a sample lost during a thermal ramp under an inert atmosphere followed by combustion and has been used to characterize the chemical composition of OM fractions (Dell'Abate et al., 2003; Plante et al., 2005), differentiate between labile and recalcitrant OM (Lopez-Capel et al., 2005), and quantify charcoal in soils (De la Rosa et al., 2008; Leifeld, 2007; Nguyen et al., 2004).

We hypothesized that (1) the adsorption capacity for phenol in field-collected charcoal will decline with TSF; (2) the adsorption capacity for phenol and the proportion of thermally stable BC in laboratory charcoal will increase with increasing temperature in *P. menziesii* charcoal and provide a frame of reference for the adsorption capacity of field-collected charcoal; and (3) the medium volatile, adsorbed C mass of field-collected charcoal, as measured by TGA, will be negatively correlated to adsorption capacity as this thermal region includes strongly adsorbed organic compounds on charcoal surfaces, which we expect to increase with TSF.

2.2 METHODS

2.2.1 *Field Sites*

Wildfire-produced charcoal was collected in the autumn of 2013 and summer of 2014 from the forest floor at nine fire chronosequence sites in the eastern Olympic Peninsula, Washington, USA. The sites, a 250 m^2 area, were selected in forest stands exposed to historic wildfires ($1898_{a,b}$, 1922), intermediate wildfires (1977, $1985_{a,b}$), and recent wildfires (2006, 2009, 2011) (n = 3, a and b are sites within the same fire perimeter separated by at least 1000 m distance) (Table 2.1). Sites were selected in the field from pre-designated areas within the North Pacific maritime dry mesic *P. menziesii T. heterophylla* potential vegetation zone, between 400 and 600 meters in elevation, and on slopes of less than 20% to avoid erosion effects using ArcGIS maps for reference (Kagan, 2010; USGS, 2009). Where applicable, fire perimeter maps were incorporated to establish the sites within the burned area of BF1, BF2, BG, CF, BH sites only (MTBS, 2013). Sites in the Elwha River Valley (IC, KT, MC, RC) were located with the guidance of fire maps published by Wendel (2009).

Soils of the northern and eastern Olympic peninsula are formed on marine deposits of basalt, colluvium, volcanic ash, and glacial till (Henderson et al., 1989; NCRS, 2014). Although there is no formal soil survey of the majority of the study sites, proximate areas are classified by the US Soil Taxonomy classification as skeletal Typic Haploxerepts (NCRS, 2014), which fits closely with our field observations at all sites. Sites were described by a census of visually estimated understory vegetation species and cover and overstory tree species and diameter (at 130 cm or diameter at breast height [DBH[) within the 250 m^2 area. Overstory composition at the chronosequence sites was dominated by *P. menziesii* and *T. heterophylla* with a minimal abundance of *Thuja plicata* and *Alnus Rubra* (5% at site RC only) (Table 2.1). Understory composition was predominantly composed of *Gaultheria shallon*, *Mahonia nervosa*, *Polystichum munitum* in historic and intermediate fire sites and *Chamerion angustifolium* at recent fire sites. Mean annual temperature from 1980–2010 averaged 8.1 ± 0.5 °C and mean annual precipitation was 2,181 ± 592 mm across all sites (Wang et al., 2012).

The feedstock for generating laboratory charcoal was collected at recreation sites along the I-90 corridor of the western slope of the Cascade Mountains, Snoqualmie Pass, Washington, USA, in the spring of 2014. Branches were collected in ecosystems similar to the chronosequence field sites where *P. menziesii* dominated the overstory species composition, which had not yet been established.

Table 2.1: Fire chronosequence site attributes for study sites on the Olympic Peninsula, Washington. Sites are dated from establishment and organic matter collection (IC, KT, MC, RC in 2013 and remaining sites in 2014). Number of fires since 1568 was determined by Wendel (2009) for sites IC, KT, MC, RC, and with fire history maps provided by the USDA Forest Service for remaining sites. Basal area is calculated with only live standing trees > 9 cm in diameter. Saplings qualify as trees taller than 130 cm and < 9 cm in diameter.

Fire History	**Site**	**Time since fire (years)**	**Number of fires since 1568**	**Basal area (m^2 ha^{-1})**	**% Basal area of *P. menziesii***	**% Basal area of *T. heterophylla***	**% Basal area of *T. plicata***	**Saplings ha^{-1}**
Historic	Idaho Creek (IC)	115	4	65	29	68	<1	1200
	Krause Top (KT)	115	5	71	100	0	0	80
	Michael's Cabin (MC)	86	7	85	100	0	0	80
Interm-ediate	Rica Canyon (RC)	36	6	38	83	0	4	6720
	Beaver Fire 1 (BF1)	29	2	97	87	1	11	7120
	Beaver Fire 2 (BF2)	29	2	82	97	<1	11	2720
Recent	Bear Gulch II (BG)	8	4	100	89	0	<1	0
	Constance Fire (CF)	5	2	51	100	0	0	0
	Big Hump (BH)	3	2	21	76	24	10	0

2.2.2 *Laboratory and Field-Collected Charcoal*

At the chronosequence field sites, we installed a contiguous grid of ten 5 m^2 plots where we randomly collected three composite OM samples (five composites at BG plot 4 due to sparse OM cover) with a 5 cm diameter ring to the entire depth of the OM, which was recorded as an average of the three or five depths (Table 2.2). The OM sample included all layers of the O horizon (L, F, H) down to the mineral soil, which was then homogenized and analyzed as a single organic layer. Charcoal was identified in the OM samples by visual observation on white paper under supplemental light and separated by hand (Table 2.2).

Table 2.2: Organic horizon soil and charcoal characteristics for the Olympic Peninsula fire chronosequence sites. Depth of organic horizon (OM) is an average of three composite samples and chemical composition is an average of ten samples. Charcoal mass was quantified from ten replicate plots. Charcoal elemental composition is an average of 9 individual samples. Standard error is given in parenthesis.

	Organic Horizon Soil Characteristics					Charcoal Composition		
Site	OM depth (cm)	Total C ($mg \cdot g^{-1}$)	Total N ($mg \cdot g^{-1}$)	Charcoal mass ($kg \cdot ha^{-1}$)	Phenol content ($mg \cdot kg^{-1}$)	Total C ($mg \cdot g^{-1}$)	Total N ($mg \cdot g^{-1}$)	Total H ($mg \cdot g^{-1}$)
IC	3.2	332.63 (18.78)	7.56 (0.45)	406 (160)	48.92 (14.27)	512.65 (15.46)	4.91 (0.40)	37.08 (1.22)
KT	4.0	364.46 (16.74)	9.72 (0.55)	139 (49)	28.72 (5.46)	570.53 (25.67)	3.82 (0.29)	38.86 (1.17)
MC	2.5	318.15 (15.32)	7.90 (0.39)	105 (59)	42.71 (9.79)	504.84 (7.34)	5.26 (0.37)	42.66 (1.03)
RC	4.2	373.69 (21.51)	10.43 (0.67)	129 (63)	66.31 (11.32)	546.05 (9.26)	4.66 (0.27)	40.18 (2.98)
BF1	2.8	335.89 (26.27)	7.12 (0.65)	535 (127)	23.39 (3.02)	628.23 (17.79)	4.43 (0.26)	29.90 (1.88)
BF2	2.3	321.14 (23.97)	5.00 (0.41)	380 (93)	26.02 (2.71)	582.77 (10.42)	4.46 (0.36)	39.41 (0.82)
BG	3.3	196.66 (18.33)	5.72 (0.56)	1,063 (212)	5.74 (1.47)	583.79 (9.88)	6.44 (0.32)	29.88 (0.51)
CF	2.2	321.00 (25.14)	11.23 (0.96)	610 (135)	16.13 (3.16)	572.48 (17.12)	9.76 (0.36)	26.44 (0.59)
BH	2.5	229.52 (14.91)	6.83 (0.42)	1,180 (251)	5.85 (1.36)	579.95 (17.75)	7.39 (0.56)	30.07 (0.33)

Laboratory charcoal samples were created from 3 cm^3 sections of live *P. menziesii* branches dried for 48 hours at 60 °C. Samples were buried in pure silica sand, in lidded crucibles to reduce O_2 availability, and heated in a muffle oven (Thermo Fisher Scientific 1100 °C box furnace BF 51800 Series) at 300 °C, 500 °C, and 800 °C. The temperature gradient encompassed the probable range of wildfire temperatures in this ecosystem (Bormann et al., 2008; Monsanto and Agee, 2008; Neary et al., 2005; Santín et al., 2016). The muffle oven was programmed to reach the target temperature at 30 minutes, heated at the target temperature for 2 hours, and decreased to 30 °C over a 2 hour period with the high-temperature alarm set at 10 °C above the target temperature. Charcoal samples were heated for 2 hours in order to ensure complete pyrolysis and combustion of the precursor wood material. Individual charcoal samples (3cm^3 segments) were ground to a fine powder with a mortar and pestle to pass a 0.2 mm sieve.

2.2.3 *Batch Sorption of Charcoal*

Batch adsorption experiments were conducted for laboratory charcoal and field-collected charcoal in 50 mL KIMAX glass centrifuge vials with Teflon-lined lids (Kimax Glass Inc. USA). Approximately 32.0 ± 0.2 mg of pulverized, homogenized charcoal was weighted into glass centrifuge tubes, and allowed to hydrate in 20 mL of distilled H_2O for a 24 hour period (Bornemann et al., 2007; Zhu et al., 2005; Zhu and Pignatello, 2005). Phenolic compounds, condensed and hydrolyzable tannins, are prevalent in forest ecosystems and known to affect substrate quality, decomposition rates, nutrient cycling (Dąbrowski et al., 2005; Hättenschwiler and Vitousek, 2000), and have been shown to increase with TSF in *P. ponderosa* forests of western Montana (DeLuca et al., 2002; MacKenzie et al., 2004). We chose simple phenol for the

adsorption experiment in order to measure the behavior of phenol in the presence of charcoal to provide a baseline of adsorption capacity. The test adsorbate, phenol (Sigma-Aldrich, ACS reagent ≥ 99.0%), was added from 1000 μg·phenol mL^{-1} stock solution into three replicate glass vials containing the adsorbate (pulverized charcoal) and distilled water to produce 2, 5, 10, 20, 50, 100, 250, and 500 ppm batch solutions. The vials were placed on a shaker table for 24 hours and allowed to equilibrate at room temperature (20 °C). Batch adsorption experiment solutions were neutral to slightly acidic, but well below than the pKa of phenol (10) and likely to resemble the protonation of OM solution at the chronosequence sites. With the method described below, phenol content was also measured by $CaCl_2$ extraction in OM samples at each plot in the study sites (Table 2.2).

Both sorbent free and 0 μg·mL^{-1} controls were analyzed to account for any bottle losses or desorption during the experiment (Sander and Pignatello, 2005). Adsorbate was removed from suspension by vacuum filtration on a vacuum manifold with Whatman #42 filter paper. The initial and equilibrium concentrations of total phenol was determined by colorimetry (Multiskan FC Microplate Photometer, Thermo Scientific) using the Folin & Ciocalteau's reagent and read at 725 nm following Box (1983). The maximum adsorption capacity of field-collected charcoal was quantified by saturating charcoal adsorbate in a solution of 500 μg phenol·mL^{-1} and following the same procedure as laboratory charcoal described above. Previous studies had shown the adsorption of charcoal to be much lower than 500 μg·mL^{-1} (Bornemann et al., 2007); therefore, we expected to exceed saturation and measure the maximum adsorption capacity.

2.2.4 *Adsorption Isotherm Model*

The initial concentration of each isotherm was calculated from the charcoal-free 0 $\mu g \cdot mL^{-1}$ control samples. Phenol desorbed from field-collected and laboratory charcoal was subtracted from the equilibrium concentration $[Phenol]_{final}$.

The adsorbed amount of sorbate q ($\mu g \cdot mL^{-1}$) was calculated using the following equation:

$$q\ (\mu g\ phenol\ mg\ charcoal^{-1}) = \frac{([Phenol\ (\mu g\ mL^{-1})]_{initial} - [Phenol\ (\mu g\ mL^{-1})]_{final}) * volume\ of\ solution\ (mL)}{charcoal\ mass\ (mg)} \quad (1)$$

The Freundlich isotherm equation is given by $q = KC^n$, where K is the Freundlich empirical constant related to sorption capacity, C is equal to the equilibrium concentration of the sorbate, and n is the Freundlich exponential coefficient indicative of the intensity of adsorption. Data were linearized to fit to the Freundlich model and coefficients were calculated from the linear model.

The disassociation constant, K_d, measures the slope of a line that is represented by the dissociation of large to smaller individuals in the isotherm model at origin and is calculated by:

$$K_d = \left(\frac{C_i - C_f}{C_f}\right)\frac{V}{M} \quad (2)$$

where C_i and C_f are the initial and final sorbate concentrations, V is the volume, and M is the mass of sorbent. The Freundlich adsorption isotherm constants, K_f and n, for phenol were determined by extracting the coefficients of the linearized isotherm model (Langmuir, 1997).

2.2.5 *Thermogravimetric Analysis of Charcoal*

Thermogravimetric analysis was performed on a TGA Q50V20, build 39 (TA Instruments). Charcoal samples of 10–12 mg were weighed into alumina sample pans. Samples were heated under $N_{2\ (gas)}$ with a balance purge flow of 40 mL·min^{-1} and sample purge flow of 60 mL·min^{-1}. Starting at an initial temperature of 30 ±7 °C, the thermal ramp increased at 10 °C·min^{-1} to 1000 °C, followed by an isothermal purge with $O_{2\ (gas)}$ for 5 minutes. Thermal decomposition data were compiled using Universal Analysis software (TA Instruments) and treated as a combination of discrete regions within the mass loss range. The segments represent water loss (highly volatile: $T_{initial}$–200 °C), lignocellulose material and occluded volatile organic compounds (medium volatile: 200–750 °C), carbonization process (low volatile: 750–1000 °C), thermally stable BC (combustible: 1000 °C under O_2), and mineral component (ash content: stable at 1000 °C under O_2) (Earnest, 1988).

2.2.6 *Statistical Analysis*

Linear regression models were used to determine the relationship between temperature or TSF in charcoal samples to the proportion of mass loss by TGA. In laboratory charcoal samples, we incorporated the effect of individual precursor wood samples as an interaction term with temperature. Similarly, field-collected charcoal models included a plot effect as an interaction with TSF in order to account for the spatial variability within each site. Adsorption capacity of field-collected charcoal (q) did not meet the assumption of homoscedasticity, therefore, we used a one-way Kruskal-Wallis (KW) test to compare non-parametric variances. No more than one outlying replicate of the laboratory charcoal adsorption isotherm data were excluded from the final isotherm data if inclusion increased the coefficient of variation by 20%. At least two of the three replicate data points were used for final analysis of the adsorption isotherms. Pearson's

correlation test was used to compare the proportion of medium volatile mass loss from TGA with the maximum adsorption capacity of laboratory charcoal (q) as the independent variable. In order to provide a balanced comparison, we randomly thinned the adsorption observations and used the excluded data as a validation. All statistical analysis was conducted in the R Statistical Environment (R Core Team, 2015).

2.3 RESULTS

Field-collected charcoal from chronosequence sites on the Olympic Peninsula measured an average 29.70 (± 6.23) μg phenol·mg charcoal^{-1} adsorption capacity (q), which did not differ significantly between TSF sites ($p > 0.1$) (Figure 2.1). In comparison, the adsorption capacity (q) of laboratory charcoal created from *P. menziesii* wood increased with formation temperature from 61.2 (± 5.8) μg phenol·mg charcoal^{-1} (300 °C) to 75.2 (± 6.4) μg phenol·mg charcoal^{-1} (500 °C), and 174.8 (± 13.7) μg phenol·mg charcoal^{-1} (800 °C) (Figure 2.2). Laboratory charcoal produced at higher temperatures showed a greater affinity for phenol in batch solution experiments (Figure 2.2) and greater sorption strength of phenol (Table 2.3). Adsorption behavior of charcoal produced at 300 °C and 500 °C was indistinguishable after 250 μg phenol·mg charcoal^{-1} (C_i), whereas 800 °C laboratory charcoal reached a maximum adsorption capacity at ~ 600 μg phenol·mg charcoal^{-1} (C_i) (Figure 2.2). Similarly, the adsorption capacity increased most rapidly in 800 °C laboratory charcoal compared to that of 500 °C and 300 °C in the lower concentration range, which cover the range of phenol concentration expected in forest floor OM (Figure 2.3, Table 2.3). Experimental data from the batch adsorption experiments were fit to both Freundlich and Langmuir isotherm models. Freundlich isotherm model linearization for 300 °C, 500 °C, and 800 °C laboratory charcoals are shown in Figure 2.4. After the Langmuir

linearization by inversion, sorbate concentrations were close to zero, which indicates that the isotherm reduces to a Freundlich model (Langmuir, 1997).

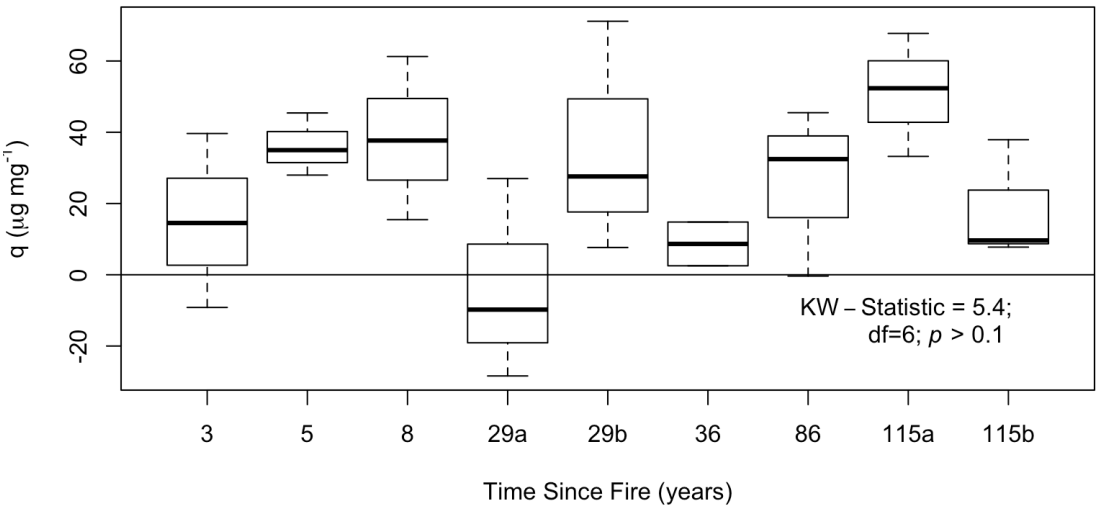

Figure 2.1: Adsorption of phenol by field-collected charcoal (q µg phenol·mg charcoal^{-1}) from a chronosequence of nine sites varying in time since fire on the Olympic Peninsula in western Washington. Boxplots of each plot show the median values (middle black line), the largest and smallest observations (vertical lines), and the 25th and 75th percentile (lower and upper bounds of boxes, respectively) (n = 3 except for year 36, where n = 2).

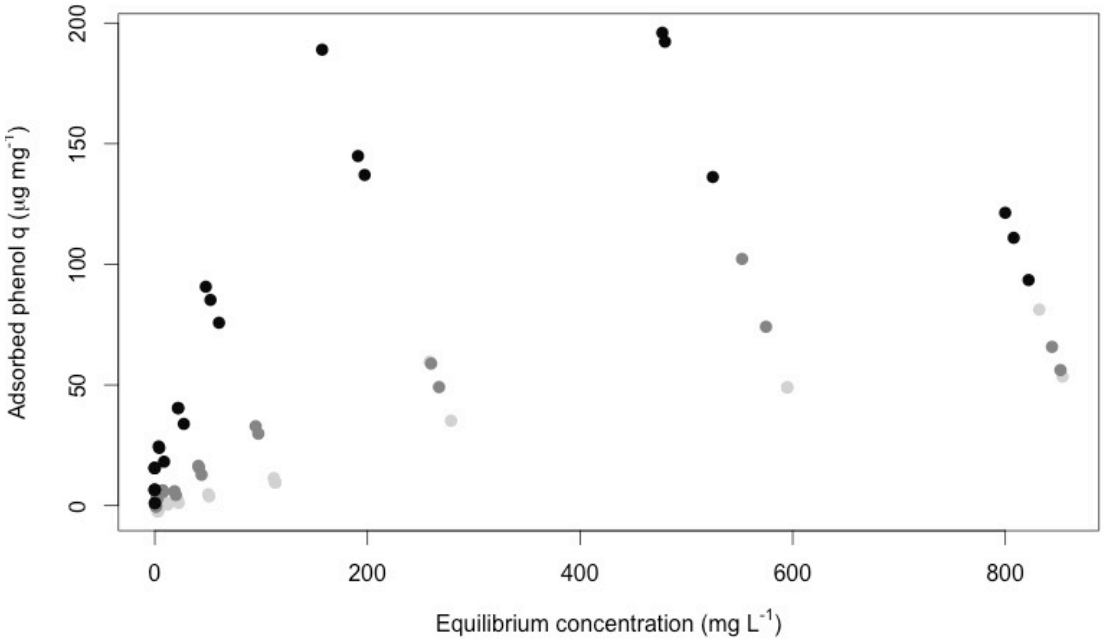

Figure 2.2: Experimental adsorption isotherms for laboratory charcoal generated from *Pseudotsuga menziesii* wood at 300 °C (in light grey), 500 °C (in dark grey), and 800 °C (in black) from 2 mg L^{-1} phenol to over 800 mg L^{-1} (n = 2 or 3).

Table 2.3: Isotherm coefficients (K_f) , sorption strength (n) , and elemental composition of laboratory charcoal samples (n = 3, standard error in brackets). K_d reported at 50 mL·mg charcoal^{-1} initial concentration. Model fit parameters are provided in Figure 2.4.

Formation Temperature	**K_f**	**n**	**Average sorption strength (K_d)**	**C g·kg^{-1}**	**H g·kg^{-1}**	**N g·kg^{-1}**	**Average H/C**
300 °C	1.72	0.88	0.08	625.02 (9.82)	40.74 (1.13)	2.99 (0.21)	0.065
500 °C	0.76	1.02	0.36	761.88 (3.26)	26.32 (0.39)	2.87 (0.04)	0.03
800 °C	0.24	1.18	1.64	822.11 (2.86)	6.51 (0.30)	4.39 (0.14)	0.008

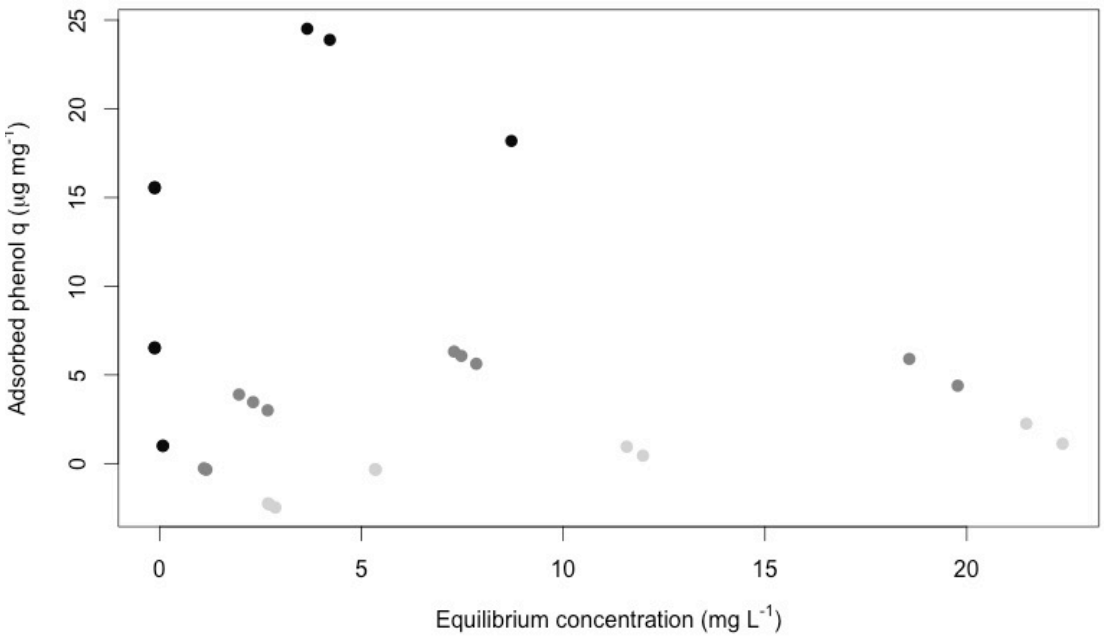

Figure 2.3: Experimental adsorption isotherms for laboratory charcoal generated from *Pseudotsuga menziesii* wood at 300 °C (in light grey), 500 °C (in dark grey), and 800 °C (in black) from 2 mg·L^{-1} phenol to 25 mg·L^{-1} (n = 2 or 3).

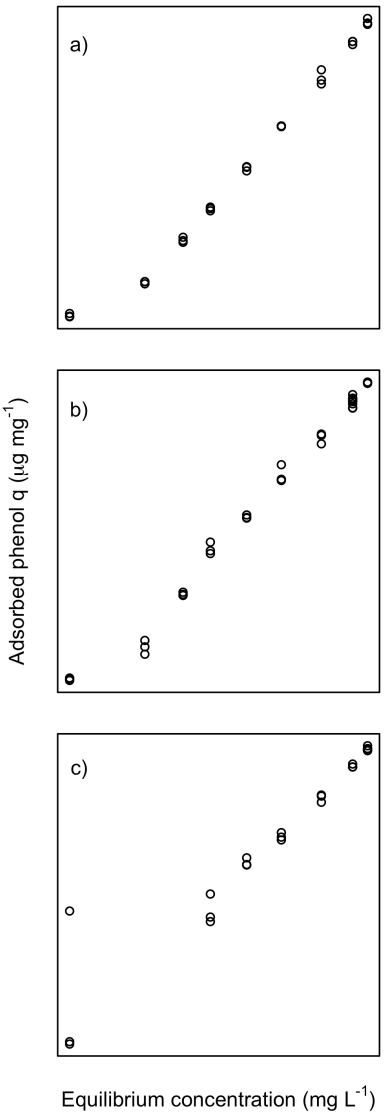

Figure 2.4: Freundlich linearization of laboratory charcoal, phenol adsorption isotherms. a) Charcoal produced at 300 °C ($r^2 = 0.98$), b) 500 °C ($r^2 = 0.99$), and c) 800 °C charcoal ($r^2 = 0.93$).

Thermogravimetric results for laboratory and field-collected charcoal are summarized in Figure 2.5 for each discrete thermal region with formation temperature and TSF, respectively. The low volatile mass loss (%) between 200 °C–750 °C represents native lignocellulosic material in laboratory charcoal as well as adsorbed organic compounds in field-collected charcoal. The log of mass loss in this region significantly decreases ($r^2 = 0.91$; $p < 0.001$) with increasing temperature in laboratory charcoal while the individual wood sample has a slightly significant interaction with temperature ($p < 0.05$), which suggests % mass loss in this thermal region is a strong indicator of formation temperature (Figure 2.5). Percent mass of field-collected charcoal samples in the medium volatile region increased slightly with TSF; however, the plot effect (location of charcoal within replicated plots at each site) had a greater contribution to the model than TSF alone, resulting in a significant and positive linear model as a whole ($r^2 = 0.72$; $p < 0.01$). The percent mass loss at 1000°C with oxidative combustion represents the BC structure of laboratory charcoal and increases with formation temperature ($r^2 = 0.82$; $p < 0.01$) without influence from the individual wood sample. The proportion of BC in charcoal samples collected along the fire chronosequence showed a significant negative relationship with TSF and plot effect resulting in a significant and negative linear model ($r^2 = 0.68$; $p < 0.01$).

Thermogravimetric analysis demonstrated a divergence between laboratory and field-collected charcoal in the regions of low volatile loss (750 °C–1000 °C) and residual ash remaining after combustion at 1000 °C (Figure 2.5). Low volatile loss released by heating of laboratory charcoal increased with increasing temperature, although individual wood sample and the interaction of these factors had a greater influence on the model ($r^2 = 0.83$; $p < 0.01$). Field-collected charcoal showed no significant trend with TSF that incorporated a minimally significant plot effect in the

overall model ($r^2 = 0.4$; $p > 0.5$). By contrast, residual ash showed no trend with temperature or individual wood sample ($r^2 = 0.5$; $p > 0.4$) but did significantly increase with TSF despite a significant plot effect ($r^2 = 0.95$; $p < 0.001$). Laboratory charcoal trends support the hypothesis that as adsorption capacity increases, the percent mass of C compounds in the medium volatile range decreases ($r^2 = 0.69$, $p < 0.05$); however, no correlation was observed for field-collected charcoal ($r^2 = 0.01$, $p > 0.5$) (Figure 2.6).

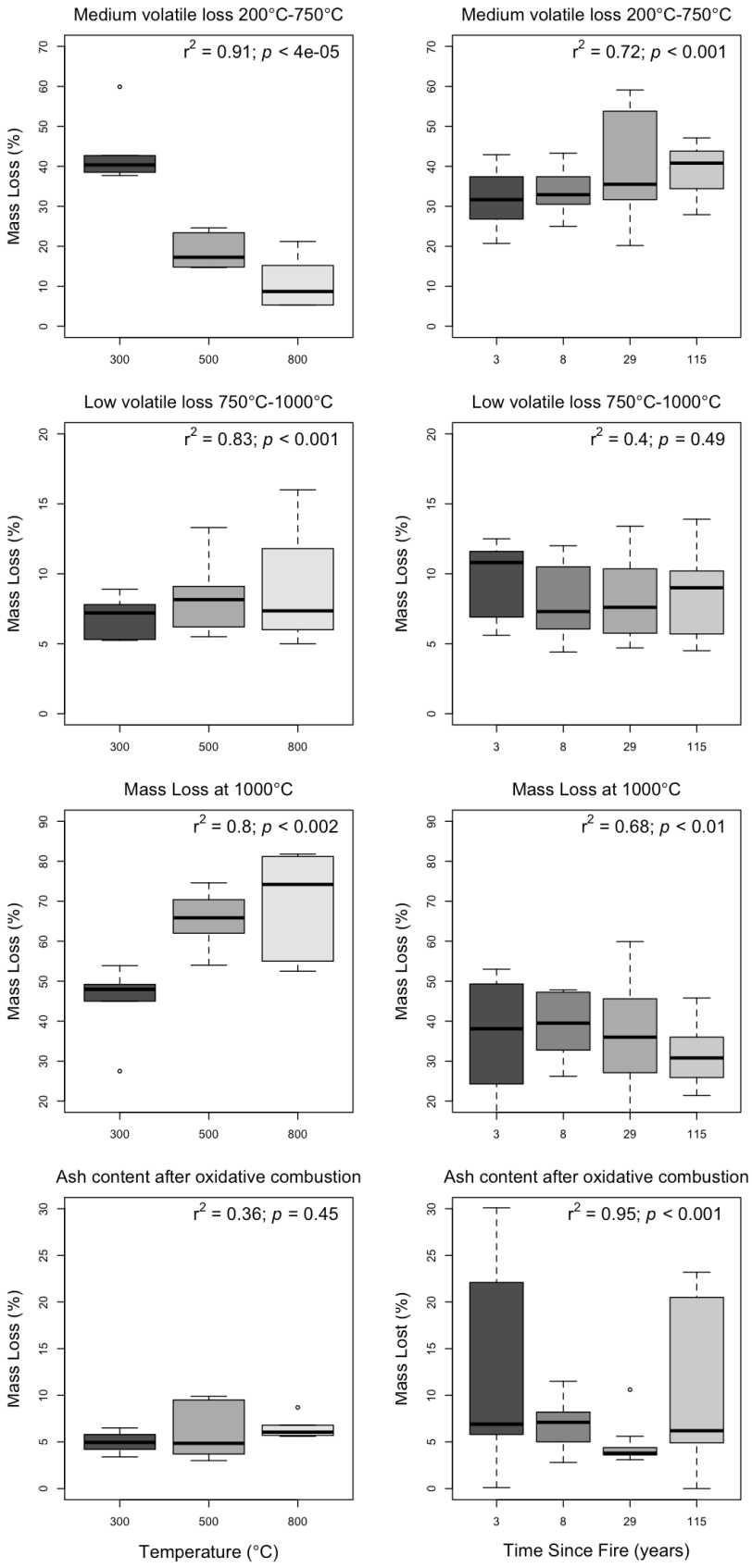
Medium volatile loss 200°C-750°C
r2 = 0.91; p < 4e-05
Mass Loss (%)
300
500
800
Medium volatile loss 200°C-750°C
r2 = 0.72; p < 0.001
3
8
29
115
Low volatile loss 750°C-1000°C
r2 = 0.83; p < 0.001
Low volatile loss 750°C-1000°C
r2 = 0.4; p = 0.49
Mass Loss at 1000°C
r2 = 0.8; p < 0.002
Mass Loss at 1000°C
r2 = 0.68; p < 0.01
Ash content after oxidative combustion
r2 = 0.36; p = 0.45
Ash content after oxidative combustion
r2 = 0.95; p < 0.001
Mass Lost (%)
Temperature (°C)
Time Since Fire (years)

Figure 2.5: Percent mass loss from T_i–1000 °C with N_2, at combustion with O_2, and ash residue after combustion for laboratory *Pseudotsuga menziesii* (left) and field-collected charcoal (right) from nine sites varying in time since fire on the Olympic Peninsula in western Washington. Linear models incorporate temperature and variation of individual charcoal samples (x-axis represents temperature of laboratory-charcoal combustion). Field-collected charcoal linear models incorporate time since fire in years and the plot effect (x-axis represents TSF in years). Model fit parameters for laboratory charcoal medium volatile and ash content are for logarithmic models, but displayed as linear for visual ease.

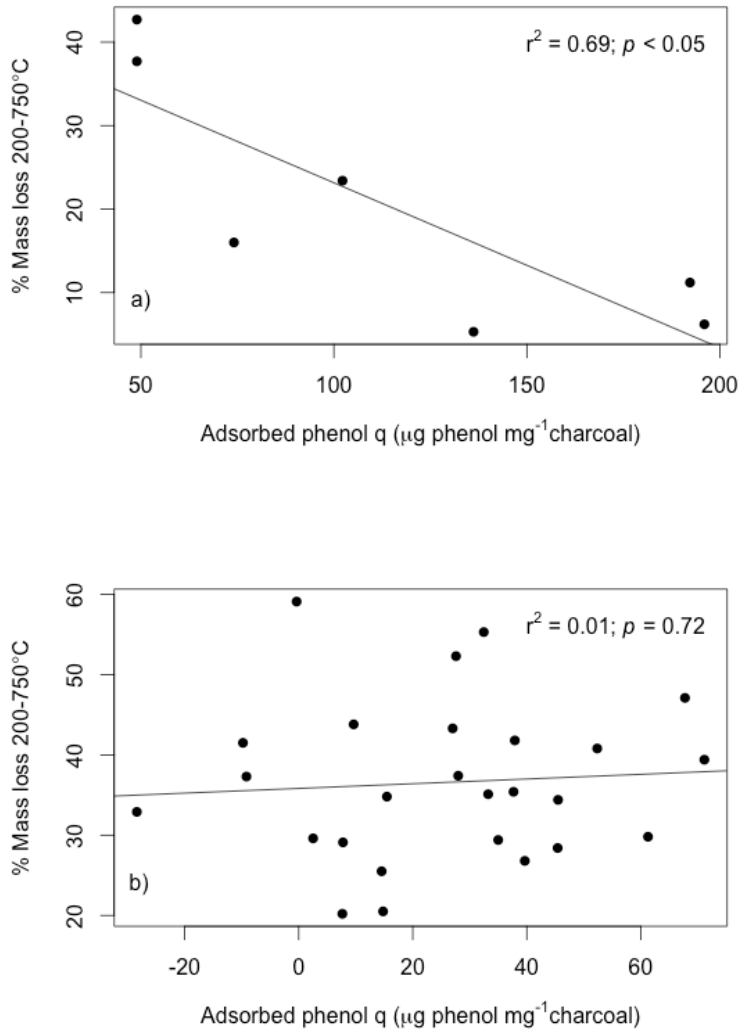

Figure 2.6: Correlation results for adsorption capacity in relation to a) medium volatile mass loss for laboratory charcoal (n = 2 for 300 °C and 500 °C, n = 3 for 800 °C) and b) field-collected charcoal from nine sites varying in time since fire on the Olympic Peninsula in western Washington (n = 3).

2.4 DISCUSSION

In the current studies, we observed a lower adsorption capacity in field-collected charcoal (Figure 2.1) compared to laboratory-produced charcoal (Figure 2.2) and attribute this to the adsorption of organic compounds and oxidation of charcoal surfaces over time, which is supported by TGA results (Figure 2.5). The average adsorption capacity of field-collected charcoal across all sites was less than 50% of the 300 °C and 17% of the 800 °C laboratory charcoals (Figures 2.1 & 2.2) and TGA results show that the proportion BC is generally lower than the 300 °C samples (Figure 2.5), suggesting that either field-collected charcoal was formed at temperatures below 300 °C or significant oxidative weathering and occlusion with OM occurred *in situ*. Charcoal collected along the fire chronosequence did not demonstrate a significant shift in phenol adsorption with TSF; however, a change in BC structure, ash residue, and mass of volatilized adsorbed compounds (or native lignocellulosic material) was observed with TSF using thermogravimetry (Figures 2.4 & 2.5). While the design of this experiment does not allow for direct comparison between adsorption and TGA data, we can use the TGA result to help characterize charcoal material collected along the chronosequence. Field-collected charcoal contained higher proportion of adsorbed compounds or experienced a low temperature pyrolysis in the original wildfire event, as a higher mass was lost at 250 °C–750 °C, and that the proportion of BC, measured as mass loss at 1000 °C with O_2, was much lower than in the laboratory charcoal are both attributes that may reduce total adsorption capacity.

As hypothesized, *P. menziesii* charcoal produced at higher temperatures increased in adsorption capacity for phenol in batch adsorption experiments (Figure 2.2, Table 2.3) as well as proportion of BC measured by TGA (Figure 2.5). Maximum adsorption values reported here are within the

scope reported by Bornemann et al. (2007) for benzene and toluene adsorption to *E. camadulensis* charcoal produced over the range of 250 °C–850 °C and about 40-fold higher than catechin adsorption reported by Brimmer (2006) for *P. ponderosa* charcoal produced at 300 °C–750 °C. Single- and bi-solute adsorption experiments using benzene, nitrobenzene, and toluene with 400 °C *Acer spp.* charcoal showed a maximum adsorption capacity of ~ 615 μg nitrobenzene·mg charcoal^{-1} (Sander and Pignatello, 2005). The experimental adsorption isotherm data from this study showed a predicted non-linear fit to the Freundlich model, despite a slight deviation in the 800 °C charcoal (Figure 2.4) that is evidenced in TGA results (Figure 2.5) where higher temperature charcoal displays higher variability in most thermal regions. Sorption behavior of charcoal is reported in literature as highly non-linear – charcoal sorption exhibits molecular sieving and multilayer sorption beyond which may be accurately described by Freundlich and Langmuir models (Pignatello et al., 2015; Sander and Pignatello, 2005). Previous studies of charcoal adsorption describe experimental data with numerous isotherm models and use a variety of charcoal-production parameters, adsorbate solutions, and adsorption techniques, which makes direct comparison of this data difficult to the majority of adsorption research. The experimental data from this study likely fit the Freundlich isotherm model due to multilayer adsorption and heterogeneous distribution of adsorption site energies and functional groups (Langmuir, 1997; Sander and Pignatello, 2005).

Theoretically, the formation temperature of field-collected charcoal can be inferred by the mass loss at combustion (1000° C with O_2), which indicates BC structure (Earnest, 1988). Our findings showed a decrease in BC structure with TSF, which might indicate that recent fire sites were exposed to higher fire temperatures, although still below 300 °C as compared to laboratory

generated charcoal (Figure 2.5). Alternatively, the observed differences within this TGA region may be due to increased chemical and biochemical oxidation of charcoal particles over time. Abiotic and biotic oxidation of charcoal and biochar in short-term studies ranging 6 months to 1.5 years (Cheng and Lehmann, 2009; Liang et al., 2008a; Nguyen et al., 2010; Zimmerman, 2010) and long-term studies of over 100 years (Cheng et al., 2008; Hockaday et al., 2007; Nguyen et al., 2008) shows the importance of these processes in the chemical composition of weathered particles, which results in higher O content, lower C content, and lower adsorption capacity.

Temperature of wildfire events represented in the chronosequence sites is impossible to infer from the existing condition of vegetation structure and composition in historic (over 100 years since fire) and intermediate sites (50–70 years since fire). Satellite data can provide a measure of overstory vegetation mortality after the fire events, which has been used as a proxy for fire temperature (Miller et al., 2009), but we hesitate to extrapolate a direct relationship to understory fire severity due to the limited connection between overstory and understory fire severity and delayed mortality of *T. heterophylla* (Franklin and Dyrness, 1973). Furthermore, fire severity and understory wildfire temperatures are not well correlated to charcoal production and consumption, which may be used to infer combustion conditions (Pingree et al., 2012; Santín et al., 2013). For example, in a temperate forest where understory temperatures during a wildfire were estimated to be > 750 °C, charcoal C formation rates were highly variable and supports the stochastic nature of wildfire events in relation to below-ground effects (Pingree et al., 2012). Charcoal mass across the fire chronosequence sites in this study is weakly, negatively correlated to TSF ($r^2 = 0.21$; $p <$

0.001), which may also support the oxidative decomposition of charcoal samples over time as opposed to wildfire conditions (Table 2.2).

Results from TGA provide a fingerprint of thermal and oxidative characteristics (thermal decomposition under N_2 and oxidative with O_2) for each charcoal specimen and are specific to the heating rate, composition of gases, and flow rate of gases during the thermal ramp (Earnest, 1988). Overall, the TGA results for laboratory-generated charcoal show a clear picture of the relationship between volatile mass loss within each thermal region and the effect of formation temperature. Generally, medium volatile mass loss (250 °C–750 °C) is slightly influenced by the individual wood type but temperature remains a strong indicator of mass loss in this region. Low volatile mass loss (750 °C–1000 °C) of laboratory charcoal is highly influenced by the individual wood chemistry and is a poor indicator of formation temperature. Oppositely, mass loss of combustion at 1000 °C and residual ash provide strong indicators of formation temperature (Figure 2.5).

Wildfire-produced charcoal in the chronosequence reflects high variability adsorption capacity, which we hypothesized could be explained by the mass loss TGA region where adsorbed compounds are volatilized (medium volatile, 250 °C–750 °C). We also expected the medium volatile mass loss to increase with TSF, which is supported by the TGA results (Figure 2.4). Although these data do not support the hypothesis that adsorption capacity is negatively correlated to the medium volatile mass loss in field–collected charcoal, laboratory charcoal samples show a significant negative correlation to adsorption capacity ($r^2 = 0.69$; $p < 0.05$) (Figure 2.6). Field-collected charcoal shows high adsorption variability both within and between

TSF sites that may be attributed to temperature and oxidation conditions during the fire event and as a result of subsequent weathering. This high variability is reflected by the strong site effect in TGA results for most thermal regions of field-collected charcoal. For example, the effect of TSF on the combustive mass loss region, which represents BC structure, equates to a 0.3% decrease per year – the effect of plot is worth 100 years of TSF.

The adsorption capacity of field-collected charcoal represents the site-specific acquired characteristics of abiotic and biotic conditions since the wildfire event (Tables 2.1 & 2.2, Figure 2.1). The presence of natural OM in soil solution can significantly reduce charcoal adsorption capacity of hydrophobic organic C compounds (Cornelissen and Gustafsson, 2004; Pignatello et al., 2006) by physical occlusion of macropores that may be alleviated over time (Braida et al., 2003; Hale et al., 2009). The occlusion of adsorption sites by mineral or organic particles could explain the decreased adsorption capacity of field-collected charcoal compared to laboratory charcoal and be further supported by the high ash content in some field-collected charcoal (Figure 2.5). Existing studies suggest a decrease in charcoal sorption capacity over time (Brimmer, 2006; DeLuca et al., 2006; Zackrisson et al., 1996), which is not supported by our direct measurement of phenol adsorption in field-collected charcoal over a 115-year fire chronosequence (Figure 2.1). In our studies, overwhelming site effects and limited recent fire sites may have negated the potential for observing the previously documented trend of adsorption capacity decreasing with TSF in the field-collected charcoal (Zackrisson et al., 1996) (Table 2.1). Our studies provide a direct quantification of charcoal adsorption capacity (Figure 2.1) and behavior (Figures 2.2 & 2.3, Table 2.3) with batch adsorption experiments. Phenol in solution clearly does not replicate the complexity of dissolved soil OM in forests soils, yet this

research provides a controlled, mechanistic evaluation of adsorption behavior *in vivo*, setting the stage for future investigations for OM adsorption to wildfire-produced charcoal in forest soils (Blum, 1996; Blum et al., 1999).

Charcoal and its adsorption capacity may play an important role in post-fire recovery through the adsorption of compounds that might otherwise interfere with seedling germination and growth (Pluchon et al., 2016; Wardle et al., 1998). The prevalence of charcoal after wildfires is documented in recent literature (Buma et al., 2014; DeLuca and Aplet, 2008; Pingree et al., 2012; Santín et al., 2015), yet the implications of this highly active C-rich material in forest soils remains poorly understood in temperate forests where fire conditions are predicted to become more frequent and extensive. The findings of this research reiterate the importance of separating the acquired effects of weathering and adsorption of organic compounds from intrinsic formation temperature in order to accurately measure adsorption capacity and define the function of charcoal in forest soils. This study suggests that charcoal adsorption capacity may influence dissolved organic C leachate rates in post-fire soils of the Olympic Peninsula, which is likely derived from formation temperature or oxidative decomposition rather than with TSF. Despite the low adsorption capacity of field-collected charcoal compared to laboratory charcoal (Figures 2.1, 2.2, and 2.3), field-collected charcoal from the chronosequence sites yielded 0.09 ± 0.04 μg phenol·mg charcoal (n=10) (Table 2.2). The adsorption capacity of field-collected charcoal will likely reduce solution concentrations of phenolic compounds in forest soils; however, we expect the capacity to be highest immediately after charcoal formation in a fire event. Due to a lack of chronosequence sites that had been recently exposed to fire (the most recent fire site was 3 years post-fire), we were unable to sample within the time frame when field-collected charcoal is

likely highest. Mixed-severity fire regime and micro-site environmental conditions of the eastern Olympic Peninsula forests added an additional layer of spatial and temporal complexity observed in this study. Future studies would benefit from a larger number of study sites across the chronosequence and a wider range of TSF values. This would allow us to overcome some of the inherent spatial variability and allow fire effects to overcome site variation effects.

Chapter 3. O-HORIZON LEACHATE IN FOREST SOILS AND CHARCOAL CHARACTERISTICS ALONG A FIRE CHRONOSEQUENCE IN THE PACIFIC NORTHWEST

3.1 INTRODUCTION

Charcoal is one of the primary soil legacies of wildfire and prescribed fire events, yet there is little understanding of how charcoal in the O-horizon or surface mineral soil influences soil dissolved organic carbon (DOC) dynamics. Charcoal present in terrestrial soils can provide adsorption surfaces for DOC species (Keech et al., 2005; Pingree et al., 2016; Zackrisson et al., 1996) and a source of dissolved black carbon (DBC) in watersheds (Ding et al., 2014; Dittmar et al., 2012; Hockaday et al., 2007; Jaffé et al., 2013). A significant ($p < 0.0001$) and positive relationship ($r^2 = 0.88$) of DOC and DBC concentrations in water samples from 27 rivers and wetlands worldwide suggests a coupled mobility of the two dissolved carbon materials from terrestrial to freshwater systems (Jaffé et al., 2013). The sorption/adsorption mechanisms responsible for this mobility are a function of soil properties and oxidation of charcoal surfaces while the export of DOC into streams and rivers is largely a function of runoff, organic matter turnover in soils, catchment size, and wetland proximity (Jaffé et al., 2013; Kalbitz and Kaiser, 2008; Kalbitz et al., 2000). In post-wildfire soils, charcoal may account for the majority of the organic component present on the forest floor (DeLuca and Aplet, 2008; Pingree et al., 2012; Santín et al., 2015).

Paleoecological and dendrochronological records provide a vivid reconstruction of fire history that demonstrate the influence of climate, human activity, and topography on fire regimes

throughout the post-glaciated history the Olympic peninsula (Fonda and Bliss, 1969; Gavin and Brubaker, 2015; Henderson et al., 1989; Wendel and Zabowski, 2010; Wetzel and Fonda, 2000). The rarity of wildfires in the western, coastal forests of the peninsula stands in contrast to the extensive and episodic fire history of the eastern, rain-shadow forests currently maintained by a mixed-severity fire regime (Agee, 1993; Gavin and Brubaker, 2015; Henderson et al., 1989; Huff, 1995). Recent dendrochronology studies in the rain-shadow forests, in the Lower Elwha River watershed and Morse Creek drainage, found a mean fire return interval of 127 years in the Lower Elwha (1800 ha) and only 21 years in Moose Creek (~200 ha) (Wendel and Zabowski, 2010; Wetzel and Fonda, 2000). This extensive record of wildfire on the Olympic peninsula, from the last glaciation period 14,000 years ago to the present emphasizes the importance of wildfire as a disturbance mechanism in this ecosystem.

Wildfire is often measured in terms of loss in aboveground and belowground productivity and loss of biomass to combustion. Only recently has the scientific community recognized the potential carbon (C) storage by the production and deposition of charcoal from wildfires (DeLuca et al., 2008; Santín et al., 2015). This concept has been popularized for agricultural applications in the form of biochar, a form of pyrogenic biomass specifically produced as a soil amendment (Barrow, 2012; Sohi et al., 2010). Charcoal is a unique byproduct of wildfires in that it is highly resistant to degradation and possesses a high surface area, aromatic C structure (Liang et al., 2008a; Schmidt and Noack, 2000; Skjemstad et al., 1996). A number of laboratory studies have established the potential for charcoal to alter forest soil biogeochemistry (DeLuca et al., 2006; Gundale and DeLuca, 2006b; Pingree et al., 2016) however; very few have tested these

concepts at an applied ecosystem scale (DeLuca and Aplet, 2008). Fire-impacted ecosystems provide an opportunity to apply processes observed in the laboratory to natural forest systems.

This high-C and low-nitrogen (N) fire residue exhibits a number of physical and chemical properties that may alter soil nutrient cycling in acidic forest soils, such as providing micro- and macro-pores (Chia et al., 2015), stimulating net and gross nitrification in forest soils with minimal net nitrification (Berglund et al., 2004; DeLuca et al., 2006; DeLuca et al., 2002), and altering soil solution chemistry by adsorption of organic compounds (Cornelissen et al. 2004, Keech et al. 2005, Gundale and DeLuca 2007, Bornemann et al. 2007). Dissolved organic matter incorporated in forest soils from O-horizon leachate represents a significant fraction of total ecosystem C, N, and phosphorus (P), and it also has the potential to alter soil solution chemistry and nutrient cycling (Qualls and Haines 1991, Michalzik et al. 2001, Kalbitz and Kaiser 2008). Dissolved organic matter is primarily provided by microbial decomposition and subsequent desorption from organic molecules from soil minerals and fresh plant litter (Currie et al., 1996; Kalbitz et al., 2000). The decomposition of organic matter provides heterotrophs with substrate for C and energy, releasing N via mineralization and consuming N via immobilization depending on the quality of the organic matter (i.e. C/N) (Paul, 2007)

The purpose of this study was to measure the quantity and quality of wildfire-generated charcoal in forest O-horizon soils of the Olympic peninsula and determine the influence of this charcoal on dissolved organic C (DOC) in O-horizon leachate released into mineral soils. Previous research in the Pacific Northwest ecosystem supports the capacity for wildfire-derived charcoal to adsorb phenol in solution (Pingree et al., 2016). These studies have also demonstrated a

negative correlation between time since fire and charcoal mass in the O-horizon (Chapter 2). In the current study we used the fire chronosequence previously established by Pingree et al. (2016) to measure the quantity, physical and chemical characteristics of O-horizon wildfire-deposited charcoal and the influence of that charcoal on O-horizon DOC leachate. First, we implemented an *in-situ* charcoal adsorption experiment to test if the presence of charcoal in non-ionic resin lysimeters decreased DOC leachate compared to lysimeters with no charcoal present. We hypothesized that O-horizon DOC leachate in charcoal-spiked resin lysimeters would be lower than those with no charcoal present due to adsorption by charcoal surfaces. We also instrumented all the sites along the fire chronosequence with non-ionic resin lysimeters in order to relate incoming O-horizon DOC leachate to soil and vegetation variables, including charcoal mass. Lastly, we employed Fourier-Transform Infrared (FTIR) spectroscopy and used the spectral response as a proxy for chemical structure thereby gathering qualitative information about native charcoal across the chronosequence sites.

3.2 METHODS

3.2.1 *Sample Collection and Measurements*

Sites were established in forest stands in the eastern Olympic Peninsula, Washington, last exposed to wildfire $1898_{a,b}$, 1922 (historic), 1922, $1985_{a,b}$ (intermediate), and 2006, 2009, 2011 (recent) (n = 3, a and b are sites within the same fire perimeter) (Figure 3.1). Sites were selected in the field within pre-designated areas within the North Pacific Maritime dry-Mesic Douglas-fir-western-hemlock potential vegetation type, between 400 and 600 meters in elevation, and on slopes of less than 20% using ArcGIS maps for reference. Where applicable, fire perimeter maps were also incorporated to establish a site within the burned area (BF sites, BG, CF, and BH)

(MTBS, 2013). Sites in the lower Elwha River Valley were located with the guidance of fire maps published by Wendel (2009).

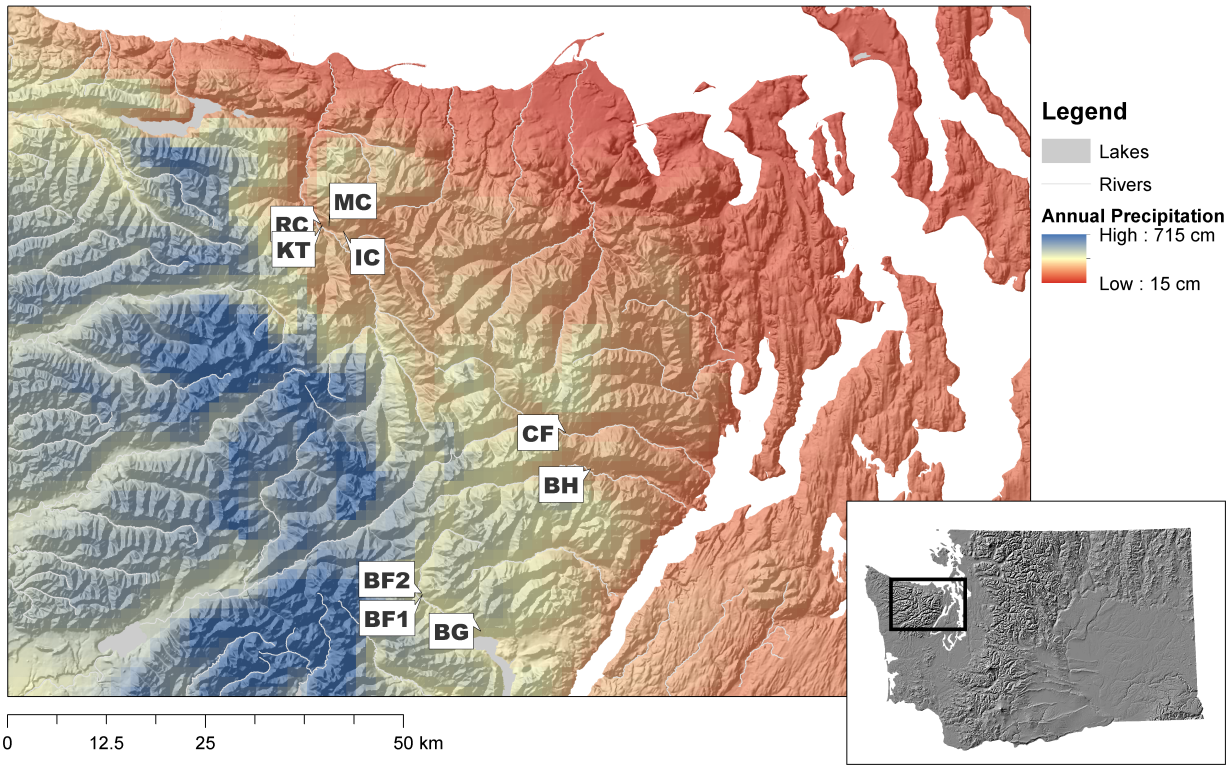

Figure 3.1: Location of fire chronosequence sites on the Olympic peninsula, Washington, USA, that were exposed to recent fires (2011 Big Hump Fire [BH], 2009 Constance Fire [CF], 2006 Bear Gulch II Fire [BG]), intermediate fires (1985a,b Beaver Fire [BF1, BF2], 1977 Rica Canyon Fire [RC] in the Elwha plots), and historical fires (1927 Michael's Cabin [MC] and 1898a,b Idaho Creek [IC] and Krause Top [KT] sites in the lower Elwha Valley watershed) (n = 3, a and b sites within the same fire perimeter separated by at least 1000 m distance).

In addition to a vegetation census and soil sample collection previously described by Pingree et al. (2016), non-ionic resin lysimeters were installed at the center of each of the ten 5 m^2 plots located within the nine 250 m^2 chronosequence sites. Lysimeters were fashioned from 50 mL plastic centrifuge tubes (Thermo Scientific, Nunc™) by removing the cap and drilling a small hole into the bottom of each tube to allow for water percolation. Approximately 1.00 g (± 0.05 g)

of non-ionic (Amberlite® XAD-7, >380 m^2 g^{-1} surface area, moderately polar) resin beads were isolated in a small nylon pouch and inserted between two 3 cm thick sections of mineral wool to avoid preferential flow of O-horizon DOC leachate. Lysimeters were placed below the O-horizon and above the mineral soil in order to capture the incoming O-horizon DOC leachate most likely to interact with charcoal particles deposited by wildfire. Lysimeters were installed for approximately 8 months through the winters of 2013-2014 and 2014-2015 in order to capture the maximum O-horizon DOC leachate rates. Three of the ten ionic and non-ionic resin lysimeters planted in the lower Elwha River watershed sites (IC, KT, MC, RC or TSF years 115, 115, 86, and 36) were spiked with 0.5 g of laboratory charcoal created at 450°C by placing the coarsely ground (< 2 mm) charcoal above the mineral wool but below the O-horizon. Resin lysimeters were collected and stored at -20°C until extraction with 10 mL of deionized water, decanted, and analyzed for total organic C on a Shimadzu TOC-VS.

At the chronosequence field sites, we randomly collected three composite O-horizon samples at each 5 m^2 plot (five composites at BG plot 4 due to sparse O-horizon cover and depth) with a 5 cm diameter ring to the entire depth of the O-horizon, which was recorded as an average of the three or five depths (Table 3.2). The sample included all layers of the O-horizon (O_i, O_e, and O_a) and charcoal was identified in the O-horizon samples by visual observation on white paper under supplemental light and separated by hand. Laboratory charcoal samples were created from 3 cm^3 sections of live *P. menziesii* branches dried for 48 hours at 60 °C. Samples were buried in pure silica sand, in lidded crucibles to reduce O_2 availability, and heated in a muffle oven (Thermo Fisher Scientific 1100 °C box furnace BF 51800 Series) at 300 °C, 500 °C, and 800 °C. The temperature gradient encompassed the probable range of wildfire temperatures in this ecosystem

(Bormann et al., 2008; Monsanto and Agee, 2008; Neary et al., 2005; Santín et al., 2016). The muffle oven was programmed to reach the target temperature at 30 minutes, heated at the target temperature for 2 hours, and decreased to 30 °C over a 2 hour period with the high-temperature alarm set at 10 °C above the target temperature. Charcoal samples were heated for 2 hours in order to ensure complete pyrolysis and combustion of the precursor wood material. Individual charcoal samples ($3cm^3$ segments) were ground to a fine powder with a mortar and pestle to pass a 0.2 mm sieve. Charcoal samples were ground and homogenized within each plot then analyzed on a Shimadzu IR-Prestige 21 infrared spectrophotometer between 4000 – 700 cm^{-1} with a resolution of 2 cm^{-1} over 48 scans per point with the common Happ-Genzel apodization model (Johnston et al., 1996).

3.2.2 *Statistical Analysis*

The effect of laboratory charcoal present in the subset of spiked lysimeters, which were planted in historic and one intermediate fire site in the lower Elwha River watershed (n = 3), were compared with a random subset of non-spike (O-horizon DOC leachate only) lysimeters. Transformed DOC values did not meet the normality assumption for analysis of variance; therefore, we used a Kruskal-Wallis test to determine significant differences between the subset groups of charcoal-spike and O-horizon DOC leachate only DOC input data. Similarly, the DOC input data across all nine sites were compared with a Kruskal-Wallis test due to non-normality and heterogeneity of variances of the DOC data. The DOC input data were regressed against time since fire (TSF) and compared to other soil and site variables with correlation analysis (Pearson's correlation coefficient). Spectra output from FTIR software were interpolated with the ChemoSpec package (Hanson, 2014) using absorbance and wavenumber after conversion by the following equation:

$$Absorbance = 2 - \log(\%\, Transmittance)$$

Spectral data were corrected for baseline drift and frequency values between 2800 – 2500 cm^{-1} were excluded because the spectra showed little variation. We also used Hierarchical Cluster Analysis (HCA) (complete cluster method and Euclidean distances) and an auto-scaled classical Principal Component Analysis (PCA), both functions are available in the ChemoSpec package (Hanson, 2014). Raw spectra were evaluated for specific differences in R without alteration to aid in PCA and clustering interpretation. All analysis were conducted in the R environment (R Core Team, 2014).

We avoided pseudo-replication of site-level variables (trees per hectare, saplings per hectare, basal area, pH) by separating any site and plot level statistical analyses. Site-level variables were not replicated (n = 1), whereas plot-level variables were replicated (n = 10) in the experimental design. Lastly, we applied previously reported adsorption capacity of charcoal collected along the fire chronosequence sites and charcoal quantity (Pingree et al., 2016) to values measured in this study of O-horizon phenol content and DOC leachate provided in Chapter 2. This calculation yielded average adsorption capacity and time of charcoal adsorption saturation.

3.3 RESULTS

3.3.1 *O-Horizon Dissolved Organic Carbon Leachate*

The O-horizon DOC leachate (g DOC m^{-2} $year^{-1}$) in charcoal-spiked resin lysimeters did not differ significantly than in non-spiked lysimeters (Kruskal-Wallis chi-squared = 0.003, *p*-value = 0.95) (Figure 3.1). The mean O-horizon DOC leachate adsorbed to non-ionic resins in the charcoal-spiked lysimeters was 1.32 (SD ± 2.70) g DOC m^{-2} $year^{-1}$ and the non-spiked random subset of O-horizon DOC leachate measured 1.67 (SD ± 2.86) g DOC m^{-2} $year^{-1}$. The mean DOC

leachate of all O-horizon samples across the nine sites averaged 1.05 (SD ± 0.34) g DOC m^{-2} $year^{-1}$ and increased significantly along the TSF gradient after a log transformation (Pearson's r = 0.52; p < 0.0001) (Figure 3.1). The rates of DOC leachate measured by non-ionic resin lysimeters did not correlate with O-horizon depth or charcoal mass, but was related to O-horizon phenol content (Pearson's r = 0.46; p < 0.001) (Figure 3.2).

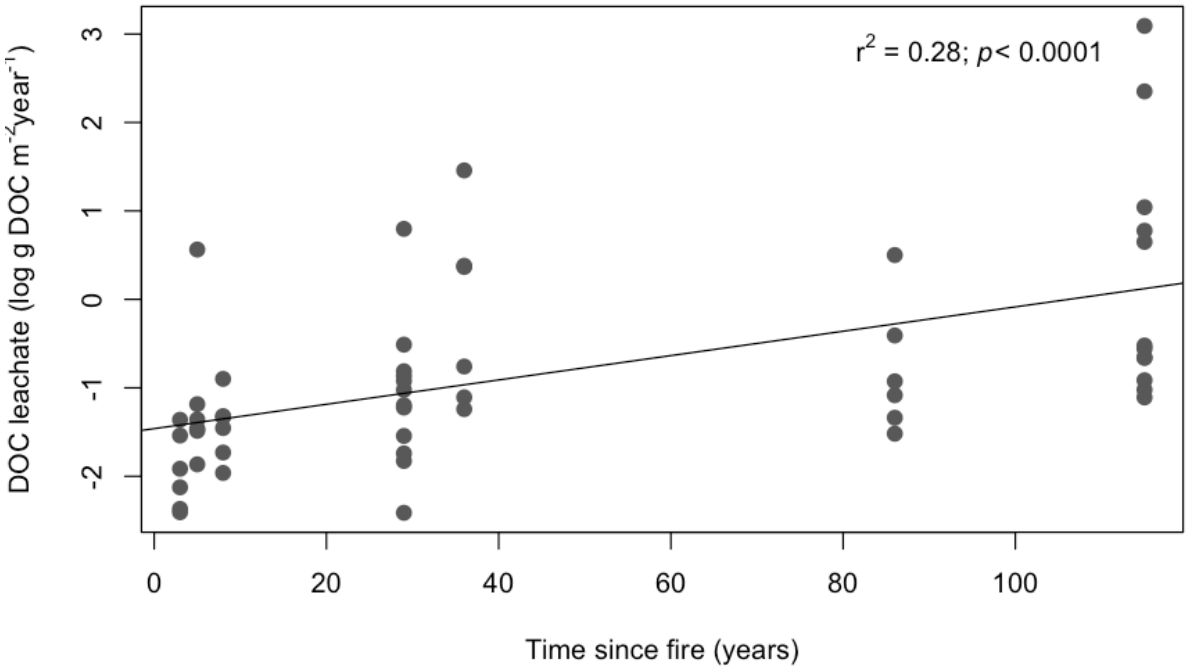

Figure 3.2: O-horizon dissolved organic carbon leachate rates measured by non-ionic resin lysimeters at a subset of plots (n = 6) within fire chronosequence sites on the east side of the Olympic peninsula, Washington. Linear model results are displayed in the top right corner.

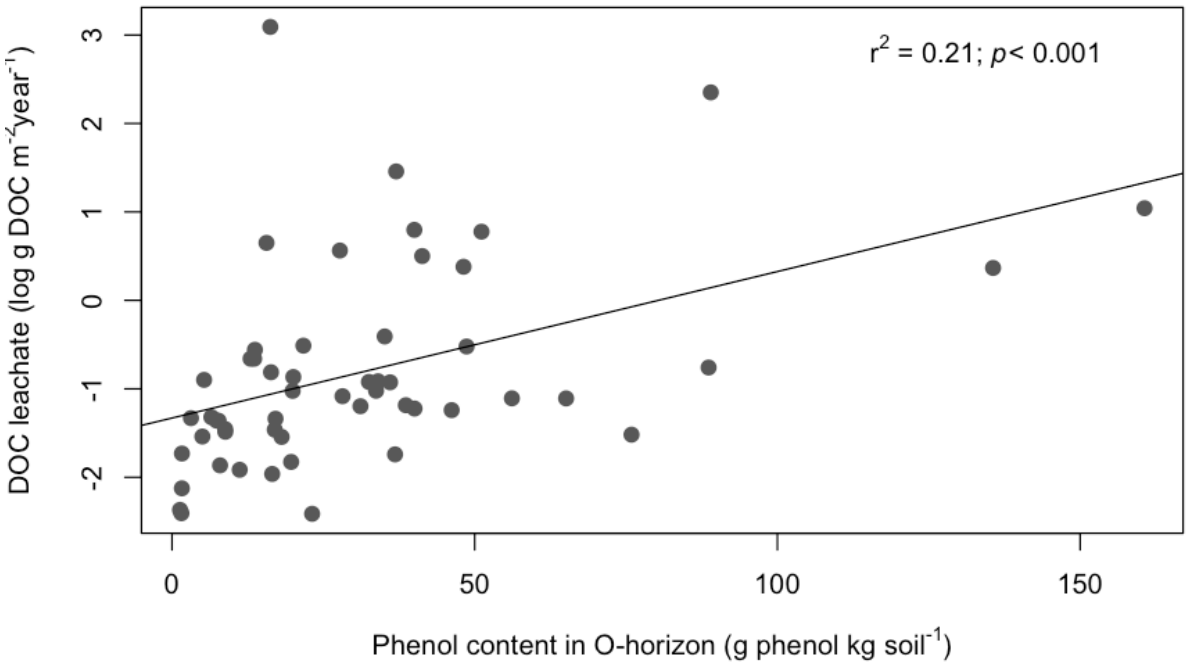

Figure 3.3: O-horizon dissolved organic carbon leachate rates measured by non-ionic resin lysimeters in relation to phenol content of O-horizon soils at a subset of plots (n = 6) within fire chronosequence sites on the east side of the Olympic peninsula, Washington. Linear model results are displayed in the top right corner.

When compared to aboveground variables, DOC leachate (g DOC m^{-2} $year^{-1}$) is weakly and positively correlated to percent moss cover (Pearson's r = 0.29, p-value < 0.05) (Figure 3.3). Site-level correlations revealed a significant positive relationship between log-transformed DOC leachate and trees per hectare (Pearson's r = 0.83, p-value < 0.01, n = 1) and similar to previous findings, a strong influence from sites IC (historic fire site last burned 115 years prior) and RC (intermediate site last burned 36 years prior) (Table 3.1). Mean annual precipitation across the fire chronosequence sites was not related significantly to O-horizon DOC leachate (Table 3.1).

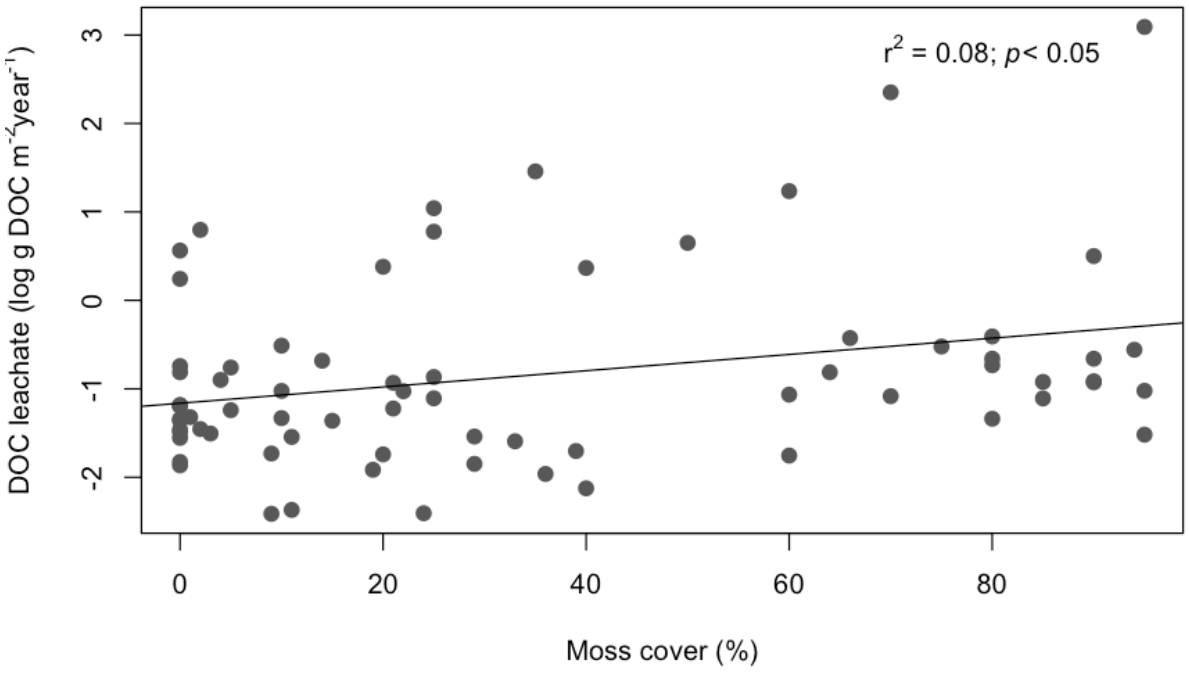

Figure 3.4: O-horizon dissolved organic carbon leachate measured by non-ionic resin lysimeters in relation percent moss cover at a subset of plots (n = 6) within fire chronosequence sites on the east side of the Olympic peninsula, Washington. Linear model results are displayed in the top right corner.

Table 3.1: A summary of dissolved organic carbon leachate rates of O-horizon soil measured by non-ionic resin lysimeters at a subset of plots (n = 6) within fire chronosequence sites on the east side of the Olympic peninsula, Washington. Standard error of plot-level variables is in brackets.

Fire History	**Site**	**Time since fire (yrs)**	**DOC input (g m^{-2} yr^{-1})**	**O-horizon phenol content (mg kg^{-1})**	**Tree density (trees ha^{-1})**	**Moss cover (%)**	**Mean annual precipitation (mm)**
Historic	IC	115	6.63 (2.64)	48.92 (14.27)	3290	60 (32)	1867
	KT	115	0.49 (0.03)	28.72 (5.46)	840	85 (7)	1544
	MC	86	0.55 (0.16)	42.71 (9.79)	520	81 (12)	1695
Intermediate	RC	36	1.38 (0.48)	66.31 (11.32)	3320	22 (15)	1499
	BF1	29	0.34 (0.05)	23.39 (3.02)	1160	37 (28)	2961
	BF2	29	0.53 (0.21)	26.02 (2.71)	240	11 (20)	2957
Recent	BG	8	0.28 (0.04)	5.74 (1.47)	600	14 (14)	2802
	CF	5	0.52 (0.17)	16.13 (3.16)	760	0	2197
	BH	3	0.57 (0.37)	5.85 (1.36)	840	29 (16)	2110

3.3.2 *Fourier Transform Infrared Spectroscopy of Charcoal*

Spectral analysis of the laboratory reference charcoal shows a broadening of the 1600 cm^{-1} region with increasing temperature, which corresponds to aromatic C=C stretching, distinct peaks in the 1700 cm^{-1} carbonyl (C=O) region diminish with increasing temperature, but do not substantial change in the O-containing function region between 3500 cm^{-1} to 3100 cm^{-1} (Figure 3.4) (Nishimiya et al., 1998; Reeves et al., 2008; Rutherford et al., 2012). The 3000 cm^{-1} to 2800 cm^{-1} region may indicate an increase in C-H aliphatic bonds with increasing temperature, as this

region has been identified by Ascough et al. (2011). Spectra from field-collected charcoal show similar distinct peaks in the aromatic C=C region (1600 cm^{-1}), carbonyl region (1700 cm^{-1}), and C-H aliphatic region (3000 cm^{-1} to 2800 cm^{-1}) (Figure 3.5).

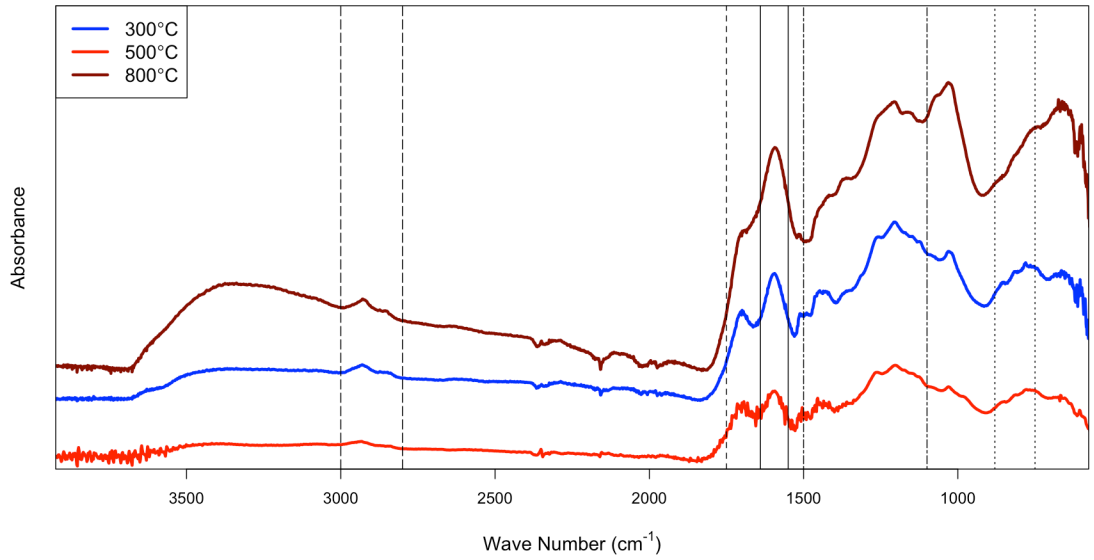

Figure 3.5: FTIR spectra of reference, laboratory Douglas-fir (*Pseudotsuga menziesii*) charcoal combusted at 300°C (blue), 500°C (red), and 800°C (dark red) in limited O_2 conditions. Solid vertical lines outline the 1600 cm^{-1} aromatic C=C region, vertical dotted lines outline the 880 cm^{-1} to 750 cm^{-1} aromatic C-H bending, 1500 cm^{-1} to 1100 cm^{-1} fingerprint region, 1700 cm^{-1} carbonyl region, and 3000 cm^{-1} to 2800 cm^{-1} hydroxyl functionality.

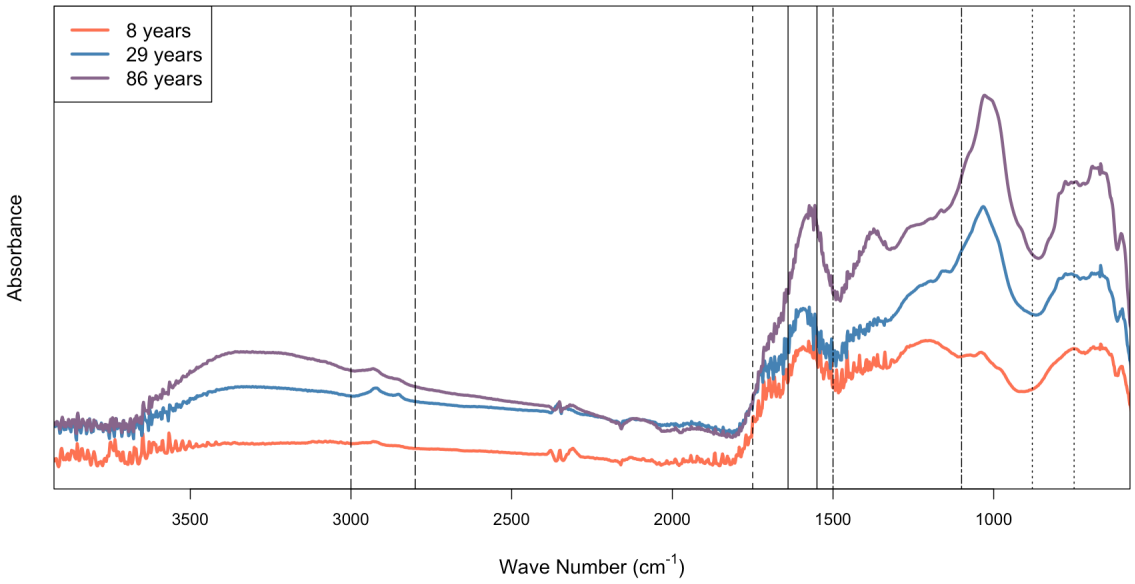

Figure 3.6: FTIR spectra of homogenized field charcoal collected in individual plots burned 8 years prior to collection (coral), 29 years prior (dark blue), and 86 years prior (purple). Solid vertical lines outline the 1600 cm^{-1} aromatic C=C region, vertical dotted lines outline the 880 cm^{-1} to 750 cm^{-1} aromatic C-H bending, 1500 cm^{-1} to 1100 cm^{-1} fingerprint region, 1700 cm^{-1} carbonyl region, and 3000 cm^{-1} to 2800 cm^{-1} hydroxyl functionality.

Field-charcoal spectra were isolated after evaluation of the PCA of all FTIR spectra (Figure 3.6), which shows these samples as grouped within fire history ellipses (group), yet also as outliers within the groups (Figure 3.6) so as to easily evaluate the differences within these spectra and aid in interpretation of PC1 and PC2 axes. The PCA of all charcoal spectra explain 52% of the overall variability and likely represent the region around 1020 cm^{-1} or 1600 cm^{-1} as these regions shows the biggest differences between the 500°C and 800°C reference charcoal, which are well separated along the PC1 axis. Samples separated most clearly along the PC2 axis also showed the largest differences between the 2500 – 2300 cm^{-1} region.

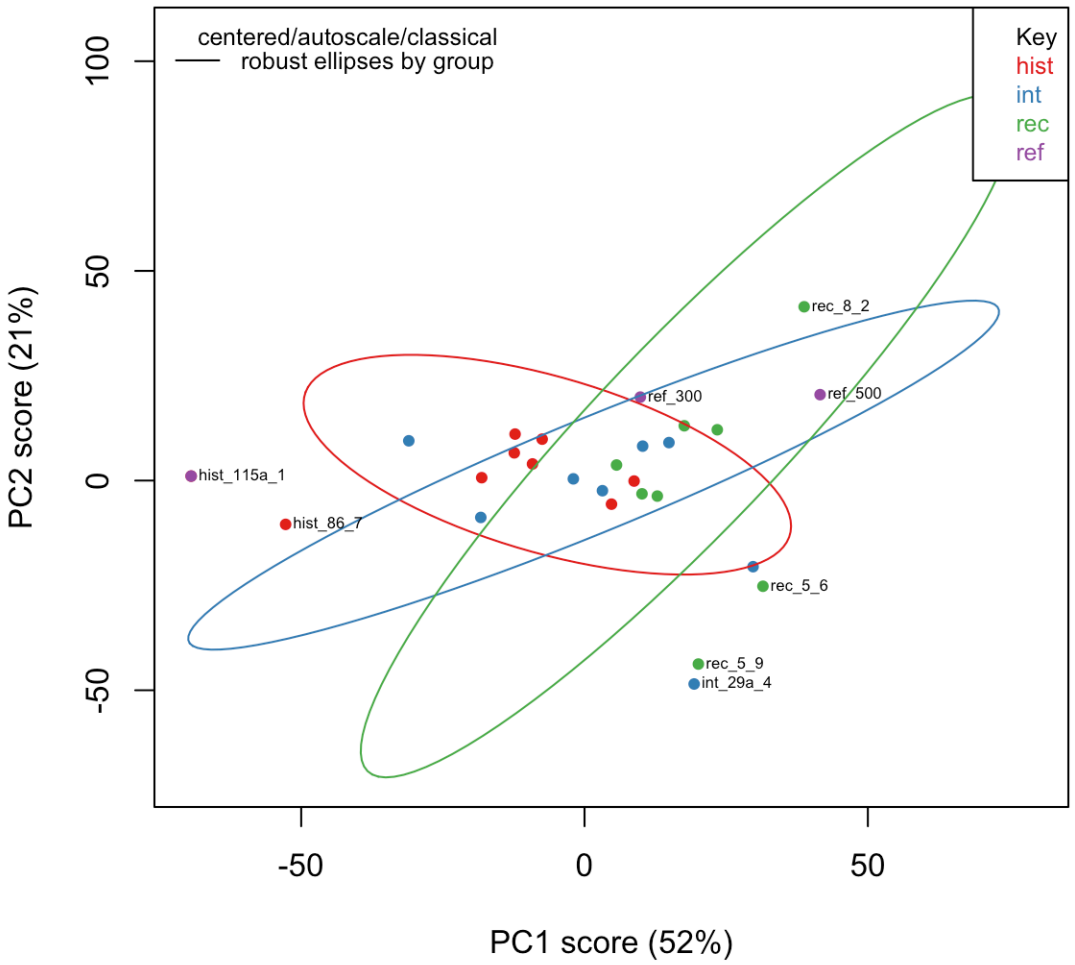

Figure 3.7: Principal Components Analysis (PCA) of FTIR spectra between 4000 cm^{-1} and 700 cm^{-1} using a centered, autoscaled, classical PCA with robust groupings shown by ellipses. Purple dots are scores from reference (ref) Douglas-fir (*Pseudotsuga menziesii*) charcoal combusted at 300°C ("ref_300"), 500°C ("ref_500"), and 800°C ("ref_800") in limited O_2 conditions. Field-collected charcoal samples represent fire history groups where red dots are site scores from historic (hist) fire sites last burned 86 years prior and 115 years prior. Blue dots are scores from intermediate (int) fire history sites last burned 36 and 29 years prior, and green dots are scores from recent (rec) fire history sites last burned 3, 5, and 8 years prior. Site names with "a" or "b" represent separate sites from within the same fire perimeter separated by 1000 m.

Results from HCA show that the majority of samples are most closely related to reference charcoal produced at 300°C while 500°C and 800°C are only related to a recent fire sample and two historic fire outliers, respectively (Figure 3.7). Furthermore, the majority of historic fire samples are more closely related to 300°C except for the two outliers ("hist_86_7" and "hist_115a_1") while intermediate and recent fire samples are arranged between 500°C and 300°C reference samples. This pattern is supported by the PCA (Figure 3.6) as most of the intermediate and recent fire samples are along PC1 between 500°C and 300°C reference samples.

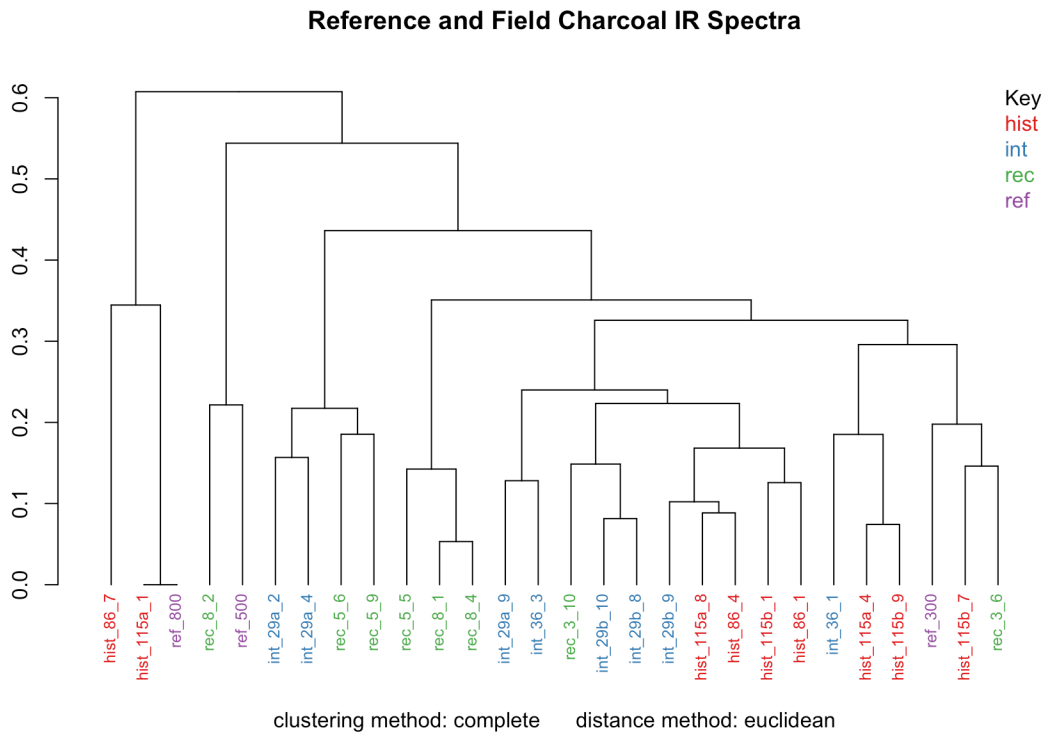

Figure 3.8: Hierarchical Clustering Analysis of reference charcoal and field-collected charcoal. Purple labels are from reference (ref) Douglas-fir (*Pseudotsuga menziesii*) charcoal combusted at 300°C ("ref_300"), 500°C ("ref_500"), and 800°C ("ref_800") in limited O_2 conditions. Field-collected charcoal samples represent fire history groups where red labels are from historic (hist) fire sites last burned 86 years prior and 115 years prior. Blue labels are from intermediate (int) fire history sites last burned 36 and 29 years prior, and green labels are from recent (rec) fire history sites last burned 3, 5, and 8 years prior. Clustering and distance method are shown on the bottom of the figure.

The adsorption capacities of wildfire-generated charcoal measured by batch adsorption laboratory experiments and reported by Pingree et al. (2016) represent the maximum adsorption capacity of the sorbate in a high sorbent concentration solution (500 µg phenol mL^{-1} charcoal), which would quickly saturate charcoal surfaces. In field conditions, the sorbent solution concentration in is not often high enough to immediately saturate charcoal surfaces. Therefore, we normalized the maximum adsorption capacity by the site conditions of O-horizon leachate

rates in order to extrapolate laboratory-measured values to ecosystem conditions. When we applied laboratory quantified maximum adsorption capacities reported by Pingree et al. (2016) to O-horizon DOC leachate rates at fire chronosequences sites, we found a range from -0.43 to 58.84 g DOC m^{-2} and average 16.64 (SE ± 6.50) g DOC m^{-2} adsorption capacity (Table 3.2). Normalized adsorption capacity values less than zero indicate an adsorption capacity that is immediately saturated by O-horizon leachate and effectively zero on an annual basis. Applied to newly formed 300°C charcoal, adsorption capacities range from 4.52 to 94.12 g DOC m^{-2} and average 37.59 (SE ± 11.39) g DOC m^{-2} (Table 3.2).

Table 3.2: Normalized adsorption capacity of field collected and reference charcoal by O-horizon dissolved organic carbon (DOC) leachate rates across east side Olympic peninsula fire chronosequence sites. Sites are dated from establishment and sample collection (IC, KT, MC, RC in 2013 and remaining sites in 2014) across the time since fire gradient ("TSF", years). Charcoal mass is reported in g m^{-2} O-horizon ("Char"), O-horizon dissolved organic carbon leachate rates are given in g m^{-2} $year^{-1}$ ("Leachate"), and the ratio of O-horizon DOC to phenol is given in g DOC g $phenol^{-1}$ ("Ratio"). Maximum adsorption capacity of field-collected and reference charcoal ("Max", g DOC g $charcoal^{-1}$) was reported by Pingree et al. (2016) and converted to normalized adsorption capacity ("Norm", g DOC m^{-2} O-horizon) by incorporating charcoal mass, O-horizon DOC leachate, and phenol concentrations given in Chapter 4. Maximum adsorption capacity of reference Douglas-fir (*Pseudotsuga menziesii*) charcoal produced at 300°C was reported by Pingree et al. (2016) and converted to normalized adsorption capacity similar to field-collected charcoal values. The number of years for saturation of charcoal adsorption capacity to occur is given by "Years". Field-collected charcoal values are shaded in grey.

Fire History	**Recent**						**Intermediate**						**Historic**					
Site	**BH**		**CF**		**BG**		**BF1**		**BF2**		**RC**		**MC**		**KT**		**IC**	
TSF	**3**		**5**		**8**		**29**		**29**		**36**		**86**		**115**		**115**	
Char	117.98		60.96		106.32		38.02		53.52		12.88		10.51		13.92		40.63	
Leachate	0.57		0.52		0.28		0.53		0.34		1.26		0.55		0.49		5.68	
Ratio	11.84		14.41		14.51		15.81		11.45		7.52		7.04		6.49		6.21	
Max	0.06	0.02	0.06	0.04	0.06	0.04	0.06	0.04	0.06	0.01	0.06	0.01	0.06	0.03	0.06	0.02	0.06	0.05
Norm	85.22	20.96	53.57	31.73	94.12	58.84	36.68	21.33	37.38	< 0	5.91	0.84	4.52	1.91	5.51	1.67	15.38	12.89
Years	149.4	36.7	103.9	61.5	341.4	213.4	69.7	40.5	109.8	< 0	4.7	0.7	8.2	3.5	11.3	3.4	2.7	2.3

3.4 DISCUSSION

Based on our results from the charcoal-spiked resin lysimeters installed *in-situ* in a subset of the fire chronosequence sites (n = 3), we found that the presence of charcoal does not significantly alter O-horizon DOC leachate when compared to non-spiked resin lysimeter measurements (Kruskal-Wallis chi-squared = 0.05, *p*-value = 0.8). These results do not support our hypothesis that the presence of charcoal would lower DOC released by the O-horizon via adsorption of non-polar C compounds as seen in previous research (Pingree et al., 2016). There are a number of factors that may contribute to this inconsistency. First, this small experiment consisted of only three replicates per treatment within each of the four sites. Lysimeters with no charcoal amendment measured DOC leachate rates with standard deviations of about half the mean values (2.13 ± 0.9 g DOC m^{-2} $year^{-1}$), which shows high variation and suggests that the number of replicates used in the experiment was not enough to capture the variability at the sites. Second, while measures of DOC adsorbed onto resin surfaces via decanting supernatant solution were sufficient in previous studies (MacKenzie and DeLuca, 2006), the highly hydrophobic material may have been mobilized into the decanted solution. Mobility of dissolved black C (DBC) into aqueous solutions is facilitated by hydrogen bonding to carbonyl and hydroxyl groups, which are polar and soluble in water, allowing physical relocation via hydrophobicity (Jaffé et al., 2013). Two individual charcoal-spiked resin lysimeters showed DOC leachate rates 20-fold and 2-fold higher than the average values for the two remaining replicates within the site that had also been spiked with charcoal. Due to the low replicates, we were not able to identify these values as outliers and thus could not discard these samples; therefore, all replicates were incorporated into the final analysis.

Despite the high variability within and among sites, the DOC leachate rate measured during the *in-situ* incubation period significantly increased with TSF (Figure 3.1). This relationship was not corroborated by charcoal mass values, which supports previous findings that demonstrate charcoal adsorption capacity is independent of TSF at these fire chronosequence sites on the east side of the Olympic Peninsula (Pingree et al., 2016). Combined, these data suggest a saturation of wildfire-deposited charcoal capacity prior to the TSF window of this study (i.e. less than 3 years). Alternatively, the high variability within and between sites calls for higher replication or blocking within fire sites for future studies. Historic fire sites had the highest contribution of O-horizon DOC leachate despite the lowest mean annual precipitation among all sites (Table 3.1). These later succession forest sites in the eastern Olympic peninsula show the greatest potential for DOC contribution by O-horizon leachate into the mineral soils.

Unmanaged forest benchmarks for ecosystem C pools and dynamics are less abundant in published literature compared to managed forests. The Oa-horizon C leachate measured in a temperate conifer forest dominated by red pine (*Pinus resinosa*) by zero-tension lysimeters in Massachusetts, USA, reported an average winter rate of 70 mg C L^{-1} (Currie et al., 1996). Values across the fire chronosequence sites in this study registered at considerably lower rates, an average 36.6 mg C L^{-1} collected over 8 – 9 months over winter. The O-horizon DOC leachate collection method used in our study was modified to isolate DOC adsorbed by non-ionic resins, the fraction of DOC most likely to also adsorb onto charcoal surfaces, and thus should be used as an internal index across the fire chronosequence sites. Non-ionic resins (Amberlite XAD-7) are effective sorbents to detect differences in total C and phenols, but should not be extrapolated to an absolute volume or mass as the total O-horizon DOC leachate was not quantified (MacKenzie

and DeLuca, 2006; Morse et al., 2000) Furthermore, O-horizon presence above the resin lysimeters may have increased DOC leachate rates or provided an adsorptive surface for incoming DOC from O-horizon DOC leachate.

Our results also show that the quantity of O-horizon DOC leachate increased concurrently with increasing phenol content in O-horizon soils, independent of the O-horizon depth, suggesting a successional shift towards organic matter that is likely influenced by phenolic compounds in the O-horizon. Phenol-rich O-horizon leachate may contribute to both positive and negative feedbacks in the plant-soil system by stimulating allelopathic interactions, forming recalcitrant organic matter in the O-horizon, and reducing decomposition rates (Hättenschwiler and Vitousek, 2000; Northup et al., 1998). As precipitation and O-horizon leachate combine and move into the mineral soils, DOM increases and accumulates extracellular enzymes from heterotrophic activity and physically fragmented litter. In optimal conditions – roughly 12% moisture, a pH of near neutral, and 10°C – heterotrophs contribute a greater proportion of DOM (Mullholland, 2003). Once in the mineral soil layer, DOC is reduced by adsorption and desorption processes associated with clay mineral surfaces and water flow transport (Kalbitz et al., 2000). The presence of phenolic compounds may alter these processes by decreasing quality of litter for decomposes and adsorption by organic-matter rich mineral soil or clay surfaces (Hättenschwiler and Vitousek, 2000). The weak, yet significant correlation between O-horizon DOC leachate and O-horizon phenol content along the fire chronosequence shows a shift in organic matter quality with implications for soil-plant interactions.

Historic fire sites may also contribute to higher O-horizon DOC leachate due to increased moss cover (Figure 3.3). Ground cover of N-fixing mosses, predominantly *Pleurozium schreberi* increased significantly along a TSF chronosequence in Swedish boreal forest ecosystems accompanied by a higher a contribution of N_2 fixation by cyanobacteria associated with the feather moss in later succession sites (DeLuca et al., 2002; Zackrisson et al., 2004). Senescence and synthesis of new cells in the moss layer may contribute to the recycling of biomass C and N in later succession sites (Chapin et al., 2011; Wang et al., 2003). Similarly, the significant and strong correlation (Pearson's $r = 0.83$, p-value < 0.01) between tree density (trees ha^{-1}) and O-horizon DOC leachate is likely a result from the interaction of rainfall with the canopy foliage. Later succession stands in the fire chronosequence provide a higher contribution of O-horizon DOC leachate that is likely influenced by the high moss cover and interaction of rainfall with the dense canopy foliage.

Data derived from FTIR measurements provide a qualitative comparison of functional group chemistry of reference and field-collected charcoal from the Olympic peninsula fire chronosequence. Reference charcoal generated under laboratory conditions clearly shows an increase in aromatic C=C bonds with increasing temperature of preparation, but the lack of change in the O-containing functional region suggests the oxidative conditions were not strict enough to show a loss of resolution in this region (Ascough et al., 2011; Nishimiya et al., 1998; Reeves et al., 2008; Rutherford et al., 2012). Biochar is typically prepared under anoxic conditions and most studies use N_2 gas during biochar formation in order to limit combustion and encourage pyrolysis of the material. Our samples were prepared under low O_2 conditions, which might provide a more accurate comparison to wildfire-produced charcoal by allowing O_2

during the combustion process similar to wildfire conditions. Interestingly, the aliphatic C-H region increases in intensity with formation temperature, which may suggest carbonization of O-containing functional groups that may eventually volatilize H ions and form aromatic C=C bonds. In the combustion process of biomass, existing organic C bonds are broken to form carbonyl and carboxyl groups, with increasing temperatures these functional groups are cleaved and yield CO_2 and CO (Kleber et al., 2015).

Field-collected charcoal patterns and relationships within the ordination space indicate that the majority of variability (PC1, 52%) across all charcoal spectra can be described by the change in quality between 500°C and 800°C in the laboratory produced charcoal, which was identified in the aromatic C=C and 1020 cm^{-1} regions. The remaining 25% of the variation between spectra can be described by the 2500 – 2300 cm^{-1}, which currently lacks a definition for biochar or black carbon material. A few outliers in recent and intermediate fire sites largely define this axis. The majority of sites are most closely related to the spectra signatures of 300°C reference charcoal, as shown both by the ordination (Figure 3.6) and hierarchical clustering (Figure 3.7). In fact, the 800°C and 500°C reference charcoal samples are most distinct from the majority of field-collected charcoal along with the same outlier which are best separated over the PC1 axis, indicating that PC1 may be best described by aromatic C=C bonds. Overall, the FTIR spectral analysis are similar to the findings from Pingree et al. (2016) that indicate highly altered functional characteristics of field-collected charcoal compared to that of fresh laboratory produced charcoal results in adsorption capacities nearly half that of the 300°C reference charcoal. Additionally, subsequent fires may reheat and recharge native charcoal particles – altering the elemental composition and functional characteristics of charcoal particles remaining

from previous fires on the forest floor (Pietikäinen et al., 2000; Zackrisson et al., 1996). Spectral characteristics show a greater distinction within the fire history samples: historic fire samples are most closely related to the 300°C reference while intermediate and recent fire samples are less so. Recent fire samples are more distinctly separated from intermediate samples, similar to the variation within O-horizon DOC leachate at these sites (Figure 3.1). Interestingly, a few outliers are most similar to 800°C and 500°C samples. One sample is from a recent fire site (BG) and may actually reflect a higher formation temperature. The two samples closely related to 800°C reference were collected in the lower Elwha River watershed, which has a rich history of human activity and may be relics from a high-temperature slash pile (Monsanto and Agee, 2008; Wendel and Zabowski, 2010).

Maximum charcoal adsorption capacity reported by Pingree et al. (2016) was applied to O-horizon DOC leachate values measured in this study in order to determine the capacity for charcoal to alter O-horizon DOC leachate rates at the fire chronosequence sites. Field-collected charcoal adsorption capacity reflects the adsorption of organic compounds and oxidation of charcoal surfaces over time, while reference charcoal reflects the effect of pyrolysis/combustion temperature on the specific precursor biomass (Pingree et al., 2016). The normalized adsorption capacity, which incorporates O-horizon characteristics and leachate rates, allows us to extrapolate the charcoal effect to a broader spatial and temporal scale. The result of applying laboratory-measured maximum adsorption capacity to O-horizon DOC leachate rates shows a higher overall adsorption capacity at recent fire sites compared to that of historic fire sites due to the slightly lower DOC leachate rates and substantially higher adsorption capacities (Tables 3.2). Intermediate fire sites (RC & BF1), where adsorption capacity and DOC leachate rates are

balanced, resulted in a neutral charcoal effect where normalized adsorption capacity would be saturated less than 3 years after a fire event. In most cases, a wildfire partially or completely volatilizes O-horizon soil, and thus the O-horizon leachate rates will also change. The east side of the Olympic peninsula, however, is characterized by a mixed-severity fire regime that often leaves unburned patches adjacent to burned patches (Henderson et al., 1989; Huff, 1995). Geomorphic events and delayed conifer mortality, particularly in the form of windthrow, provide an opportunity for soil mixing and incorporation of adjacent charcoal particles into unburned patches (Franklin and Dyrness, 1973; Henderson et al., 1989).

The forests of the east side of the Olympic peninsula provide an interesting case study in the biogeochemical cycles and successional patterns of a mixed-severity fire regime class that is narrowly and poorly defined by a broad range of overstory mortality. Our findings show, despite high site variability, a significant correlation between O-horizon DOC leachate rates and time since fire. Late succession sites measured in this study are dominated by moss ground cover and recalcitrant, phenolic-rich O-horizon soils similar to findings in boreal ecosystems. This study also demonstrates that the adsorption capacity of fresh 300°C charcoal and recently deposited field-collected charcoal are highly should be evaluated in context of charcoal mass on the forest floor, O-horizon characteristics, and leachate rates in order to provide the most accurate measure of the charcoal adsorption affect.

Chapter 4. FOREST SOIL BIOGEOCHEMISTRY AND CHARCOAL CONTENT ALONG A WILDFIRE CHRONOSEQUENCE IN THE RAIN SHADOW FORESTS OF THE EAST SIDE OLYMPIC PENINSULA, WASHINGTON

4.1 INTRODUCTION

Wildfire is a major disturbance in the east side forests of the Olympic Peninsula yet little is known about the effects of wildfire on soil biogeochemistry, nutrient pools, and nutrient cycles essential to the ecosystem function of these forests. Timber harvest practices and fire exclusion in western Washington have led to increased forest density and decreased diversity, where historically non-lethal wildfires had maintained more resilient and diverse forest conditions (Franklin and Dyrness, 1973; Franklin and Johnson, 2012; Weisberg, 2004). These forests have historically been characterized by frequent low- to moderate-intensity fires occurring between infrequent high-intensity, stand-replacing fires (Fonda and Binney, 2011; Henderson et al., 1989). The fire return interval of this region historically ranged from 120 to 300 years (Fonda and Bliss, 1969; Henderson et al., 1989; Wendel and Zabowski, 2010; Wetzel and Fonda, 2000) making wildfire a dominant disturbance in *Tsuga heterophylla/Pseudotsuga menziesii* forests of the rain shadow Olympic peninsula. Prescribed fire in this region remains a viable option to reincorporate low-intensity surface fire as a restoration tool in the old growth *P. menziesii* dominated forests (Fonda and Binney 2011). These forests represent a unique

ecosystem where spatial and temporal heterogeneity of fire severity may have significant implications for belowground and aboveground post-fire recovery. The mixed-severity fire regime forests of eastern and northeastern region of the Olympic peninsula is defined by fires that result in 20-70% mortality of the overstory vegetation or basal area (Agee, 1993). In addition to the historical fires of this region, recent wildfires, namely the 2009 Constance Fire on the Olympic National Park and the 2011 Big Hump Fire on the Olympic National Forest, provide an opportunity to assess the influence of wildfire on these highly productive forests. To date there has been limited effort to evaluate the influence of fire or fire exclusion on soil nutrient dynamics in these east side forests of the Olympic Peninsula.

A suite of studies in temperate and boreal forests provide evidence that collectively supports the hypothesis that the occurrence of fire in historically fire-maintained ecosystems contributes to the long-term sustainability and resilience of forest ecosystem processes mediated by above-ground and below ground interactions (DeLuca et al., 2006; DeLuca and Sala, 2006; MacKenzie and DeLuca, 2006; MacKenzie et al., 2004; Wardle et al., 2003). The ecological disturbance of fire in Swedish boreal forests provides an a pathway for succession trajectories mediated through plant-soil feedbacks, which over time results in net N immobilization and creation of an N limited ecosystem (DeLuca et al., 2002; Zackrisson et al., 1996). Fire chronosequence studies in northern Sweden were used to evaluate the influence of secondary post-fire succession on vegetation and soil responses (DeLuca et al. 2002). The authors used a total of 34 forest reserve sites varying in age (time since last fire, TSF) from 3 – 352 years since the last fire. Vegetation

communities and depth of soil humus were measured at all 34 sites while N variables were measured at a subset of eight sites. Net N mineralization was found to decrease linearly and nitrification rates decreased exponentially while feather mosses (mainly *Pleurozium schreberi*) and ericaceous shrubs (*Empetrum hermaphroditum*) increased logarithmically with TSF (DeLuca et al., 2002). The presence of wildfire-derived charcoal in mineral soils increased nitrification rates, which was shown to be unrelated to labile organic N substrate (DeLuca et al., 2002), a phenomena likely driven by adsorption of compounds that otherwise inhibit net nitrification (Berglund et al., 2004; DeLuca et al., 2006; Gundale and DeLuca, 2006b). In a low elevation *Pinus ponderosa* ecosystem, frequent fires stimulated N cycling rates notwithstanding a reduction in total N and litter quality (C:N) over the fire chronosequence – nitrification potential was similarly stimulated by charcoal additions in mineral soil (DeLuca et al., 2006; DeLuca and Sala, 2006; MacKenzie et al., 2004). Wildfire events and the recurrence of wildfires in these ecosystems provide a driver of nutrient availability and vegetation regeneration mediated by N cycling and the presence of charcoal in forest soils.

The fate of nutrient quantity and quality in forest soils has been found to be intimately linked to ecosystem function throughout a fire cycle (Chapin et al., 2011; MacKenzie et al., 2004; Wardle et al., 2003). Fire chronosequence studies provide a space-for-time substitution, operating under the assumption that initial disturbance characteristics and succession patterns are equivalent in older and younger sites (Walker et al., 2010). A 361-year fire chronosequence in Swedish boreal forests showed evidence of increased N fixation by cyanobacteria associated with feather mosses and greater organic N uptake

via mycorrhizal fungi possibly to compensate soil inorganic N deficiencies in late succession stands (DeLuca et al., 2002; Hyodo et al., 2013; Zackrisson et al., 2004). Spatial analysis of a 79-year chronosequence revealed homogeneous bulk C and N pools with time since fire and, oppositely, heterogeneous biotic variables (e.g. microbial biomass, N mineralization) and O-horizon depth with time since fire (Lavoie and Mack, 2012). This analysis of an Alaskan boreal ecosystem suggests that wildfires create spatial heterogeneity favorable for N cycling and decouples the tight relationship between soil and forest floor cover dominated by moss and lichen. Long-term studies of fire disturbances, such as provided by fire chronosequence designs that span the historical fire return interval, provide a balanced assessment of the function of wildfires as opposed to short-term fire effects weighted on early succession interactions (Johnson and Miyanishi, 2008; Walker et al., 2010).

In this study we aimed to evaluate the influence of fire and time since fire (TSF) on soil C & N pools, N cycling, and forest composition in the east side forests of the Olympic peninsula where climate change is predicted to alter fire occurrence and extent via an increase in annual temperature by 0.6 – 1.9ºC and drier summer conditions (-8.5%) (Halofsky et al., 2011b). The majority of increased annual temperature is predicted to occur in the summer, which will also increase summer potential evapotranspiration (5 – 18 mm by 2040); conditions that will be concentrated in lower elevation, northeast forests encompassing the study sites (Halofsky et al., 2011b). A current synthesis of aboveground and belowground forest biogeochemical interactions in these forests will help provide context for the current ecological function of wildfires. As the predicted changes

will directly alter the fire regime and, thus, biogeochemical cycles of the Olympic peninsula's fire-maintained forests, so will these studies provide a baseline for the magnitude of ecological change. Although climate models do not incorporate storm tracks, where lightning ignition would play an important role in fire occurrence, these predictions are a recipe for higher fire frequency and larger fire extent.

The purpose of the research presented herein was to evaluate how time since fire (TSF) influences vegetative composition and the quantity and character of soil C and N pools in organic and surface mineral soils of the east side of the Olympic Peninsula, WA. Specific objectives of the study were to: (1) determine whether O-horizon C and N increases with TSF; (2) evaluate how TSF influences O-horizon and mineral soil inorganic N and potentially mineralizable N (PMN); (3) determine whether charcoal accumulated in the O-horizon influences soil phenolic concentrations; (4) assess whether sites recently exposed to fire have increased net nitrification compared to paired unburned sites.

4.2 METHODS

4.2.1 *Study Sites*

We evaluated the soils, understory vegetation, and overstory density in nine forest stands in the Olympic peninsula, Washington in the summers of 2013 and 2014 (Figure 4.1), previously described in (Pingree et al., 2016). Sites were selected along a gradient of years since the last wildfire, referred to as time since fire (TSF), within a day travel from the laboratory and accessible from a hiking trail for immediate processing of fresh soil samples. The TSF gradient encompasses the fire return interval of previously studies forests on the eastern Olympic peninsula (Franklin and Dyrness, 1973; Henderson et al.,

1989; Wendel and Zabowski, 2010). The time constraints of this study, distances traveled to sites, and heterogeneous slope of the sites prohibited the use of transect lines or a blocked design. Sites were distributed across a gradient of TSF intervals except for TSF years 29 and 115 where two sites occur in the same TSF level (9 sites and 7 levels of TSF). These sites were separated by at least 1,000 m distance. A site was established with a 10 m by 25 m area, 250 m^2, within the North Pacific maritime dry mesic *P. menziesii, T. heterophylla* potential vegetation zone, between 400 and 600 meters in elevation, and on slopes of less than 20% to avoid erosion effects using ArcGIS maps for reference (Kagan, 2010; USGS, 2009). Soils of the northern and eastern Olympic peninsula are formed on marine deposits of basalt, colluvium, volcanic ash, and glacial till (Henderson et al., 1989; NCRS, 2014). Although there is no formal soil survey of the majority of the study sites, proximate areas are classified by the US Soil Taxonomy classification as skeletal Typic Haploxerepts (NCRS, 2014), which fits closely with our field observations at all sites. Mean annual temperature from 1980–2010 averaged 8.1 ± 0.5 °C and mean annual precipitation was 2,181 ± 592 mm across all sites (Wang et al., 2012).

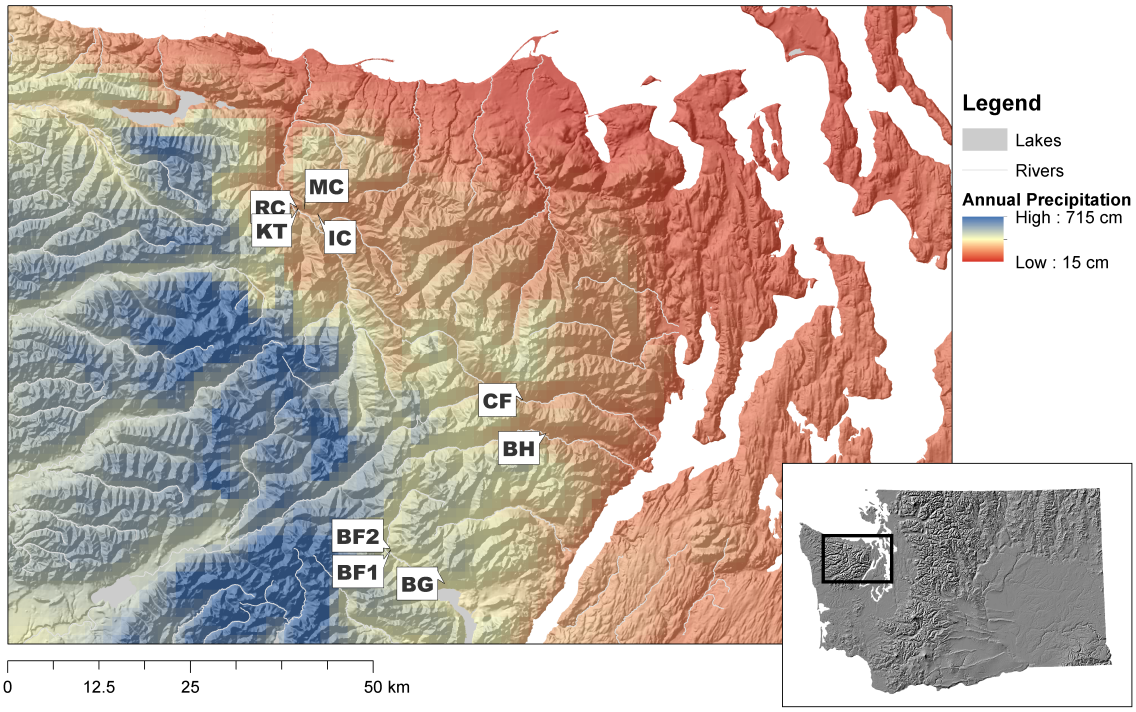

Figure 4.1: Location of fire chronosequence sites on the Olympic peninsula, Washington, USA, that were exposed to recent fires (2011 Big Hump Fire [BH], 2009 Constance Fire [CF], 2006 Bear Gulch II Fire [BG]), intermediate fires (1985a,b Beaver Fire [BF1, BF2], 1977 Rica Canyon Fire [RC] in the Elwha plots), and historical fires (1927 Michael's Cabin [MC] and 1898a,b Idaho Creek [IC] and Krause Top [KT] sites in the lower Elwha Valley watershed) (n = 3, a and b sites within the same fire perimeter separated by at least 1000 m distance).

4.2.2 *Understory and Overstory Vegetation*

Sites were further described by a census of visually estimated understory vegetation species and percent cover determined within each 5 m^2 plot. Ground cover was estimated by visual percent of rock, bare ground, vegetation, moss, coarse woody debris, and O-horizon. If understory vegetation consisted of over five different species, the plot was divided into quadrants and percent cover was estimated visually within each quadrant. The average percent cover for each plot was determined with quadrant estimates. At each

site, every standing tree and snag larger than 6 cm in diameter at breast height (DBH) was recorded by diameter and species. Saplings with a DBH less than 6 cm were counted and identified if they were higher than breast height but were not measured for DBH. At recent fire sites, seedlings (< DBH) were counted as percent vegetation cover.

4.2.3 *Soil Sampling and Analysis*

Within each site, a contiguous grid of ten 5 m^2 plots was installed for collection of O-horizon and mineral soil samples. Due to the highly variable terrain, plots were arranged contiguously in order to cover the greatest area of similar slope. Within each plot, three composite O-horizon samples were collected with a 5 cm diameter ring to the entire depth of the layer with Oi, Oe, and Oa combined (five samples were collected in BG plot 4 due to minimal O-horizon depth, Figure 4.1). Due to the high rock content of mineral soils (> 40% by volume), one 10 cm diameter soil sample was collected to a depth of 10 cm at the center of each plot. Samples were transported to the laboratory on the day of collection, stored at 7°C, sieved to <2mm, and extracted within 3 days of sample collection by the methods below. Approximately 10 g (± 0.01) of field-moist mineral or O-horizon soils were extracted for DOC, total N, and phenol by adding to 30 ml of 0.01 M CaCl2, agitating for 30 minutes on a reciprocal table, and filtering with Whatman CF/G glass filters. Mineral soils were extracted for ammonium and nitrate by adding 6 g (± 0.01) field-moist soil to 25 ml of 1 M KCl solution; the mixture were shaken for 30 minutes on a reciprocal table and filtering with Whatman #42 filter paper. Final extraction concentrations were corrected for moisture.

We performed a 14 d anaerobic incubation to determine the maximum mineralizable N (PMN) available for plant growth in one season given optimal moisture, temperature, and N substrate (Powers, 1980). One the same day as mineral soil extractions (day 0), approximately 6 g (± 0.01) of field-moist mineral soils were added to 12.5 mL of deionized water in a 50 mL plastic centrifuge tube. Oxygen was displaced by adding N^2 (gas) for one minute in the slurry and, using Parafilm as a seal, displacing oxygen in the headspace for 30 seconds, then quickly capped and incubated for 14 days at 25°C. At the end of the 14-day period, we added 12.5 mL of 2 M KCl and extracted using the method described above for mineral soils. After correcting for moisture content, PMN was determined by subtracting NH_4^+ at day 14 from NH_4^+ at day 0, and reported as mg NH_4^+ kg dry $soil^{-1}$ day^{-1}. Extracts from $CaCl_2$ extractions were analyzed for total dissolved organic C and N (TOC-VS, Shimadzu) and total phenol determined by colorimetry (Multiskan FC Microplate Photometer, Thermo Scientific) using the Folin & Ciocalteau's reagent and read at 725 nm (Box, 1983). Mineral soil extracts of KCl were analyzed for NH_4^+ by colorimetery (Multiskan FC Microplate Photometer, Thermo Scientific) following the salicylate-nitroprusside method (Mulvaney, 1996).

Air-dried O-horizon and oven-dried mineral soils (60°C) were homogenized with a mortar and pestle and analyzed for total C, H, and N by dry combustion using an elemental analyzer (Model 2400, PerkinElmer). Soil was determined by combining roughly 1:1 ratio of soil to distilled (DI) water to create a saturated slurry for mineral soils and completely inundating about 30 ml volume of O-horizon soil with DI water (Thomas, 1996). We allowed the slurry to equilibrate for 30 minutes before reading the

pH 700 benchtop meter (Oakton Instruments, USA). Two replicate composite samples from each of the 10 plots were combined for the pH average value. One composite 40 g mineral soil sample for each site, comprised of ~ 4 g of oven-dry mineral soil from each plot, was used to determine soil texture by the hydrometer method with pre-treatment for organic matter and iron oxide removal (Gee and Or, 2002). Mineral soil bulk density was determined from three samples per site with a 5 cm^2 diameter core pressed lightly into the top 5 cm of mineral soil, dried at 70°C and sieved to < 2 mm. Soil moisture content was determined gravimetrically by drying 6 g mineral soil and 10 g (± 0.01) O-horizon soil for 48 hours at 60°C.

In the spring of 2016, soils were collected from paired burned and unburned plots in sites BH (Big Hump Fire 2011), CF (Constance Fire 2009), and BF (Beaver Fire 1985) for an aerobic incubation to measure net N mineralization and nitrification. Fire perimeters were delineated from GIS data and visually confirmed by fire scars on mature conifers in order to establish paired plots within and outside of fire perimeters separated by at least 200 m. At each plot, we established a simple random design based on a 100 m^2 grid wherein we randomly selected 12 sample points within the grid. At each random grid cell, after removing the O-horizon we collected mineral soil to a depth of 10 cm and volume of about 400 g. Soil samples were transported to the lab within 24 hours, kept at 6°C. Within two days of sample collection, samples were coarse-sieved by hand to remove large roots and rocks larger than 2 cm. Due to the high moisture content of soil samples we were unable to sieve with a standard screen device. Approximately 5.00 g was separated for moisture content determined after 24 hours at 105°C and 5.00 g was

separated for immediate 1M KCl extraction, shaken with 25 mL solution for 30 minutes, and extracted with Whatman #42 filter paper. We then added approximately 300 g of field moist soil into 1L wide-mouth Ball jars fitted with a septa valve and sealed. Jars were kept in the dark at a constant temperature of 23°C for 24 hours after which the headspace was sampled for CO^2 concentration, jars were fitted with permeable lids, and the incubation was allowed to continue under aerobic conditions for 28-41 days. Gas samples were analyzed on a Shimadzu GC-2014 with an AOC 5000 Auto Injector (MSH-02-00B, 2.5 mL, 60 mm). Soils were kept at field moisture by the weekly addition of deionized water allocated evenly over the soil surface; this process generally added only 1-2 g of water per week. After the incubation period, we separated approximately 5.00 g for extraction and followed the procedure previously described.

4.2.4 *Statistical Analysis*

Multivariate, non-parametric data analyses provided an opportunity to summarize how samples (e.g. plots) are related to each other given interdependent response variables. This data reduction summarized a large number of observations and expressed the interrelated response variables in a compact way where traditional methods would be weak or ineffective given that the majority of variables in this study did not meet assumptions of normality or homoscedastic variances (McCune and Grace, 2002). Data were first analyzed with Nonmetric Multidimensional Scaling (NMDS), which included separate ordinations for soil variables (pH, mineral and O-horizon total C, total N, mineral soil moisture content, mineral soil available inorganic NH_4^+ -N and NO_3^--N, phenol content of mineral and O-horizon, PMN) and vegetation variables (percent cover

of all vegetation, moss, bare ground, and species over 5% cover) in order to the explore the structure of the data, which did not meet assumptions of normality or linearity among variables. Overstory vegetation variables were excluded from both NMDS models (basal area, trees per hectare, saplings per hectare), due to the lack of replication. Euclidean distances were applied to soil NMDS ordination and Bray-Curtis distances in the vegetation ordination. We used the ecodist package version 1.2.9 for the NMDS visualization and outlined the site groups by TSF (Oksanen et al., 2013). Before the ordination, data were standardized by the maxima in order compare different scales for many variables (e.g.: mineral soil C, percent cover, PMN, etc.) using the *metaMDS* function in the vegan package (Oksanen et al., 2013).

The NMDS visualizations were followed by two separate Permutational Multivariate Analysis of Variances (PERMANOVA) for soil variables using Euclidean distances measures and vegetation variables with Bray-Curtis distance measures. In order to properly test the nested design of this experiment (Site is nested within TSF) we applied PERMANOVA tests to within-site and between-site distance matrices. Within-site distances were calculated by using the mean value for the distance between observations within each site. Permutations were restrained for within-site distances by site and allowed for free permutations between sites then executed with the *adonis* function in the vegan package (Oksanen et al., 2013).

We circumvented pseudo-replication of site-level variables (trees per hectare, saplings per hectare, basal area, and pH) by separating any site- and plot-level exploratory and

statistical analyses. Site-level variables were not replicated (n = 1), whereas plot-level variables were replicated (n = 10) and were tested with site as a random factor in order to partition the variance according to the experimental design.

Soil and vegetation variables were compared in a correlation matrix to determine relationships and significance between all variables including TSF. Soil response variables that met the assumptions of normality and homoscedasticity (*p*-value cut off > 0.05) were tested with an analysis of variance (ANOVA) against TSF. This case occurred for O-horizon C content only. Distribution of response variable O-horizon depth was normal but variances were not homoscedastic; therefore, we used linear models (LM) for analysis. Remaining response variables were log transformed due to the lognormal distributions and then tested statistically with LMs. Final LMs were determined with a backwards model selection, which started with soil or vegetation variables correlated with the response variable, which all always included TSF. The least significant variable (using *p*-values) was discarded and the model rerun sequentially until the final model consisted of significant explanatory variables. We found significant correlations for five response variables: O-horizon C content, O-horizon depth, O-horizon phenol content, mineral soil phenol content, PMN, and charcoal content. The TSF variable was tested with the significant co-variables against each soil parameter, listed previously, in order to determine the degree to which co-variables influenced the relationship between TSF and the specific soil parameter.

Soil basal respiration data from the aerobic incubation met normality and homoscedasticity assumptions and were tested with a 2-way ANOVA against sites and the treatment factor (soils collected from burned or unburned sites). In this experimental design, both site and burn history are considered fixed factors because we deliberately included sites from recent and intermediate fire history. We conducted pairwise comparisons of mean values by using a Tukey's Honest Significant Differences test. One missing value (BHB7) was estimated by the mean of the site/treatment group to complete the Tukey's test. Significant differences of net NH_4^+ and NO_3^- accumulation rates (mg N kg dry $soil^{-1}$ 20 $days^{-1}$) in sites and treatments (paired burned and unburned plots) were tested with a PERMANOVA using Euclidean distance measures and restricting the permutation to within sites.

4.3 RESULTS

4.3.1 *Aboveground composition and trends along the fire chronosequence*

Overstory composition at the chronosequence sites was dominated by *P. menziesii* (average 85% across all sites) and *T. heterophylla* (at historic fire site Idaho Creek and recent fire site Big Hump) with minimal abundance of *Thuja plicata* at intermediate and recent fire sites and *Alnus rubra* at one recent fire site (Table A1). Understory composition was predominantly composed of Gaultheria shallon (GASH) and *Mahonia nervosa* (MANE) at all but the two most recent fire sites, *Polystichum munitum* (POMU) in historic and intermediate fire sites, and *Chamerion angustifolium* (CHAN), *A. rubra* (ALRU), and *Salix* spp. at recent fire sites (Figure 4.2). The NMDS of vegetation attributes had a stress of 0.202, which suggest that the interpretation is not definitive (Clarke, 1993), a non-metric fit R^2 of 0.959, and linear fit R^2 of 0.808. Time since fire

(TSF) significantly affected the composition of vegetation between sites (p-value < 0.01), but not within sites (Table A4).

The NMDS ordination (Figure 4.2) is derived from a distance matrix, which summarizes the differences between each sample unit (i.e. plots) in terms of the vegetation cover (bare ground, moss, and vegetation) and abundance of the most abundant species. The distances among site loadings in the ordination space are in the same rank order as the distances among plots as measured by the original distance matrix. Loading points that are closer together symbolize more similar sample units (i.e. plots) while dissimilar units are farther away in the ordination space. The loadings where vegetation variables are most abundant are shown with the variable code (see Table A3 for descriptions) and by proximity to the site loadings.

Vegetation loadings are grouped by TSF and show high variability for intermediate sites and one 115 TSF site. Loadings show smaller clusters in recent fire sites and one of the two 115 TSF groups, while all others are highly variable. Early succession species, i.e. Salix species, red alder (*A. rubra*), fireweed (*C. angustifolium*), bear grass (*X. tenax*) and abundance of saplings, are most abundant closer to the recent fire loadings as well as the absence of any vegetation, moss, or O-horizon cover. Intermediate sites are most abundant in phenolic-producing *Vaccinium* shrubs and salal (*G. shallon*). Moss cover is highest in historic fire sites where Oregon grape (*M. repens*) and baldhip rose (*Rosa gymnocarpa*) also dominate.

Linear model results for vegetation parameters related to TSF are given in Table A5 and show significant vegetation co-variable factors as well as the final model for each hypothesis. While TSF was significantly related to O-horizon C content, O-horizon depth, O-horizon phenol content, and mineral soil phenol content, in addition to co-variable parameters, it was non-significant in the final model determined by backwards selection for PMN and Charcoal mass (Figure A1, Table A5).

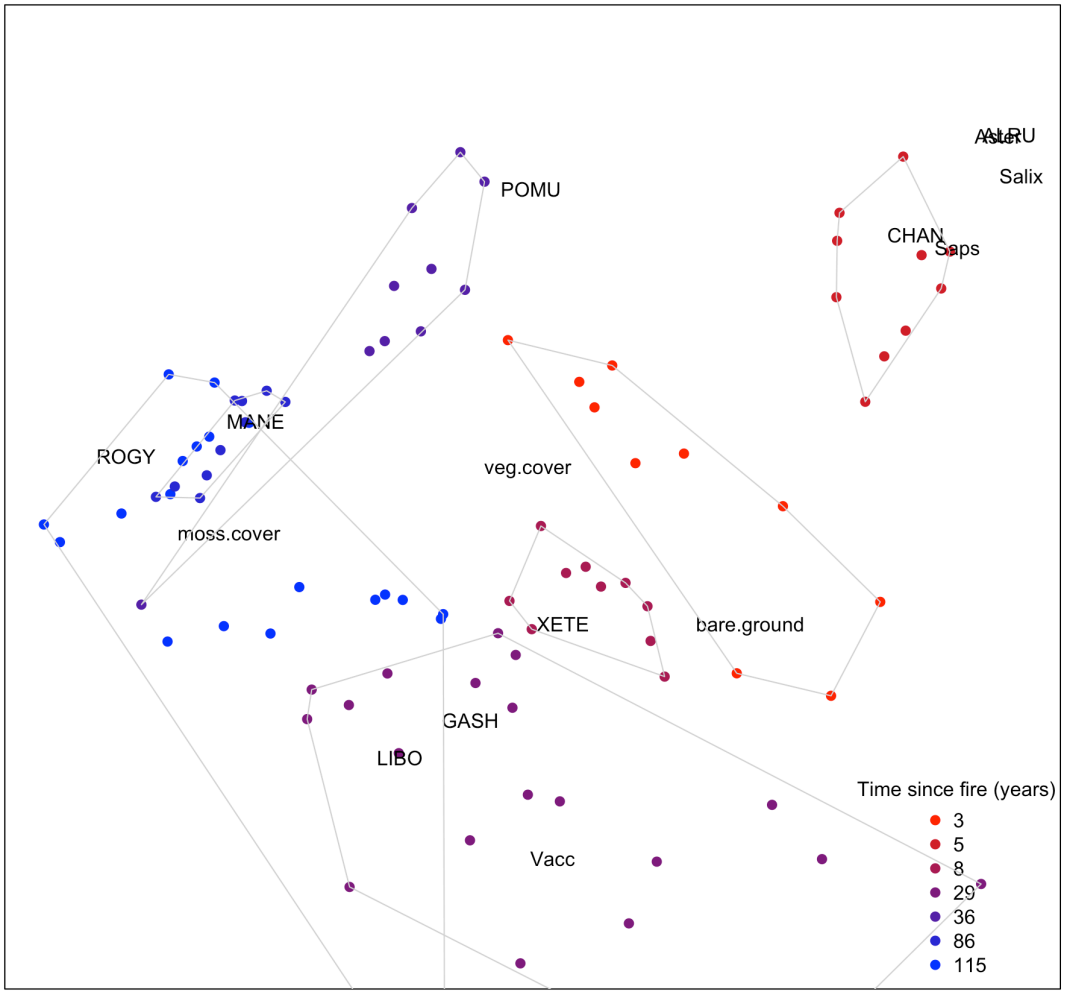

Figure 4.2: Nonmetric multidimensional scaling (NMDS) for vegetation variables measured at sites located along fire chronosequence on the east side Olympic peninsula, Washington. Groups are outlined by a gray line and colored to match the level of time since fire (years). Distance measures were calculated by the Bray-Curtis method.

4.3.2 *Belowground soil characteristics and trends along the fire chronosequence*

In the ordination space, NMDS visualizations of soil attributes show less separation than vegetation attributes, but a clear clockwise pattern of recent, intermediate, and historic fire history site loadings (stress = 0.181, Non-metric fit $R^2 = 0.967$, linear fit $R^2 = 0.864$) (Figure 4.3). Similar also to the vegetation NMDS, the majority of soil parameter variability within TSF loadings is attributed to intermediate and one historic fire history site (Figures 4.2 & 4.3). Soil variables were also significantly affected by TSF between sites (p-value < 0.01), but not within sites (Table A6). Soil C concentration in the O-horizon was significantly affected by TSF, as shown by Figure 4.4 and Table A8, although groupings do not suggest a strong linear relationship with the TSF gradient (Figure A1). Recent fire history site loadings are most strongly related to mineral soil C, mineral soil N, mineral soil NH_4^+-N, and have the highest vegetation cover. Intermediate fire history loadings are more closely related to high C/N ratios in O-horizon and mineral soils, and, as reiterated in Figure 4.4, have higher C concentrations in the O-horizon. Nitrate concentrations in mineral soil are more closely related a select few recent and intermediate fire sites, whereas historical site loadings are more related to phenol content in O-horizon and mineral soils, PMN, and moss cover (Figure 4.3). Linear model results show TSF as a significant co-variable when tested against O-horizon C content, O-horizon phenol content, mineral soil phenol content, PMN, and charcoal mass (Table A7).

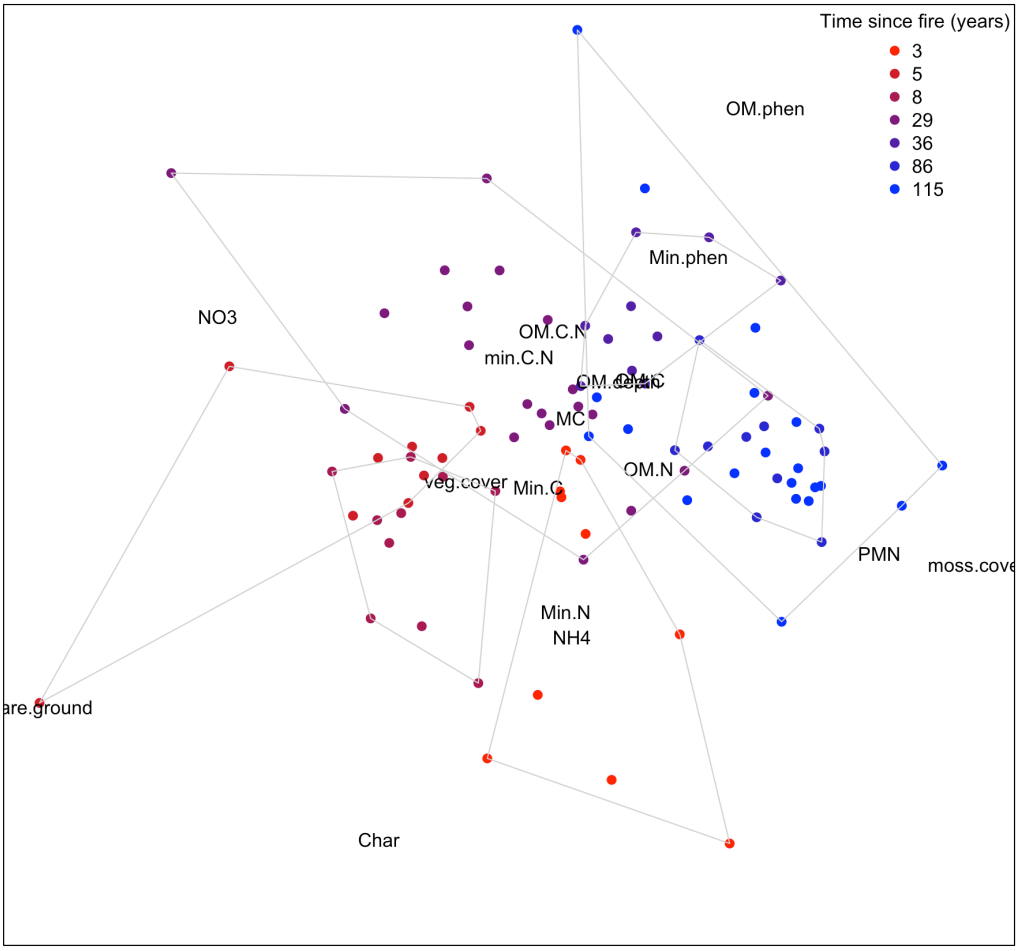

Figure 4.3: Nonmetric multidimensional scaling (NMDS) for soil variables measured at sites located along fire chronosequence on the east side Olympic peninsula, Washington. Groups are outlined by a gray line and colored to match the level of time since fire (years). Distance measures were calculated by the Euclidean method.

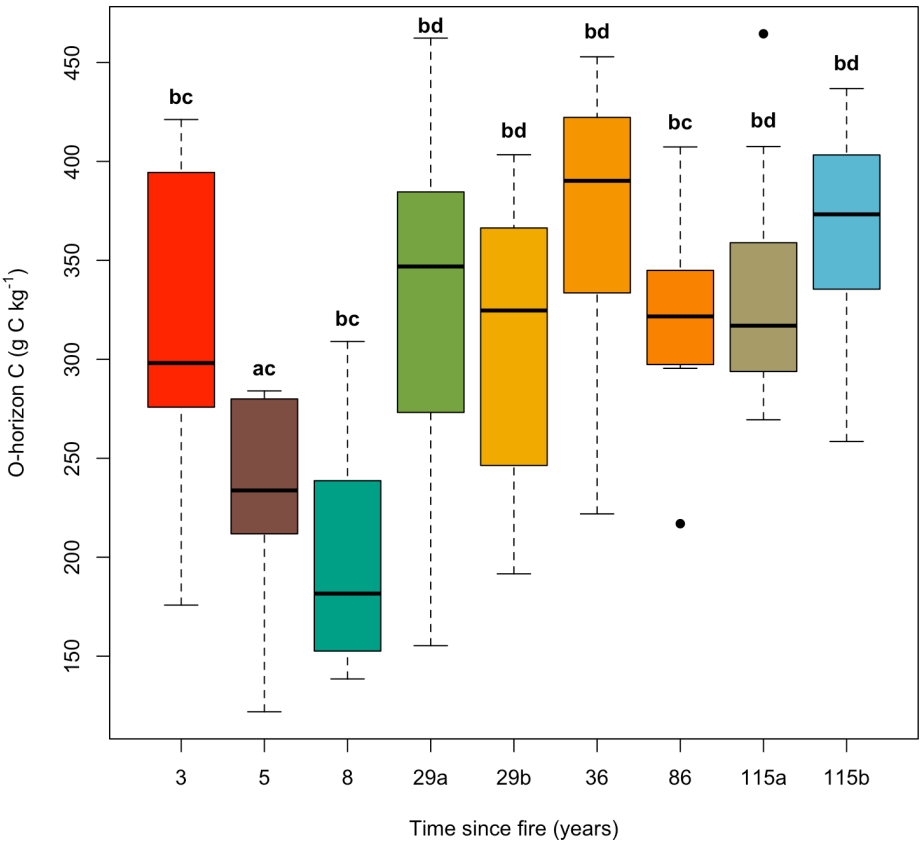

Figure 4.4: O-horizon C concentration along a fire chronosequence on the east side Olympic peninsula, Washington. Lettering denotes significant differences (p-value < 0.05). Boxplots of each plot show the median values (middle black line), the largest and smallest observations (vertical lines), and the 25th and 75th percentile (lower and upper bounds of boxes, respectively) (n = 10).

4.3.3 *Nitrogen cycling in burned and unburned paired plots*

Mineral soil collected from paired burned and unburned plots show significantly higher basal respiration rates (Figure 4.5 and Table A9). There was no significant interaction between burn history and the site factor. Net N mineralization (accumulation of NH_4^+-N) over the aerobic incubation yielded significant differences only by the site (TSF) and not burn history (Burn) (Figure 4.6 and Table A10). Mineralization rates were higher in the

most recently burned sites, and lowest in the burned site from 2011 (7 years since fire). Overall, net N mineralization rates decrease with TSF but show no significant difference from the effect of fire. Net nitrification rates were significantly different by site and there was a significant interaction between site and fire history, but no significant differences in fire history (Figure 4.8 and Table A12). Net nitrification rates were substantially higher in the most recently burned site and decrease after 5 years TSF to rates of unburned soils. Net nitrification rates compared by site and burn history showed a significant interaction between the two factors (Table A12).

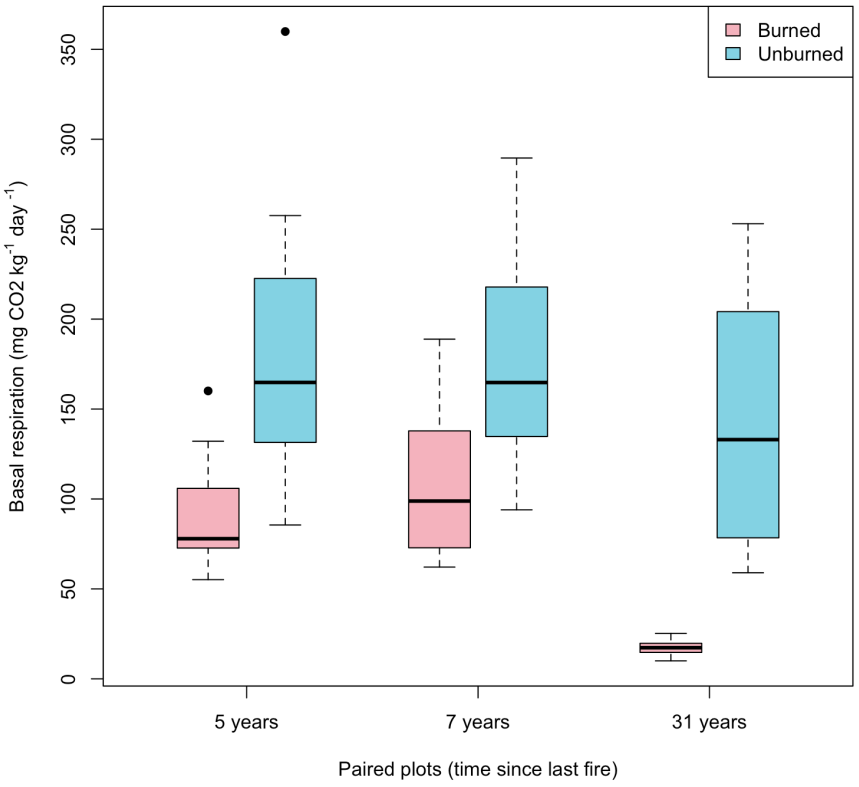

Figure 4.5: Soil basal respiration after a 24-hour period in mineral soils collected at paired burned and unburned plots located in the eastern Olympic peninsula, Washington (n = 12).

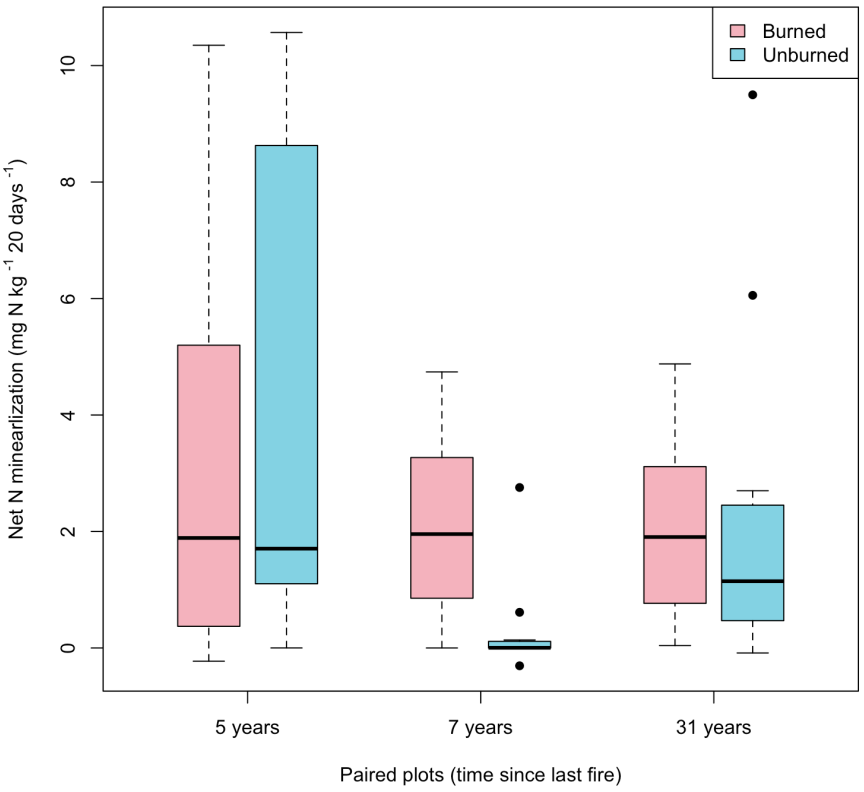

Figure 4.6: Net nitrogen mineralization rates after an aerobic incubation of mineral soils collected at paired burned and unburned plots located in the eastern Olympic peninsula, Washington (n = 12).

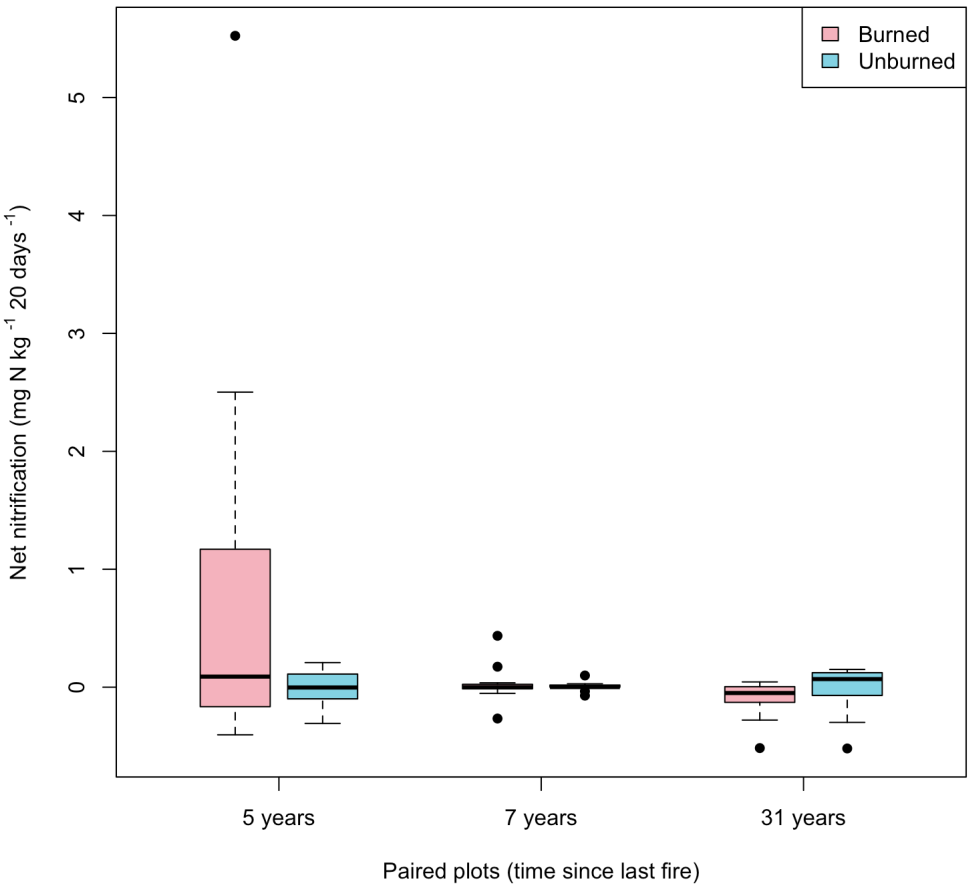

Figure 4.7: Net nitrification rates after an aerobic incubation of mineral soils collected at paired burned and unburned plots located in the eastern Olympic peninsula, Washington (n = 12).

4.4 DISCUSSION

Multivariate exploration of vegetation and soil responses along a fire chronosequence show significant groupings along the TSF gradient (Figures 4.2 & 4.3, Tables A4 & A5, *p*-value < 0.01) and suggests a successional progression most strongly pronounced in vegetation abundance and composition in these east side Olympic peninsula forest stands after wildfire events (Figures 4.2 & 4.3). Vegetation variables show greater separation in the ordination space and have more significant, linear correlations with TSF compared to soil variables (Figure A1), which suggests that vegetation abundance is more strongly affected by fire disturbances in these stands. The two TSF levels with replicate sites (115 and 29) show the highest variability in soil and vegetation variables, indicating heterogeneity within the fire perimeters was not captured by this study. Recent fire sites clearly show early succession vegetation dominated by the presence of *A. rubra*, *Salix* spp., and *C. angustifolium*. Recent sites also contain higher charcoal mass, mineral soil total N and inorganic available NH_4^+, though not significantly correlated with the TSF gradient (Figure 4.3). Intermediate fire sites show high variability in soil and vegetation parameters and acting as an intermediary transition in soil variables, but not in vegetation variables. Over time, soils shift toward phenolic-rich organic and mineral soils, high moss cover, and a high PMN index. This study provides evidence of a belowground response that is less sensitive to wildfire disturbances than the aboveground vegetation. High heterogeneity within soil variables and lack of strong soil variable correlations along the TSF gradient suggest that surface soils in forests of the eastern Olympic peninsula are robust in the face of fire disturbances. Alternatively, the study design may

not have captured wildfire effect trends outside the chronosequence range of 3 – 115 years since the last fire event.

Across multiple ecosystem types and fire regimes, studies illustrate trends in accumulation of C content in O-horizon soils and increase in O-horizon depth in the prolonged absence of a fire event (DeLuca et al., 2002; Lavoie and Mack, 2012; MacKenzie et al., 2004; Rothstein et al., 2004; Wardle et al., 2003). Our findings support previously described trends of O-horizon depth and O-horizon C content increasing with TSF in these chronosequence sites ($r = 0.22$, p-value < 0.05 and $r = 0.28$, p-value < 0.01, respectively). The depth of the O-horizon was strongly influenced by the presence of *Vaccinium* spp., a common component of frequently burned boreal forests (Zackrisson, 1977) and a perennial forb (*X. tenax*), which spreads by rhizomes and is possibly a relic of anthropogenic fire use in the region (Shebitz et al., 2008). The O-horizon depth was also correlated with O-horizon phenol content ($r = 0.21$, < 0.05), indicating phenolic-rich biomass or a byproduct of lignin decomposition (Hättenschwiler and Vitousek, 2000). Similarly, as C content of the O-horizon increases so did the content of N in O-horizon soils, and yet we found no correlations with C/N ratio (Figure A1, Table A7). These trends may indicate a shift towards recalcitrant, N-rich O-horizon in older secondary succession sites (Figures 4.2 & 4.3).

Contrary to previous studies, this study did not show any significant correlations in total or available N content along the TSF gradient. Previous studies in temperate and boreal forest ecosystems display an immediate increase in N availability that declined with time

after the wildfire events (DeLuca et al., 2002; Lavoie and Mack, 2012; MacKenzie et al., 2004; Rothstein et al., 2004), which was not detected in the recent fire sites of this study. The mass-based accounting of organic C and N in this study may have overwhelmed the effect of fire due to the high rock content in mineral soils. The lack of detectable differences in available N in recent fire sites and in N transformations of paired burned and unburned soil incubations further implies that the fire chronosequence design did not capture immediate fire effects by measuring sites burned less than 3 years prior. Carbon mineralization, as measured by 24-hour CO_2 evolution, was higher in unburned soils, but there was no difference in N mineralization of burned and unburned soils (Figures 4.6 & 4.7, Tables A10 & A11), signifying higher microbial activity and substrate decomposition, but also possible heterotrophic competition for N substrates (Kaye and Hart, 1997). Differences in N mineralization rates are a product of site-specific variability rather than fire effects (Figure 4.6 & Table A10). Interestingly, nitrification rates were significantly highest in the most recently burned plot (5 years TSF), a trend that may suggest a previously documented release of nitrification rates attributed to adsorption of inhibiting phenolic compounds by charcoal surfaces (DeLuca et al., 2002). While adsorption capacity of wildfire-produced charcoal collected from these sites does not change significantly with TSF (Pingree et al., 2016), the higher charcoal mass in recent fire sites may contribute to a greater adsorption effect of charcoal in recent fire sites (Chapter 3). Lastly, we found no changes in total and available N along the fire chronosequence sites; however, the index of PMN significantly increased ($r = 0.4$, $p < 0.001$). Forest soils in this fire chronosequence may accumulate less labile organic matter

over time, hindering the mineralization of N by relatively high phenol concentrations in O-horizon and mineral soils.

In summary, findings from this study show that forest stands on the east side Olympic peninsula, Washington, are more sensitive to wildfire events in aboveground abundance and composition compared to surface organic and mineral soil C and N pools. Total O-horizon C, but not total N, was significantly and positively correlated with TSF ($r = 0.38$, p-value < 0.001, Figure A1). Linear models of O-horizon pools (C and phenol) show vegetation and soil co-variates explain a greater proportion of variance than TSF (Tables A5 & A7). Over the fire chronosequence, the amount of N released by anaerobic incubation was significantly and positively correlated to TSF ($r = 0.4$, p-value < 0.001, Figure A1) and was also influenced by percent of moss cover, *Vaccinium* spp. cover, and C:N ratios in both organic and surface mineral soils, which may suggest a shift towards more recalcitrant N forms in later succession sites. Charcoal mass over the TSF gradient ($r = -0.44$, p-value < 0.001, Figure A1) was similar in magnitude to O-horizon phenol content ($r = 0.36$, p-value < 0.001, Figure A1), but it is likely that the adsorption capacity of charcoal particles present in the O-horizon are saturated and display insignificant adsorption capacities soon after a wildfire event (Pingree et al., 2016). Lastly, net nitrification rates are highly influenced by site characteristics that either overcome post-wildfire stimulation or sites have returned to pre-fire nitrification rates (Figure 4.7 & 4.8, Table A11).

These results show similar successional pathways described for the *P. menziesii-T. heterophylla* potential vegetation zone (Franklin and Dyrness, 1973; Henderson et al., 1989) and illustrate aboveground sensitivity to wildfire events. Vegetation is dominated by early seral species such as *A. rubra*, *Salix* spp., *C. angustifolium* in recent fire sites, *Vaccinium* spp. and *G. shallon* in intermediate sites, and finally *M. repens* and moss cover at historic fire sites. Mixed-severity fire regimes result in heterogeneity that may contribute to the robust belowground surface soil patterns described herein. Fewer soil variables measured in this study were correlated to TSF compared to vegetation variables. Vegetation variables displayed clearer separation in TSF groupings with NMDS ordination corresponding to a slightly higher *p*-value in PERMANOVA. This assessment of aboveground and belowground characteristics in mixed-severity fire regime forests suggests that soils are more resilient and recover to pre-fire conditions earlier than vegetation – the function of wildfires in this region may be more closely aligned with vegetation composition than nutrient cycling dynamics.

Chapter 5. SYNTHESIS

This dissertation comprises three primary research papers with Chapters 2, 3, and 4 that were written to assess the influence of charcoal and quantify the impact of wildfire on C and N pools in soils of mixed-severity fire regime, *P. menziesii* dominated forest stands. The first chapter of this dissertation identifies a need to apply concepts of charcoal adsorption capacity to a forest stand scale, test previously documented trends of wildfire effects to this mixed-severity fire ecosystem, and provide a baseline of wildfire effects in the rain shadow Olympic peninsula forests that are expected to experience more extensive and frequent wildfire events with changing climate conditions (Halofsky et al., 2011b).

The research findings from Chapter 2 stand in contrast to the previously documented trend of a decreasing adsorption capacity over a fire chronosequence gradient of time-since-fire (Keech et al., 2005; Zackrisson et al., 1996), which is likely a result of differences in the adsorption capacity measurement techniques and adsorbent saturation, differences in ecosystem type, and differences in the number and range of age of chronosequence sites (a range of 115 years versus 365 years) used in the studies. A common measure of charcoal adsorption capacity involved an indirect method where the inhibitory effect of seedling germination was a proxy for adsorption of phenolic compounds in the solution to charcoal particles. Adsorption batch experiments with simple phenol in solution show no change in maximum adsorption capacity, but do not evaluate adsorption behavior at concentrations lower than 500 ppm in wildfire-produced charcoal particles. We did not find evidence of adsorption capacity as a driving mechanism in O-horizon DOC leachate rates at the 3 – 115 year fire chronosequence sites. Average maximum adsorption

capacity was extrapolated to forest O-horizon soil characteristics in Chapter 3 and this normalization suggests that adsorption capacity was likely saturated at the earliest TSF site (BH, 3 years), which helps explain the findings in Chapters 2 (Figure 2.1) and the lack of correlation between charcoal mass and O-horizon DOC leachate rates ($R^2 = 0.03$, p-value > 0.05). These findings illustrate the importance of applying field conditions and ecosystem parameters in order to extrapolate laboratory-measured phenomena to heterogeneous and dynamic systems.

Multivariate, non-parametric ordination of surface soil and vegetation response variables across the eastern Olympic peninsula fire chronosequence provides a comprehensive visualization of plot relationships and patterns. Vegetation variables are clearly grouped by TSF and soil variables are more dispersed in NMDS visualizations although both soil and vegetation PERMANOVA results showed a significant influence of TSF on response variables between sites. Linear models adhere to the assumptions of traditional statistics and display the importance of co-variant plot-level response variables (Tables A5 & A7), while the multivariate, non-parametric techniques give a holistic and broad perspective of these co-correlated response variables along the fire chronosequence. Chronosequence designs are best suited for such broad generalizations along a TSF gradient and encourage mechanistic inquiry into specific patterns and relationships. Forest soils of the eastern Olympic peninsula yielded a short-term increase in net nitrification in burned soils, an increase in depth, phenolic content, O-horizon C content, and O-horizon DOC leachate over the TSF gradient which may be related to vegetation species composition (e.g. moss cover) or humification processes that also result in higher PMN index in historic fire sites. These relationships, however, are speculative without reductionist experimentation to measure specific mechanisms. Research findings from this study provide

impetus for future studies in mechanisms of post-fire surface soil patterns in this mixed-severity fire regime ecosystem.

Wildfire effects across the chronosequence sites indicate that forest soils in the rain shadow forests of the Olympic peninsula may be more resilient to mixed-severity fire disturbances than the understory vegetation community and able to recover more quickly from a single wildfire event within the historical fire regime. These studies do not encompass immediate post-fire effects (< 3 years since the last fire event), which may be important when assessing fire effects on charcoal adsorption capacity, microbial activity, and N cycling (Choromanska and DeLuca, 2001; Choromanska and DeLuca, 2002). The findings of these studies are also limited to current and historic fire history and fire severity regimes defined by moderate severity and spatial and temporal heterogeneity. Given a shift in fire frequency and extend that increases fire severity, forest soil C and N pools may be significantly depleted (Bormann et al., 2008; Homann et al., 2011). Further research would be necessary in this highly productive and highly heterogeneous ecosystem to better understand the capacity of these forest soils to buffer wildfire impacts on C and N pools and N cycling after future fire events. Furthermore, the high variability and complex nature of co-correlated response variables limits the extrapolation of these findings to different mixed-severity fire regime ecosystems, which should be avoided without preliminary exploration.

BIBLIOGRAPHY

Agee, J.K., 1993. Fire Ecology of Pacific Northwet Forests. Island Press, Covelo, CA.

Ascough, P.L., Bird, M.I., Francis, S.M., Thornton, B., Midwood, A.J., Scott, A.C., Apperley, D., 2011. Variability in oxidative degradation of charcoal: Influence of production conditions and environmental exposure. Geochimica et Cosmochimica Acta 75(9), 2361-2378.

Baird, M., Zabowski, D., Everett, R.L., 1999. Wildfire effects on carbon and nitrogen in inland coniferous forests. Plant and Soil 209(2), 233-243.

Baldock, J.A., Smernik, R.J., 2002. Chemical composition and bioavailability of thermally altered Pinus resinosa (Red pine) wood. Organic Geochemistry 33(9), 1093-1109.

Ball, P.N., MacKenzie, M.D., DeLuca, T.H., Montana, W.E.H., 2010. Wildfire and Charcoal Enhance Nitrification and Ammonium-Oxidizing Bacterial Abundance in Dry Montane Forest Soils. Journal of Environmental Quality 39(4), 1243-1253.

Barrow, C.J., 2012. Biochar: Potential for countering land degradation and for improving agriculture. Applied Geography 34, 21-28.

Barto, E.K., Hilker, M., Müller, F., Mohney, B.K., Weidenhamer, J.D., Rillig, M.C., 2011. The Fungal Fast Lane: Common Mycorrhizal Networks Extend Bioactive Zones of Allelochemicals in Soils. PLOS ONE 6(11), e27195.

Bélanger, N., Pinno, B.D., 2008. Carbon sequestration, vegetation dynamics and soil development in the Boreal Transition ecoregion of Saskatchewan during the Holocene. CATENA 74(1), 65-72.

Berglund, L.M., DeLuca, T.H., Zackrisson, O., 2004. Activated carbon amendments to soil alters nitrification rates in Scots pine forests. Soil Biology and Biochemistry 36(12), 2067-2073.

Blum, U., 1996. Allelopathic interactions involving phenolic acids. Journal of Nematology 28(3), 259.

Blum, U., Shafer, S.R., Lehman, M.E., 1999. Evidence for inhibitory allelopathic interactions involving phenolic acids in field soils: concepts vs. an experimental model. Critical Reviews in Plant Sciences 18(5), 673-693.

Bormann, B.T., Homann, P.S., Darbyshire, R.L., Morrissette, B.A., 2008. Intense forest wildfire sharply reduces mineral soil C and N: the first direct evidence. Canadian Journal of Forest Research 38(11), 2771-2783.

Bornemann, L.C., Kookana, R.S., Welp, G., 2007. Differential sorption behaviour of aromatic hydrocarbons on charcoals prepared at different temperatures from grass and wood. Chemosphere 67(5), 1033-1042.

Box, J.D., 1983. Investigation of the Folin-Ciocalteau phenol reagent for the determination of polyphenolic substances in natural waters. Water Research 17(5), 511-525.

Braida, W.J., Pignatello, J.J., Lu, Y., Ravikovitch, P.I., Neimark, A.V., Xing, B., 2003. Sorption Hysteresis of Benzene in Charcoal Particles. Environmental Science & Technology 37(2), 409-417.

Bremner, J.M., McCarty, G.W., 1988. Effects of Terpenoids on Nitrification in Soil. Soil Science Society of America Journal 52(6), 1630-1633.

Brimmer, R.J., 2006. Sorption potential of naturally occurring charcoal in ponderosa pine forests of western Montana (MS thesis). Missoula, MT: University of Montana.

Buma, B., Poore, R.E., Wessman, C.A., 2014. Disturbances, Their Interactions, and Cumulative Effects on Carbon and Charcoal Stocks in a Forested Ecosystem. Ecosystems 17(6), 947-959.

Certini, G., 2005. Effects of fire on properties of forest soils: a review. Oecologia 143(1), 1-10.

Certini, G., 2014. Fire as a Soil-Forming Factor. AMBIO 43(2), 191-195.

Chapin, F.S., Matson, P.A., Vitousek, P., 2011. Principles of Terrestrial Ecosystem Ecology. 2nd ed. Springer-Verlag, New York.

Cheng, C.-H., Lehmann, J., 2009. Ageing of black carbon along a temperature gradient. Chemosphere 75(8), 1021-1027.

Cheng, C.-H., Lehmann, J., Engelhard, M.H., 2008. Natural oxidation of black carbon in soils: changes in molecular form and surface charge along a climosequence. Geochimica et Cosmochimica Acta 72(6), 1598-1610.

Cheng, C.-H., Lehmann, J., Thies, J.E., Burton, S.D., Engelhard, M.H., 2006. Oxidation of black carbon by biotic and abiotic processes. Organic Geochemistry 37(11), 1477-1488.

Chia, C.H., Downie, A., Munroe, P., 2015. Characteristics of biochar: physical and structural properties. In: J. Lehmann, S. Joseph (Eds.), Biochar for Enviornmental Management: Science, Technology and Implementation. Routledge, New York, pp. 89-109.

Choromanska, U., DeLuca, T.H., 2001. Prescribed Fire Alters the Impact of Wildfire on Soil Biochemical Properties in a Ponderosa Pine Forest. Soil Science Society of America Journal 65(1), 232-238.

Choromanska, U., DeLuca, T.H., 2002. Microbial activity and nitrogen mineralization in forest mineral soils following heating: evaluation of post-fire effects. Soil Biology and Biochemistry 34(2), 263-271.

Clark, J.S., Lynch, J., Stocks, B.J., Goldammer, J.G., 1998. Relationships between charcoal particles in air and sediments in west-central Siberia. The Holocene 8(1), 19-29.

Clarke, K.R., 1993. Non-parametric multivariate analyses of changes in community structure. Australian Journal of Ecology 18(1), 117-143.

Cornelissen, G., Elmquist, M., Groth, I., Gustafsson, Ö., 2004. Effect of sorbate planarity on environmental black carbon sorption. Environmental Science & Technology 38(13), 3574-3580.

Cornelissen, G., Gustafsson, Ö., 2004. Sorption of Phenanthrene to Environmental Black Carbon in Sediment with and without Organic Matter and Native Sorbates. Environmental Science & Technology 38(1), 148-155.

Currie, W.S., Aber, J.D., McDowell, W.H., Boone, R.D., Magill, A.H., 1996. Vertical transport of dissolved organic C and N under long-term N amendments in pine and hardwood forests. Biogeochemistry 35(3), 471-505.

Cutler, N.A., Arróniz-Crespo, M., Street, L.E., Jones, D.L., Chaput, D.L., DeLuca, T.H., 2016. Long-Term Recovery of Microbial Communities in the Boreal Bryosphere Following Fire Disturbance. Microbial Ecology, 1-16.

Dąbrowski, A., Podkościelny, P., Hubicki, Z., Barczak, M., 2005. Adsorption of phenolic compounds by activated carbon—a critical review. Chemosphere 58(8), 1049-1070.

Daly, C., Gibson, W.P., Taylor, G.H., Johnson, G.L., Pasteris, P., 2002. A knowledge-based approach to the statistical mapping of climate. Climate Research 22(2), 99-113.

Das Gupta, S., Mackenzie, M.D., 2016. Spatial Patterns of Soil Respiration Links Above and Belowground Processes along a Boreal Aspen Fire Chronosequence. PLOS ONE 11(11), e0165602.

De la Rosa, J.M., Knicker, H., López-Capel, E., Manning, D.A.C., González-Perez, J.A., González-Vila, F.J., 2008. Direct Detection of Black Carbon in Soils by Py-GC/MS, Carbon-13 NMR Spectroscopy and Thermogravimetric Techniques. Soil Science Society of America Journal 72(1).

Dell'Abate, M.T., Benedetti, A., Brookes, P.C., 2003. Hyphenated techniques of thermal analysis for characterisation of soil humic substances. Journal of Separation Science 26(5), 433-440.

DeLuca, T.H., Aplet, G.H., 2008. Charcoal and carbon storage in forest soils of the Rocky Mountain West. Frontiers in Ecology and the Environment 6(1), 18-24.

DeLuca, T.H., Boisvenue, C., 2012. Boreal forest soil carbon: distribution, function and modelling. Forestry.

DeLuca, T.H., MacKenzie, M.D., Gundale, M.J., Holben, W.E., 2006. Wildfire-Produced Charcoal Directly Influences Nitrogen Cycling in Ponderosa Pine Forests. Soil Science Society of America Journal 70(2), 448.

DeLuca, T.H., Nilsson, M., Zackrisson, O., 2002. Nitrogen mineralization and phenol accumulation along a fire chronosequence in northern Sweden. Oecologia 133(2), 206-214.

DeLuca, T.H., Sala, A., 2006. Frequent fire alters nitrogen transformations in ponderosa pine stands of the inland northwest. Ecology 87(10), 2511-2522.

DeLuca, T.H., Zackrisson, O., Gundale, M.J., Nilsson, M.-C., 2008. Ecosystem Feedbacks and Nitrogen Fixation in Boreal Forests. Science 320(5880), 1181-1181.

Ding, Y., Cawley, K.M., da Cunha, C.N., Jaffé, R., 2014. Environmental dynamics of dissolved black carbon in wetlands. Biogeochemistry 119(1), 259-273.

Dittmar, T., de Rezende, C.E., Manecki, M., Niggemann, J., Coelho Ovalle, A.R., Stubbins, A., Bernardes, M.C., 2012. Continuous flux of dissolved black carbon from a vanished tropical forest biome. Nature Geosci 5(9), 618-622.

Dooley, S.R., Treseder, K.K., 2012. The effect of fire on microbial biomass: a meta-analysis of field studies. Biogeochemistry 109(1-3), 49-61.

Earnest, C.M., 1988. The Modern Thermogravimetric Approach to the Compositional Analysis of Materials. In: C.M. Earnest (Ed.), Compositional Analysis by Thermogravimetry. American Society for Testing and Materials, Baltimore, pp. 1-18.

Fahnestock, G.R., Agee, J.K., 1983. Biomass Consumption and Smoke Production by Prehistoric and Modern Forest Fires in Western Washington. Journal of Forestry 81(10), 653-657.

Fastie, C.L., 1995. Causes and Ecosystem Consequences of Multiple Pathways of Primary Succession at Glacier Bay, Alaska. Ecology 76(6), 1899-1916.

Fonda, R.W., Binney, E.P., 2011. Vegetation Response to Prescribed Fire in Douglas-Fir Forests, Olympic National Park. Northwest Science 85(1), 30-40.

Fonda, R.W., Bliss, L.C., 1969. Forest Vegetation of the Montane and Subalpine Zones, Olympic Mountains, Washington. Ecological Monographs 39(3), 271-301.

Forbes, M.S., Raison, R.J., Skjemstad, J.O., 2006. Formation, transformation and transport of black carbon (charcoal) in terrestrial and aquatic ecosystems. Science of The Total Environment 370(1), 190-206.

Franklin, J.F., Dyrness, C.T., 1973. Natural Vegetation of Oregon and Washington. USDA Forest Service General Technical Report, Pacific Northwest Forest and Range Experiment Station (PNW-8).

Franklin, J.F., Johnson, K.N., 2012. A Restoration Framework for Federal Forests in the Pacific Northwest. Journal of Forestry 110(8), 429-439.

Franklin, R.E., 1951. Crystallite Growth in Graphitizing and Non-Graphitizing Carbons. Proceedings of the Royal Society of London. Series A. Mathematical and Physical Sciences 209(1097), 196-218.

Fukami, T., Wardle, D.A., 2005. Long-term ecological dynamics: reciprocal insights from natural and anthropogenic gradients. Proceedings of the Royal Society B: Biological Sciences 272(1577), 2105-2115.

Gavin, G.D., Brubaker, B.L., 2015. Late Quaternary Vegetation and Fire History of the Olympic Peninsula, Late Pleistocene and Holocene Environmental Change on the Olympic Peninsula, Washington. Springer International Publishing, Cham, pp. 61-106.

Gee, G.W., Or, D., 2002. 2.4 Particle-Size Analysis. In: J.H. Dane, C.G. Topp (Eds.), Methods of Soil Analysis: Part 4 Physical Methods. SSSA Book Series. Soil Science Society of America, Madison, WI, pp. 255-293.

Glaser, B., Haumaier, L., Guggenberger, G., Zech, W., 1998. Black carbon in soils: the use of benzenecarboxylic acids as specific markers. Organic Geochemistry 29(4), 811-819.

Glaser, B., Haumaier, L., Guggenberger, G., Zech, W., 2001. The 'Terra Preta' phenomenon: a model for sustainable agriculture in the humid tropics. Naturwissenschaften 88(1), 37-41.

Glaser, B., Lehmann, J., Zech, W., 2002. Ameliorating physical and chemical properties of highly weathered soils in the tropics with charcoal – a review. Biology and Fertility of Soils 35(4), 219-230.

Glasspool, I.J., Edwards, D., Axe, L., 2006. Charcoal in the Early Devonian: A wildfire-derived Konservat–Lagerstätte. Review of Palaeobotany and Palynology 142(3–4), 131-136.

Gundale, M.J., DeLuca, T.H., 2006a. Temperature and source material influence ecological attributes of ponderosa pine and Douglas-fir charcoal. Forest Ecology and Management 231(1), 86-93.

Gundale, M.J., DeLuca, T.H., 2006b. Temperature and source material influence ecological attributes of ponderosa pine and Douglas-fir charcoal. Forest Ecology and Management 231(1-3), 86-93.

Gundale, M.J., DeLuca, T.H., 2007. Charcoal effects on soil solution chemistry and growth of Koeleria macrantha in the ponderosa pine/Douglas-fir ecosystem. Biology and Fertility of Soils 43(3), 303-311.

Gundale, M.J., Sverker, J., Albrectsen, B.R., Nilsson, M.-C., Wardle, D.A., 2010. Variation in protein complexation capacity among and within six plant species across a boreal forest chronosequence. Plant Ecology 211(2), 253-266.

Guo, Y., Bustin, R.M., 1998. FTIR spectroscopy and reflectance of modern charcoals and fungal decayed woods: implications for studies of inertinite in coals. International Journal of Coal Geology 37(1–2), 29-53.

Hale, S.E., Cornelissen, G., Werner, D., 2015. Sorption and remediation of organic compounds in soils and sediments by (activated) biochar. In: J. Lehmann, S. Joseph (Eds.), Biochar for Enviornmental Management: Science, Technology and Implementation. Routledge, New York, pp. 625-678.

Hale, S.E., Tomaszewski, J.E., Luthy, R.G., Werner, D., 2009. Sorption of dichlorodiphenyltrichloroethane (DDT) and its metabolites by activated carbon in clean water and sediment slurries. Water Research 43(17), 4336-4346.

Halofsky, J., Donato, D., Hibbs, D., Campbell, J., Cannon, M.D., Fontaine, J., Thompson, J., Anthony, R., Bormann, B., Kayes, L., 2011a. Mixed-severity fire regimes: lessons and hypotheses from the Klamath-Siskiyou Ecoregion. Ecosphere 2(4), 40.

Halofsky, J.E., Peterson, D.L., O'Halloran, K.A., 2011b. Adapting to climate change at Olympic National Forest and Olympic National Park. Gen. Tech. Rep. PNW-GTR-844. In: F.S. U.S. Department of Agriculture, Pacific Northwest Research Station (Ed.), Portland, OR, pp. 130.

Hammes, K., Schmidt, M.W.I., Smernik, R.J., Currie, L.A., Ball, W.P., Nguyen, T.H., Louchouarn, P., Houel, S., Gustafsson, Ö., Elmquist, M., Cornelissen, G., Skjemstad, J.O., Masiello, C.A., Song, J., Peng, P.a., Mitra, S., Dunn, J.C., Hatcher, P.G., Hockaday, W.C., Smith, D.M., Hartkopf-Fröder, C., Böhmer, A., Lüer, B., Huebert, B.J., Amelung, W., Brodowski, S., Huang, L., Zhang, W., Gschwend, P.M., Flores-Cervantes, D.X., Largeau, C., Rouzaud, J.-N., Rumpel, C., Guggenberger, G., Kaiser, K., Rodionov, A., Gonzalez-Vila, F.J., Gonzalez-Perez, J.A., de la Rosa, J.M., Manning, D.A.C., López-Capél, E., Ding, L., 2007. Comparison of quantification methods to measure fire-derived (black/elemental) carbon in soils and sediments using reference materials from soil, water, sediment and the atmosphere. Global Biogeochemical Cycles 21(3), n/a-n/a.

Hanson, B.A., 2014. ChemoSpec: Exploratory Chemometrics for Spectroscopy.

Hargreaves, G.H., 1975. Moisture Availability and Crop Production. 18(5).

Hart, S.C., DeLuca, T.H., Newman, G.S., MacKenzie, M.D., Boyle, S.I., 2005. Post-fire vegetative dynamics as drivers of microbial community structure and function in forest soils. Forest Ecology and Management 220(1), 166-184.

Hart, S.C., Stark, J.M., Davidson, E.A., Firestone, M.K., 1994. Nitrogen Minearlization, Immobilization, and Nitrification, Methods of Soil Analysis: Part 2—Microbiological and Biochemical Properties. SSSA Book Series, Madison, WI, pp. 985-1018.

Hatten, J., Zabowski, D., Scherer, G., Dolan, E., 2005. A comparison of soil properties after contemporary wildfire and fire suppression. Forest Ecology and Management 220(1–3), 227-241.

Hättenschwiler, S., Vitousek, P.M., 2000. The role of polyphenols in terrestrial ecosystem nutrient cycling. Trends in Ecology & Evolution 15(6), 238-243.

Hedges, J.I., Eglinton, G., Hatcher, P.G., Kirchman, D.L., Arnosti, C., Derenne, S., Evershed, R.P., Kögel-Knabner, I., de Leeuw, J.W., Littke, R., Michaelis, W., Rullkötter, J., 2000. The molecularly-uncharacterized component of nonliving organic matter in natural environments. Organic Geochemistry 31(10), 945-958.

Henderson, J.A., Peter, D.H., Lesher, R.D., Shaw, D.C., 1989. Forested plant associations of the Olympic National Forest. In: F.S. U.S. Department of Agriculture, Pacific Northwest Research Station (Ed.).

Hockaday, W.C., Grannas, A.M., Kim, S., Hatcher, P.G., 2007. The transformation and mobility of charcoal in a fire-impacted watershed. Geochimica et Cosmochimica Acta 71(14), 3432-3445.

Homann, P.S., Bormann, B.T., Darbyshire, R.L., Morrissette, B.A., 2011. Forest Soil Carbon and Nitrogen Losses Associated with Wildfire and Prescribed Fire. Soil Science Society of America Journal 75(5), 1926-1934.

Homann, P.S., Harmon, M., Remillard, S., Smithwick, E.A.H., 2005. What the soil reveals: Potential total ecosystem C stores of the Pacific Northwest region, USA. Forest Ecology and Management 220(1–3), 270-283.

Huff, M.H., 1995. Forest Age Structure and Development Following Wildfires in the Western Olympic Mountains, Washington. Ecological Applications 5(2), 471-483.

Hyodo, F., Kusaka, S., Wardle, D.A., Nilsson, M.-C., 2013. Changes in stable nitrogen and carbon isotope ratios of plants and soil across a boreal forest fire chronosequence. Plant and Soil 364(1), 315-323.

Jaafar, N.M., Clode, P.L., Abbott, L.K., 2015. Soil Microbial Responses to Biochars Varying in Particle Size, Surface and Pore Properties. Pedosphere 25(5), 770-780.

Jaffé, R., Ding, Y., Niggemann, J., Vähätalo, A.V., Stubbins, A., Spencer, R.G.M., Campbell, J., Dittmar, T., 2013. Global Charcoal Mobilization from Soils via Dissolution and Riverine Transport to the Oceans. Science 340(6130), 345-347.

Johnson, E.A., Miyanishi, K., 2008. Testing the assumptions of chronosequences in succession. Ecology Letters 11(5), 419-431.

Johnston, C., Aochi, Y., Sparks, D., Page, A., Helmke, P., Loeppert, R., Soltanpour, P., Tabatabai, M., Sumner, M., 1996. Fourier transform infrared and Raman spectroscopy, Methods of Soil Analysis. Part 3 - Chemical Methods. Soil Science Society of America and American Society of Agronomy, Madison, WI, pp. 269-321.

Jones, D.L., Murphy, D.V., Khalid, M., Ahmad, W., Edwards-Jones, G., DeLuca, T.H., 2011. Short-term biochar-induced increase in soil CO2 release is both biotically and abiotically mediated. Soil Biology and Biochemistry 43(8), 1723-1731.

Kagan, J., 2010. Oregon and Washington Potential Vegetation Type. Institute for Natural Resources, Portland, Oregon.

Kalbitz, K., Kaiser, K., 2008. Contribution of dissolved organic matter to carbon storage in forest mineral soils. Journal of Plant Nutrition and Soil Science 171(1), 52-60.

Kalbitz, K., Solinger, S., Park, J.-H., Michalzik, B., Matzner, E., 2000. CONTROLS ON THE DYNAMICS OF DISSOLVED ORGANIC MATTER IN SOILS: A REVIEW. Soil Science 165(4), 277-304.

Kaye, J.P., Hart, S.C., 1997. Competition for nitrogen between plants and soil microorganisms. Trends in Ecology & Evolution 12(4), 139-143.

Keech, O., Carcaillet, C., Nilsson, M.-C., 2005. Adsorption of allelopathic compounds by wood-derived charcoal: the role of wood porosity. Plant and Soil 272(1-2), 291-300.

Keiluweit, M., Kleber, M., 2009. Molecular-Level Interactions in Soils and Sediments: The Role of Aromatic π-Systems. Environmental Science & Technology 43(10), 3421-3429.

Kleber, M., Hockaday, W.C., Nico, P.S., 2015. Characteristics of biochar: macro-molecular properties. In: J. Lehmann, S. Joseph (Eds.), Biochar for Enviornmental Management: Science, Technology and Implementation. Routledge, New York, pp. 111-137.

Knapp, P.A., Hadley, K.S., 2012. A 300-year history of Pacific Northwest windstorms inferred from tree rings. Global and Planetary Change 92–93, 257-266.

Knicker, H., 2007. How does fire affect the nature and stability of soil organic nitrogen and carbon? A review. Biogeochemistry 85(1), 91-118.

Kraus, T.E.C., Dahlgren, R.A., Zasoski, R.J., 2003. Tannins in nutrient dynamics of forest ecosystems - a review. Plant and Soil 256(1), 41-66.

Kurth, V.J., Hart, S.C., Ross, C.S., Kaye, J.P., Fulé, P.Z., 2014. Stand-replacing wildfires increase nitrification for decades in southwestern ponderosa pine forests. Oecologia 175(1), 395-407.

Kurth, V.J., MacKenzie, M.D., DeLuca, T.H., 2006. Estimating charcoal content in forest mineral soils. Geoderma 137(1–2), 135-139.

Langmuir, D., 1997. Aqueous environmental geochemistry. Prentice Hall, Upper Saddle River, NJ.

Lavoie, M., Mack, M.C., 2012. Spatial heterogeneity of understory vegetation and soil in an Alaskan upland boreal forest fire chronosequence Biogeochemistry (107), 227-239.

Law, B.E., Thornton, P.E., Irvine, J., Anthoni, P.M., Van Tuyl, S., 2001. Carbon storage and fluxes in ponderosa pine forests at different developmental stages. Global Change Biology 7(7), 755-777.

Leifeld, J., 2007. Thermal stability of black carbon characterised by oxidative differential scanning calorimetry. Organic Geochemistry 38(1), 112-127.

Liang, B., Lehmann, J., Solomon, D., Sohi, S., Thies, J.E., Skjemstad, J.O., Luizao, F.J., Engelhard, M.H., Neves, E.G., Wirick, S., 2008a. Stability of biomass-derived black carbon in soils. Geochimica et Cosmochimica Acta 72(24), 6069-6078.

Liang, B., Lehmann, J., Solomon, D., Sohi, S., Thies, J.E., Skjemstad, J.O., Luizão, F.J., Engelhard, M.H., Neves, E.G., Wirick, S., 2008b. Stability of biomass-derived black carbon in soils. Geochimica et Cosmochimica Acta 72(24), 6069-6078.

Lopez-Capel, E., Sohi, S.P., Gaunt, J.L., Manning, D.A.C., 2005. Use of thermogravimetry-differential scanning calorimetry to characterize modelable soil organic matter fractions. Soil Science Society of America Journal 69(1).

Lua, A.C., Yang, T., Guo, J., 2004. Effects of pyrolysis conditions on the properties of activated carbons prepared from pistachio-nut shells. Journal of Analytical and Applied Pyrolysis 72(2), 279-287.

MacKenzie, M.D., DeLuca, T.H., 2006. Charcoal and shrubs modify soil processes in ponderosa pine forests of western Montana. Plant and Soil 287(1-2), 257-266.

MacKenzie, M.D., DeLuca, T.H., Sala, A., 2004. Forest structure and organic horizon analysis along a fire chronosequence in the low elevation forests of western Montana. Forest Ecology and Management 203(1), 331-343.

MacKenzie, M.D., McIntire, E.J.B., Quideau, S.A., Graham, R.C., 2008. Charcoal Distribution Affects Carbon and Nitrogen Contents in Forest Soils of California. Soil Science Society of America Journal 72(6), 1774-1785.

Makoto, K., Kamata, N., Kamibayashi, N., Koike, T., Tani, H., 2012. Bark-beetle-attacked trees produced more charcoal than unattacked trees during a forest fire on the Kenai Peninsula, Southern Alaska. Scandinavian Journal of Forest Research 27(1), 30-35.

Manyà, J.J., 2012. Pyrolysis for Biochar Purposes: A Review to Establish Current Knowledge Gaps and Research Needs. Environmental Science & Technology 46(15), 7939-7954.

Marcoux, H.M., Gergel, S.E., Daniels, L.D., 2013. Mixed-severity fire regimes: How well are they represented by existing fire-regime classification systems? Canadian Journal of Forest Research 43(7), 658-668.

Mataix-Solera, J., Arcenegui, V., Tessler, N., Zornoza, R., Wittenberg, L., Martínez, C., Caselles, P., Pérez-Bejarano, A., Malkinson, D., Jordán, M.M., 2013. Soil properties as key factors controlling water repellency in fire-affected areas: Evidences from burned sites in Spain and Israel. CATENA 108, 6-13.

McCune, B., Grace, J.B., 2002. Analysis of Ecological Communities MjM Software Design, Glenden Beach, Oregon.

Michalzik, B., Kalbitz, K., Park, J.-H., Solinger, S., Matzner, E., 2001. Fluxes and concentrations of dissolved organic carbon and nitrogen – a synthesis for temperate forests. Biogeochemistry 52(2), 173-205.

Miller, J.D., Knapp, E.E., Key, C.H., Skinner, C.N., Isbell, C.J., Creasy, R.M., Sherlock, J.W., 2009. Calibration and validation of the relative differenced Normalized Burn Ratio (RdNBR) to three measures of fire severity in the Sierra Nevada and Klamath Mountains, California, USA. Remote Sensing of Environment 113(3), 645-656.

Monsanto, P.G., Agee, J.K., 2008. Long-term post-wildfire dynamics of coarse woody debris after salvage logging and implications for soil heating in dry forests of the eastern Cascades, Washington. Forest Ecology and Management 255(12), 3952-3961.

Morse, C.C., Yevdokimov, I.V., DeLuca, T.H., 2000. In Situ extraction of rhizosphere organic compounds from contrasting plant communities. Communications in Soil Science and Plant Analysis 31(5-6), 725-742.

MTBS, 2013. Monitoring Trends in Burn Severity Assessment of Fire Information. http://www.mtbs.gov. U.S. Geological Survey and U.S.D.A. Forest Service, Sioux Falls, South Dakota.

Mullholland, P.J., 2003. Large-Scale Patterns in Dissolved Organic Carbon Concentration, Flux, and Sources. In: S.E.G. Findlay, R.L. Sinsabaugh (Eds.), Aquatic Ecosystems: Interactivity of dissolved organic matter. Aquatic Ecology. Academic Press, San Diego, California, pp. 139-157.

Mulvaney, R.L., 1996. Nitrogen—Inorganic Forms. In: D.L. Sparks, A.L. Page, P.A. Helmke, R.H. Loeppert (Eds.), Methods of Soil Analysis Part 3—Chemical Methods. SSSA Book Series. Soil Science Society of America, American Society of Agronomy, Madison, WI, pp. 1123-1184.

NCRS, 2014. Keys to Soil Taxonomy. In: N.R.C.S. United States Department of Agriculture (Ed.).

Neary, D.G., Klopatek, C.C., DeBano, L.F., Ffolliott, P.F., 1999. Fire effects on belowground sustainability: a review and synthesis. Forest Ecology and Management 122(1–2), 51-71.

Neary, D.G., Ryan, K.C., DeBano, L.F., 2005. Wildland fire in ecosystems: Effects of fire on soils and water. In: F.S. U.S. Department of Agriculture, Rocky Mountain Research Station (Ed.), Odgen, UT, pp. 250.

Nguyen, B.T., Lehmann, J., Hockaday, W.C., Joseph, S., Masiello, C.A., 2010. Temperature sensitivity of black carbon decomposition and oxidation. Environmental Science & Technology 44(9), 3324-3331.

Nguyen, B.T., Lehmann, J., Kinyangi, J., Smernik, R., Riha, S.J., Engelhard, M.H., 2008. Long-term black carbon dynamics in cultivated soil. Biogeochemistry 92(1), 163-176.

Nguyen, T.H., Brown, R.A., Ball, W.P., 2004. An evaluation of thermal resistance as a measure of black carbon content in diesel soot, wood char, and sediment. Organic Geochemistry 35(3), 217-234.

Nishimiya, K., Hata, T., Imamura, Y., Ishihara, S., 1998. Analysis of chemical structure of wood charcoal by X-ray photoelectron spectroscopy. Journal of Wood Science 44(1), 56-61.

Northup, R.R., Dahlgren, R.A., McColl, J.G., 1998. Polyphenols as Regulators of Plant-litter-soil Interactions in Northern California's Pygmy Forest: A Positive Feedback? Biogeochemistry 42(1), 189-220.

Oksanen, J., Blanchet, F.G., Kindt, R., Legendre, P., Minchin, P.R., O'Hara, R.B., Simpson, G.L., Peter Solymos, Stevens, M.H.H., Wagner, H., 2013. Community Ecology Package. CRAN.

Paavolainen, L., Kitunen, V., Smolander, A., 1998. Inhibition of nitrification in forest soil by monoterpenes. Plant and Soil 205(2), 147-154.

Paul, E.A., 2007. Soil Microbiology, Ecology, and Biochemistry. 3rd ed. Academic Press, San Francisco, California.

Perry, D.A., Hessburg, P.F., Skinner, C.N., Spies, T.A., Stephens, S.L., Taylor, A.H., Franklin, J.F., McComb, B., Riegel, G., 2011. The ecology of mixed severity fire regimes in Washington, Oregon, and Northern California. Forest Ecology and Management 262(5), 703-717.

Peterson, D.L., Schreiner, E.G., Buckingham, N.M., 1997. Gradients, Vegetation and Climate: Spatial and Temporal Dynamics in the Olympic Mountains, U.S.A. Global Ecology and Biogeography Letters 6(1), 7-17.

Pietikäinen, J., Kiikkilä, O., Fritze, H., 2000. Charcoal as a habitat for microbes and its effect on the microbial community of the underlying humus. Oikos 89(2), 231-242.

Pignatello, J.J., Kwon, S., Lu, Y., 2006. Effect of Natural Organic Substances on the Surface and Adsorptive Properties of Environmental Black Carbon (Char): Attenuation of Surface Activity by Humic and Fulvic Acids. Environmental Science & Technology 40(24), 7757-7763.

Pignatello, J.J., Uchimiya, M., Abiven, M., Schmidt, M.W.I., 2015. Evolution of biochar properties in soil. In: J. Lehmann, S. Joseph (Eds.), Biochar for Enviornmental Management: Science, Technology and Implementation. Routledge, New York, pp. 195-233.

Pingree, M.R.A., 2011. The first pre-and post-wildfire charcoal quantification using peroxide-acid digestion. Masters Thesis, Western Washington University, WWU Masters Thesis Collection, 30 pp.

Pingree, M.R.A., DeLuca, E.E., Schwartz, D.T., DeLuca, T.H., 2016. Adsorption capacity of wildfire-produced charcoal from Pacific Northwest forests. Geoderma 283, 68-77.

Pingree, M.R.A., Homann, P.S., Morrissette, B., Darbyshire, R., 2012. Long and Short-Term Effects of Fire on Soil Charcoal of a Conifer Forest in Southwest Oregon. Forests 3(4), 353-369.

Plante, A.F., Pernes, M., Chenu, C., 2005. Changes in clay-associated organic matter quality in a C depletion sequence as measured by differential thermal analyses. Geoderma 129(3–4), 186-199.

Pluchon, N., Vincent, A.G., Gundale, M.J., Nilsson, M.-C., Kardol, P., Wardle, D.A., 2016. The impact of charcoal and soil mixtures on decomposition and soil microbial communities in boreal forest. Applied Soil Ecology 99, 40-50.

Powers, R.F., 1980. Mineralizable Soil Nitrogen as an Index of Nitrogen Availability to Forest Trees1. Soil Science Society of America Journal 44(6), 1314-1320.

Preston, C.M., Schmidt, M.W.I., 2006. Black (pyrogenic) carbon: a synthesis of current knowledge and uncertainties with special consideration of boreal regions. Biogeosciences 3(4), 397-420.

Qualls, R.G., Haines, B.L., 1991. Geochemistry of Dissolved Organic Nutrients in Water Percolating through a Forest Ecosystem. Soil Science Society of America Journal 55(4), 1112-1123.

Quilliam, R.S., Glanville, H.C., Wade, S.C., Jones, D.L., 2013. Life in the 'charosphere' – Does biochar in agricultural soil provide a significant habitat for microorganisms? Soil Biology and Biochemistry 65, 287-293.

R Core Team, 2014. R: A Language and Environment for Statistical Computing. R Foundation for Statistical Computing, Vienna, Austria.

Reeves, J.B., McCarty, G.W., Rutherford, D.W., Wershaw, R.L., 2008. Mid-Infrared Diffuse Reflectance Spectroscopic Examination of Charred Pine Wood, Bark, Cellulose, and Lignin: Implications for the Quantitative Determination of Charcoal in Soils. Appl. Spectrosc. 62(2), 182-189.

Reisser, M., Purves, R.S., Schmidt, M.W.I., Abiven, S., 2016. Pyrogenic Carbon in Soils: A Literature-Based Inventory and a Global Estimation of Its Content in Soil Organic Carbon and Stocks. Frontiers in Earth Science 4(80).

Rothstein, D.E., Yermakov, Z., Buell, A.L., 2004. Loss and recovery of ecosystem carbon pools following stand-replacing wildfire in Michigan jack pine forests. Canadian Journal of Forest Research 34(9), 1908-1918.

Rutherford, D.W., Wershaw, R.L., Rostad, C.E., Kelly, C.N., 2012. Effect of formation conditions on biochars: Compositional and structural properties of cellulose, lignin, and pine biochars. Biomass and Bioenergy 46, 693-701.

Sander, M., Pignatello, J.J., 2005. Characterization of charcoal adsorption sites for aromatic compounds: insights drawn from single-solute and bi-solute competitive experiments. Environmental Science & Technology 39(6), 1606-1615.

Sanford, R.L., Saldarriaga, J., Clark, K.E., Uhl, C., Herrera, R., 1985. Amazon Rain-Forest Fires. Science 227(4682), 53-55.

Santín, C., Doerr, S.H., Merino, A., Bryant, R., Loader, N.J., 2016. Forest floor chemical transformations in a boreal forest fire and their correlations with temperature and heating duration. Geoderma 264, Part A, 71-80.

Santín, C., Doerr, S.H., Preston, C., Bryant, R., 2013. Consumption of residual pyrogenic carbon by wildfire. International Journal of Wildland Fire 22(8), 1072-1077.

Santín, C., Doerr, S.H., Preston, C.M., González-Rodríguez, G., 2015. Pyrogenic organic matter production from wildfires: a missing sink in the global carbon cycle. Global Change Biology 21(4), 1621-1633.

Schmidt, M.W.I., Noack, A.G., 2000. Black carbon in soils and sediments: Analysis, distribution, implications, and current challenges. Global Biogeochemical Cycles 14(3), 777-793.

Scott, A.C., 2000. The Pre-Quaternary history of fire. Palaeogeography, Palaeoclimatology, Palaeoecology 164(1–4), 281-329.

Scott, A.C., Damblon, F., 2010. Charcoal: Taphonomy and significance in geology, botany and archaeology. Palaeogeography, Palaeoclimatology, Palaeoecology 291(1–2), 1-10.

Shebitz, D.J., Reichard, S.H., Woubneh, W., 2008. Beargrass (Xerophyllum tenax) on the Olympic Peninsula, Washington: Autecology and Population Status. Northwest Science 82(2), 128-140.

Singh, B.P., Cowie, A.L., Smernik, R.J., 2012. Biochar Carbon Stability in a Clayey Soil As a Function of Feedstock and Pyrolysis Temperature. Environmental Science & Technology 46(21), 11770-11778.

Skjemstad, J., Clarke, P., Taylor, J., Oades, J., Mcclure, S., 1996. The chemistry and nature of protected carbon in soil. Soil Research 34(2), 251-271.

Sohi, S.P., Krull, E., Lopez-Capel, E., Bol, R., 2010. Chapter 2 - A Review of Biochar and Its Use and Function in Soil, Advances in Agronomy. Academic Press, pp. 47-82.

Stoof, C.R., Moore, D., Fernandes, P.M., Stoorvogel, J.J., Fernandes, R.E.S., Ferreira, A.J.D., Ritsema, C.J., 2013. Hot fire, cool soil. Geophysical Research Letters 40(8), 1534-1539.

Taylor, T.N., Taylor, E.L., Krings, M., 2009. Paleobotany: The biology and evolution of fossil plants. 2nd ed. Academic Press, Boston, MA.

Tepley, A.J., Swanson, F.J., Spies, T.A., 2013. Fire-mediated pathways of stand development in Douglas-fir/western hemlock forests of the Pacific Northwest, USA. Ecology 94(8), 1729-1743.

Thies, J.E., Rillig, M.C., Graber, E.R., 2015. Biochar effects on the abundance, activity and diversity of the soil biota. In: J. Lehmann, S. Joseph (Eds.), Biochar for Environmental Management: Science, Technology and Implementation. Routledge, New York, NY, pp. 327-390.

Thomas, G., 1996. Soil pH and soil acidity, Methods of Soil Analysis Part 3—Chemical Methods. Soil Science Society of America and American Society of Agronomy, Madison, WI, pp. 475-490.

Thomas, J.W., Franklin, J.F., Gordon, J., Johnson, K.N., 2006. The Northwest Forest Plan: Origins, Components, Implementation Experience, and Suggestions for Change

El Plan Forestal del Noroeste: Oigenes, Componentes, Experiencia de Implementación y Sugerencias de Cambio. Conservation Biology 20(2), 277-287.

Tryon, E.H., 1948. Effect of Charcoal on Certain Physical, Chemical, and Biological Properties of Forest Soils. Ecological Monographs 18(1), 81-115.

USGS, 2009. National Elevation Dataset (NED). http://nationalmap.gov. U.S. Geological Survey, Sioux Falls, SD.

Uusitalo, M., Kitunen, V., Smolander, A., 2008. Response of C and N transformations in birch soil to coniferous resin volatiles. Soil Biology and Biochemistry 40(10), 2643-2649.

Vitousek, P.M., Howarth, R.W., 1991. Nitrogen limitation on land and in the sea: How can it occur? Biogeochemistry 13(2), 87-115.

Walker, L.R., Wardle, D.A., Bardgett, R.D., Clarkson, B.D., 2010. The use of chronosequences in studies of ecological succession and soil development. Journal of Ecology 98(4), 725-736.

Wang, C., Bond-Lamberty, B.E.N., Gower, S.T., 2003. Carbon distribution of a well- and poorly-drained black spruce fire chronosequence. Global Change Biology 9(7), 1066-1079.

Wang, T., Hamann, A., Spittlehouse, D.L., Murdock, T.Q., 2012. ClimateWNA—High-Resolution Spatial Climate Data for Western North America. Journal of Applied Meteorology and Climatology 51(1), 16-29.

Wardle, D.A., Hörnberg, G., Zackrisson, O., Kalela-Brundin, M., Coomes, D.A., 2003. Long-Term Effects of Wildfire on Ecosystem Properties Across an Island Area Gradient. Science 300(5621), 972-975.

Wardle, D.A., Zackrisson, O., Nilsson, M.-C., 1998. The charcoal effect in Boreal forests: mechanisms and ecological consequences. Oecologia 115(3), 419-426.

Weisberg, P.J., 2004. Importance of non-stand-replacing fire for development of forest structure in the Pacific Northwest, USA. Forest Science 50(2), 245-258.

Wendel, R., 2009. Forests and fire history of the Geyser Valley area, Olympic National Park, Washington State, University of Washington, Seattle, 103 pp.

Wendel, R., Zabowski, D., 2010. Fire history within the lower Elwha river watershed, Olympic National Park, Washington. Northwest Science 84(1), 88-97.

Wetzel, S.A., Fonda, R., 2000. Fire history of Douglas-fir forests in the Morse Creek drainage of Olympic National Park, Washington. Northwest Science 74(4), 263.

Wiedner, K., Glaser, B., 2015. Traditional use of biochar. In: J. Lehmann, S. Joseph (Eds.), Biochar for Environmental Management: Science, Technology and Implementation. Routledge, New York, pp. 15-37.

Wildman, J., Derbyshire, F., 1991. Origins and functions of macroporosity in activated carbons from coal and wood precursors. Fuel 70(5), 655-661.

Wray, J., Anderson, M.K., 2003. Restoring Indian-Set Fires to Prairie Ecosystems on the Olympic Peninsula. Ecological Restoration 21(4), 296-301.

Zackrisson, O., 1977. Influence of Forest Fires on the North Swedish Boreal Forest. Oikos 29(1), 22-32.

Zackrisson, O., DeLuca, T.H., Nilsson, M.C., Sellstedt, A., Berglund, L.M., 2004. Nitrogen fixation increases with successional age in boreal forests. Ecology 85(12), 3327-3334.

Zackrisson, O., Nilsson, M.-C., Wardle, D.A., 1996. Key ecological function of charcoal from wildfire in the Boreal forest. Oikos, 10-19.

Zhu, D., Kwon, S., Pignatello, J.J., 2005. Adsorption of Single-Ring Organic Compounds to Wood Charcoals Prepared under Different Thermochemical Conditions. Environmental Science & Technology 39(11), 3990-3998.

Zhu, D., Pignatello, J.J., 2005. Characterization of aromatic compound sorptive interactions with black carbon (charcoal) assisted by graphite as a model. Environmental Science & Technology 39(7), 2033-2041.

Zimmerman, A.R., 2010. Abiotic and microbial oxidation of laboratory-produced black carbon (biochar). Environmental Science & Technology 44(4), 1295-1301.

APPENDIX

Table A1: Aboveground characteristics of the nine 250 m^2 fire chronosequence sites across the eastern Olympic Peninsula, Washington. Time since fire was dated from site establishment and soil sample collection (IC, KT, MC, RC in 2013 and remaining sites in 2014). The number of fires since 1568 was determined by Wendel (2009) for sites IC, KT, MC, RC, and with fire history maps provided by the USDA Forest Service for the remaining sites. Climate variables were calculated as an average from 1981-2010 by Wang et al. (2012). The Hargreaves climate moisture deficit is the sum of the monthly difference between the potential and actual moisture deficit (Hargreaves, 1975). Basal area was calculated from live standing trees > 9 cm in diameter at breast height and saplings were trees taller than breast height and < 9 cm in diameter.

Fire History	Site	Time since fire (years)	Number of fires since 1568	Elevation (m)	Mean annual temperature (°C)	Mean annual precipitation (mm)	Hargreaves climate moisture deficit	Basal area (m^2 ha^{-1})	% Basal area *P. menziesii*	% Basal area *T. heterophylla*	% Basal area *T. plicata*	Saplings ha^{-1}
Historic	IC	115	4	520	8.7	1867	252	65	29	68	<1	1200
	KT	115	5	360	8.7	1544	289	71	100	0	0	80
	MC	86	7	396	8.8	1695	278	85	100	0	0	80
Interm-ediate	RC	36	6	385	8.6	1499	291	38	83	0	4	6720
	BF1	29	2	457	7.7	2961	166	97	87	1	11	7120
	BF2	29	2	457	7.7	2957	164	82	97	<1	11	2720
Recent	BG	8	4	608	7.9	2802	174	100	89	0	<1	0
	CF	5	2	452	7.7	2197	145	51	100	0	0	0
	BH	3	2	525	7.5	2110	163	21	76	24	10	0

Table A2: Soil characteristics of the nine 250 m^2 sites across the eastern Olympic Peninsula, Washington. Sites are dated by time since fire from establishment and soil sample collection (IC, KT, MC, RC in 2013 and remaining sites in 2014). The O-horizon depth is an average of three composite samples within each of the ten 5 m^2 plots. Mineral soil pH and texture was measured from a composite samples composed of equal parts of all plots in the site. Chemical composition is reported as an average of all plots (n = 10). Standard error is given in parenthesis.

Fire History	Site	Time since fire (years)	O-horizon depth (cm)	Mineral soil pH	% Sand	% Silt	% Clay	O-horizon soil C ($g\ kg^{-1}$)	O-horizon soil N ($g\ kg^{-1}$)	O-horizon soil C:N	Mineral soil C ($g\ kg^{-1}$)	Mineral soil N ($g\ kg^{-1}$)	Mineral soil C:N
Historic	IC	115	3.2 (0.1)	5.12	52	30	18	332.6 (18.8)	7.6 (0.5)	44	56.1 (17.7)	1.2 (0.2)	46
	KT	115	4.0 (0.2)	5.44	38	39	23	364.5 (16.7)	9.7 (0.5)	37	44.4 (4.6)	1.5 (0.1)	29
	MC	86	2.5 (0.2)	5.11	48	35	17	318.2 (15.3)	7.9 (0.4)	40	47.6 (5.0)	1.4 (0.1)	33
Interm-ediate	RC	36	4.2 (0.1)	5.56	48	36	16	373.7 (21.5)	10.4 (0.7)	36	37.0 (4.2)	1.2 (0.1)	31
	BF1	29	2.8 (0.1)	5.58	57	24	19	335.9 (26.3)	7.1 (0.7)	47	29.3 (3.5)	0.8 (0.1)	35
	BF2	29	2.2 (0.8)	5.98	50	31	19	321.1 (24.0)	5.0 (0.4)	64	33.7 (3.5)	0.8 (0.1)	43
Recent	BG	8	3.3 (0.4)	5.26	60	27	13	196.7 (18.3)	5.7 (0.6)	34	53.9 (4.6)	1.3 (0.1)	42
	CF	5	2.2 (0.2)	5.85	61	18	21	321.0 (25.1)	11.2 (1.0)	29	53.1 (10.4)	2.1 (0.5)	25
	BH	3	2.5 (0.2)	5.30	50	28	22	229.5 (14.9)	6.8 (0.4)	34	56.1 (12.3)	1.5 (0.5)	37

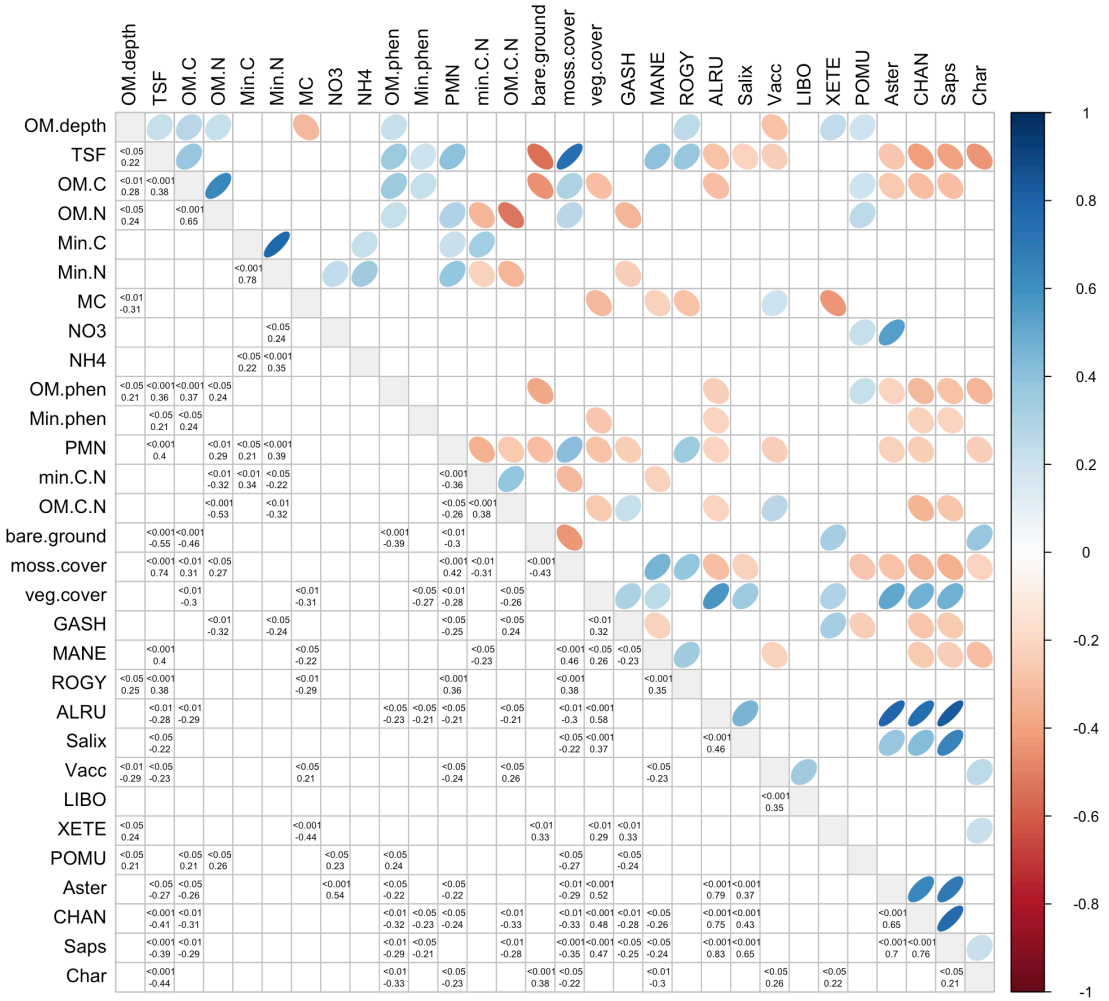

Figure A1: Correlation matrix of soil and vegetation variables measured along the fire chronosequence in the eastern Olympic peninsula, Washington (n=10). The right-hand side displays correlations with ellipses and on a color-scale. The left-hand side shows significance values (upper) and Pearson correlation values (lower). See Table A1 for a description of the variable names and units.

Table A3: A description of soil and vegetation variables measured in fire chronosequence sites in the eastern Olympic peninsula, Washington. Variable descriptions include acronym or abbreviation (code) used in all figures and units thereof.

Variable code	**Description**	**Units**
TSF	Time since fire chronosequence gradient	Years since the last fire
OM depth	Depth of O-horizon	cm
OM C	Carbon concentration of O-horizon	mg C g dry soil^{-1}
OM N	Nitrogen concentration of O-horizon	mg N g dry soil^{-1}
Min C	Carbon concentration of 0-10 cm mineral soil	mg C g dry soil^{-1}
Min N	Nitrogen concentration of 0-10 cm mineral soil	mg N g dry soil^{-1}
MC	Moisture content	Dry soil weight (g) / field-moist soil weight (g)
NO3	Nitrate-N concentration of mineral soil KCl extracts	mg N kg dry soil^{-1}
NH4	Ammonium-N concentration of mineral soil KCl extracts	mg N kg dry soil^{-1}
OM phen	Phenol concentration in O-horizon soils from $CaCl_2$ extracts	mg phenol kg dry soil^{-1}
Min phen	Phenol concentration in 0-10 cm minearl soils from $CaCl_2$ extracts	mg phenol kg dry soil^{-1}
PMN	Potentially mineralizable nitrogen from anaerobic incubation	mg N kg dry soil^{-1} day^{-1}
Min CN	Ratio of carbon to nitrogen concentration in 0-10 cm mineral soil	NA
OM CN	Ratio of carbon to nitrogen concentration in O-horizon soils	NA
Bare ground	Percent cover of visually estimated bare ground (devoid of O-horizon, moss, or vegetation)	%
Moss cover	Percent cover of visually estimated moss	%
Veg cover	Percent cover of visually estimated vegetation	%
GASH	Percent cover of visually estimated salal *(Gaultheria shallon)*	%
MANE	Percent cover of visually estimated Oregon grape *(Mahonia nervosa)*	%
ROGY	Percent cover of visually estimated baldhip rose *(Rosa gymnocarpa)*	%
ALRU	Percent cover of visually estimated red alder *(Alnus rubra)*	%
Salix	Percent cover of visually estimated shrubs in the *Salix* genus	%
Vacc	Percent cover of visually estimated shrubs in the *Vaccinium* genus	%
LIBO	Percent cover of visually estimated of twinflower *(Linnaea borealis)*	%
XETE	Percent cover of visually estimated of bear grass *(Xerophyllum tenax)*	%
POMU	Percent cover of visually estimated of sword fern *(Polystichum munitum)*	%
Aster	Percent cover of visually estimated of flowering plants in the *Aster* genus	%
CHAN	Percent cover of visually estimated of fireweed *(Chamerion angustifolium)*	%
Char	Charcoal mass hand-separated from O-horizon	kg charcoal hectare^{-1}

Table A4: Permutational analysis of variance (PERMANOVA) results for vegetation and overstory parameters. The first three lines are testing the significance of distances between observations, restricted to permute only within Site. The last three lines test the significant differences within site, as site is nested within time since fire (TSF). ** p-value < 0.01.

	Df	**SS**	**MSS**	**F model**	**r^2**	**P value**
TSF	1	0.50764	0.50764	2.3078	0.24795	0.0048 **
Residuals	7	1.53973	0.21996		0.75205	
Total	8	2.04737			1.0000	
Site	8	14.3917	1.79896	19.728	0.66084	1
Residuals	81	7.3862	0.09119		0.33916	
Total	89	21.7778			1.00000	

Table A5: Linear model results for vegetation variables related to TSF. Full models and final selected models are listed above the final model results.

Full model: OM.C ~ TSF + bare.ground + moss.cover + veg.cover + ALRU + POMU + Aster + CHAN + Saps				
Final model: OM.C ~ TSF + bare.ground + veg.cover + POMU				
Factor	**Estimate**	**Std Error**	**t value**	**P value**
Intercept	325.3430	20.8941	15.571	< 0.001
TSF	0.5054	0.2144	2.357	< 0.05
Bare.ground	-1.4252	0.6456	-2.208	< 0.05
Veg.cover	-0.6189	0.2108	-2.936	< 0.01
POMU	2.0926	0.8357	2.505	< 0.05
R^2	0.3419			
Full model: OM.depth ~ TSF + ROGY + Vacc + XETE + POMU				
Final model: OM.depth ~ TSF + Vacc + XETE + POMU				
Factor	**Estimate**	**Std Error**	**t value**	**P value**
Intercept	2.467414	0.220615	11.184	< 0.001
TSF	0.008387	0.002921	2.871	< 0.01
Vacc	-0.106798	0.052694	-2.027	< 0.05
XETE	0.13223	0.038678	3.419	< 0.001
POMU	0.035068	0.012945	2.709	< 0.01
R^2	0.2568			
Full model: log(OM.phen) ~ TSF + bare.ground + ALRU + POMU + Aster + Saps + CHAN				
Final model: log(OM.phen) ~ TSF + bare.ground + POMU + CHAN				
Factor	**Estimate**	**Std Error**	**t value**	**p value**
Intercept	2.877118	0.217488	13.229	< 0.001
TSF	0.005938	0.00259	2.293	< 0.05
bare.ground	-0.019669	0.00723	-2.721	< 0.01

POMU	0.028144	0.009358	3.007	< 0.01
CHAN	-0.02606	0.005862	-4.446	< 0.001
R^2	0.4956			
Full model: log(Min.phen) ~ TSF + veg.cover + ALRU + CHAN + Saps				
Final model: log(Min.phen) ~ TSF + veg.cover + CHAN				
Factor	**Estimate**	**Std Error**	**t value**	**p value**
Intercept	0.955942	0.489301	1.954	0.054
TSF	0.011029	0.005498	2.006	< 0.05
veg.cover	-0.01765	0.007037	-2.508	< 0.05
CHAN	-0.069109	0.017498	-3.95	< 0.001
R^2	0.4169			
Full model: log(PMN) ~ TSF + bare.ground + moss.cover + veg.cover + GASH + ROGY + ALRU + Vacc + Aster + CHAN				
Final model: log(PMN) ~ moss.cover + Vacc				
Factor	**Estimate**	**Std Error**	**t value**	**p value**
Intercept	-0.737863	0.347735	-2.122	< 0.05
moss.cover	0.026597	0.006619	4.018	< 0.001
Vacc	-0.322879	0.098069	-3.292	< 0.05
R^2	0.2552			
Full model: log(Char) ~ TSF + bare.ground + moss.cover + MANE + Vacc + XETE + Saps				
Final model: log(Char) ~ bare.ground + MANE				
Factor	**Estimate**	**Std Error**	**t value**	**p value**
Intercept	5.60633	0.34563	16.22	< 0.001
bare.ground	0.04569	0.01725	2.648	< 0.01
MANE	-0.06507	0.01008	-6.459	< 0.001
R^2	0.3871			

Table A6: Permutational analysis of variance (PERMANOVA) results for all soil parameters. The first three lines are testing the significance of distances between observations, restricted to permute only within Site. The last three lines test the significant differences within site, as site is nested within time since fire (TSF). ** P value < 0.01.

	Df	**SS**	**MSS**	**F model**	**r^2**	**P value**
TSF	1	1.3527	1.35275	2.7983	0.28559	0.0042 **
Residuals	7	3.3840	0.48342		0.71441	
Total	8	4.7367			1.0000	
Site	8	24.551	3.06891	8.8296	0.46583	1
Residuals	81	28.153	0.34757		0.53417	
Total	89	52.704			1.00000	

Table A7: Linear model results for soil variables related to TSF. Full models and final selected models are listed above the final model results.

Full model: OM.C ~ TSF + OM.N + OM.phen + Min.phen				
Final model: OM.C ~ TSF + OM.N				
Factor	**Estimate**	**Std Error**	**t value**	**P value**
Intercept	132.0586	19.8070	6.667	< 0.001
TSF	0.5941	0.1442	4.119	< 0.001
OM.N	18.7541	2.3003	8.153	< 0.001
R^2	0.5145			
Full model: OM.depth ~ TSF + OM.C + OM.N + MC + OM.phen				
Final model: OM.depth ~ MC + OM.phen				
Factor	**Estimate**	**Std Error**	**t value**	**p value**
Intercept	5.502035	0.763846	7.203	< 0.001
MC	-4.364236	1.1679	-3.737	< 0.001
OM.phen	0.012212	0.004249	2.874	< 0.01
Multiple R^2	0.1767			
Full model: log(OM.phen) ~ TSF + OM.depth + OM.C + OM.N + Char				
Final model: log(OM.phen) ~ TSF + OM.C + Char				
Factor	**Estimate**	**Std Error**	**t value**	**p value**
Intercept	0.983069	0.3513205	2.798	< 0.01
TSF	0.0056281	0.0023056	2.441	< 0.05
OM.C	0.0059872	0.0010967	5.459	< 0.001
Char	-0.0003677	0.000164	-2.243	< 0.05
R^2	0.4614			
Full model: log(Min.phen) ~ TSF + OM.C				
Final model: log(Min.phen) ~ TSF + OM.C				
Factor	**Estimate**	**Std Error**	**t value**	**p value**
Intercept	-3.400448	0.96883	-3.51	< 0.001
TSF	0.016401	0.006242	2.627	< 0.05
OM.C	0.008646	0.003254	2.657	< 0.01
R^2	0.2053			
Full model: log(PMN) ~ TSF + OM.N + Min.C + Min.N + min.C.N + OM.C.N				
Final model: log(PMN) ~ TSF + min.C.N + OM.C.N				
Factor	**Estimate**	**Std Error**	**t value**	**p value**
Intercept	4.279136	0.855156	5.004	< 0.001
TSF	0.020108	0.004742	4.241	< 0.001
Min.C.N	-5.09E-02	0.020475	-2.485	< 0.05
OM.C.N	-0.084576	0.017526	-4.826	< 0.001
R^2	0.4175			

Full model: log(Char) ~ TSF + OM.phen + PMN				
Final model: log(Char) ~ TSF				
Factor	**Estimate**	**Std Error**	**t value**	**p value**
Intercept	6.216336	0.425593	14.606	< 0.001
TSF	-0.025538	0.006645	-3.843	< 0.001
R^2	0.1437			

Table A8: Analysis of Variance (ANOVA) results for O-horizon carbon concentration (g C kg dry soil^{-1}) tested against time since fire (TSF) and the random site factor (Site) (n=10). *** p-value < 0.001.

	Df	**SS**	**MSS**	**F value**	**P value**
TSF	6	253577	42263	9.625	5.58e-08 ***
Site	2	7329	3665	0.835	0.438
Residuals	81	355685	4391		
Total	89				

Table A9: Analysis of Variance (ANOVA) results from soil basal respiration rates (mg CO_2 g dry soil^{-1} day^{-1}) tested against years since the last fire (TSF) and burn history (Burn) (n = 12). ** P value < 0.01. *** P value < 0.001.

	Df	**SS**	**MSS**	**F value**	**P value**
TSF	2	57222	28611	9.922	0.000171 **
Burn History	1	162767	162767	56.446	1.97e-10 ***
TSF * Burn	2	9748	4874	1.690	0.192
Residuals	66	190318	2884		
Total	71				

Table A10: Permutational Multivariate Analysis of Variances (PERMANOVA) results of net ammonium accumulation rates during the aerobic incubation (mg N kg dry soil^{-1} 20 days^{-1}) using Euclidean distances measures and a constrained permutation within sites. * P value < 0.05.

	Df	**SS**	**MSS**	**F value**	**r^2**	**P value**
TSF	2	67.79	33.897	4.9988	0.12575	0.011 *
Burn History	1	0.95	0.949	0.1400	0.00176	0.708
TSF * Burn	2	22.81	11.405	1.6819	0.04231	0.176
Residuals	66	447.55	6.781		0.83017	
Total	71	539.10			1.00000	

Table A11: Permutational Multivariate Analysis of Variances (PERMANOVA) results for net nitrate accumulation during the aerobic incubation (mg N kg dry soil^{-1} 20 days^{-1}) using Euclidean distances measures and a constrained permutation within sites. * P value < 0.05.

	Df	**SS**	**MSS**	**F value**	**r^2**	**P value**
TSF	2	2.944	1.4721	2.9302	0.07322	0.020 *
Burn History	1	1.157	1.1566	2.3021	0.02876	0.105
TSF * Burn	2	2.949	1.4745	2.9348	0.07334	0.013 *
Residuals	66	33.159	0.5024		0.82467	
Total	71	40.208			1.00000	

VITA

Melissa R.A. Pingree received her bachelor's of science in resource conservation with an emphasis in terrestrial science at the University of Montana's College of Forestry in December of 2006. After working as a civilian for the Department of Defense in Forestry at Fort Lewis she began her master's of science degree program at Western Washington University. Working intermittently in the summer on Type 2 wildland fire hand crews with the U.S. Forest Service, she completed her master's of science at Western Washington University under the mentorship of Peter S. Homann graduating in 2011 from the Huxley College of the Environment. After two seasons with the National Park Service as a wildland fire crew member, she started her doctoral program at the University of Washington in January of 2013.